Multimessenger signals from dark photons around black holes

Masha Baryakhtar

University of Washington

May 3, 2023

New Particles in the Sky

- Axions and their relatives are ultralight and weakly coupled: a window into the **highest scales**
- Dense, large astrophysical objects can provide good testing grounds

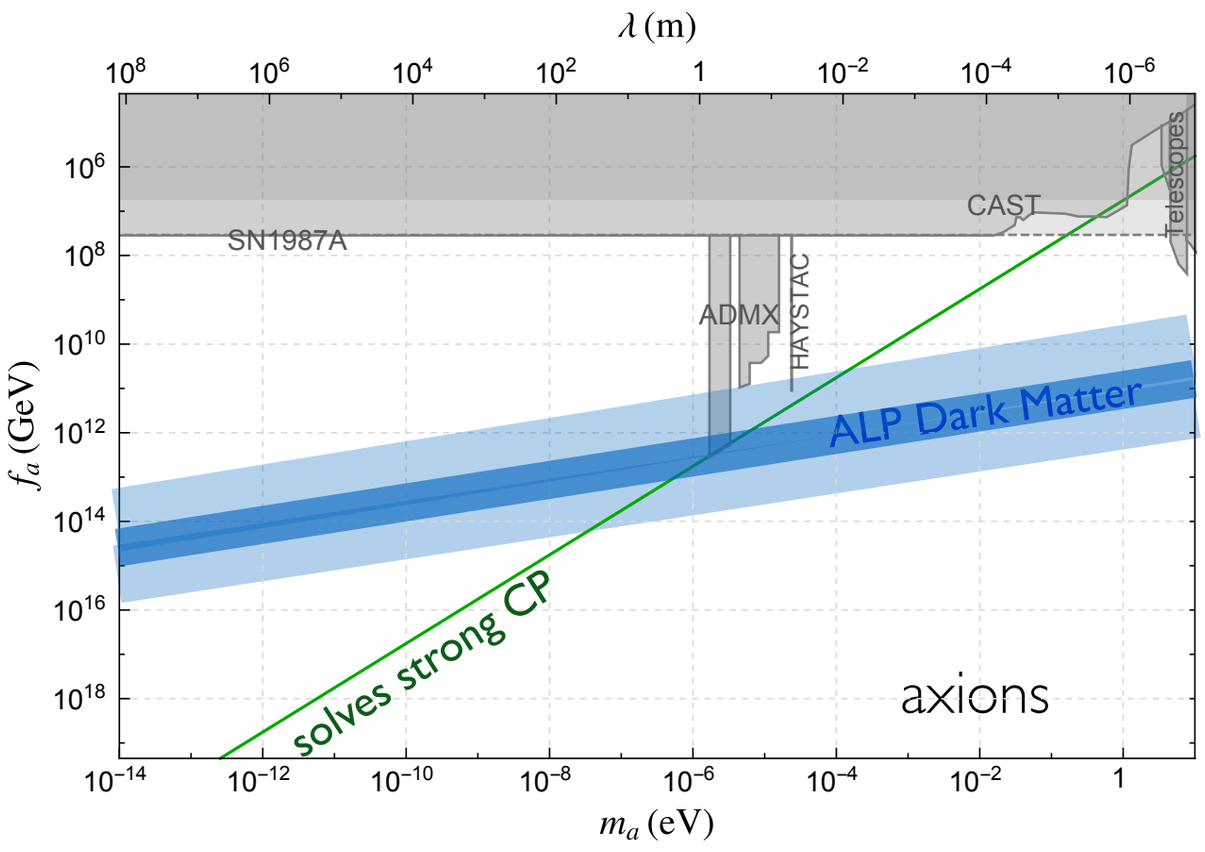

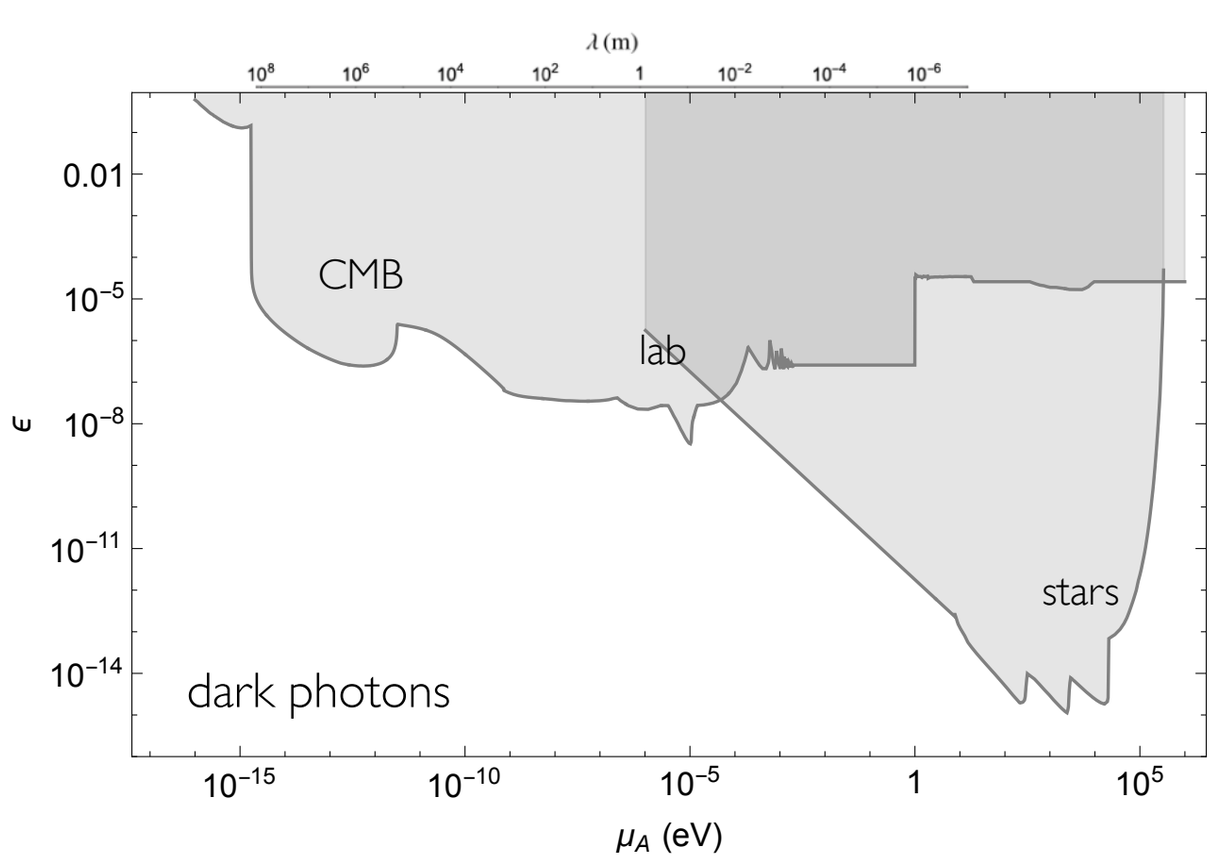

cajohare.github.io/axionlimits/

Black holes as laboratories for ultralight particles

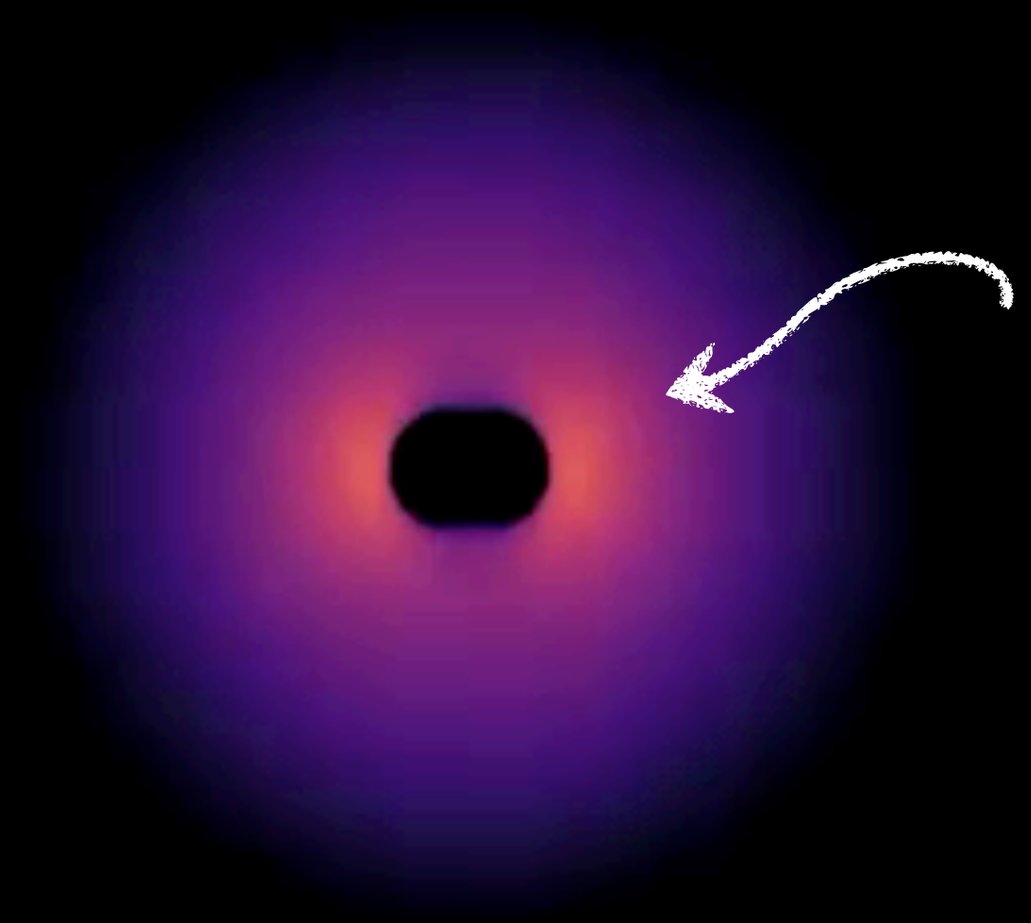

Density comparable to neutron star densities

Few percent of black hole mass distributed over (tens of black hole radii)^3 volume

Numerical GR simulation by Will East

Superradiance

- A wave scattering off a rotating object increases in amplitude by extracting angular momentum and energy.
- Growth proportional to probability of absorption when rotating object is at rest: **dissipation** necessary to increase wave amplitude

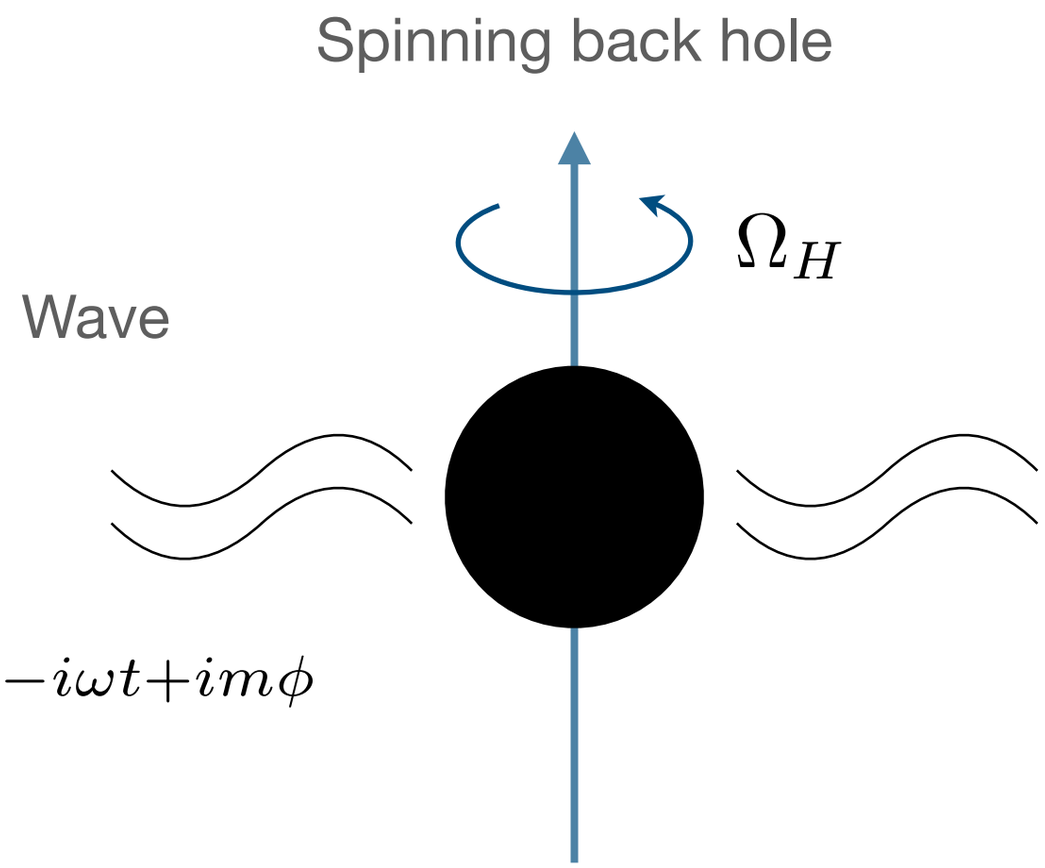

Superradiance condition:

Angular phase velocity of wave slower than angular velocity of BH horizon,

$$\omega/m < \Omega_{BH}$$

Zel'dovich; Starobinskii; Misner

Superradiance

- A wave scattering off a rotating object increases in amplitude by extracting angular momentum and energy.
- Growth proportional to probability of absorption when rotating object is at rest: **dissipation** necessary to increase wave amplitude

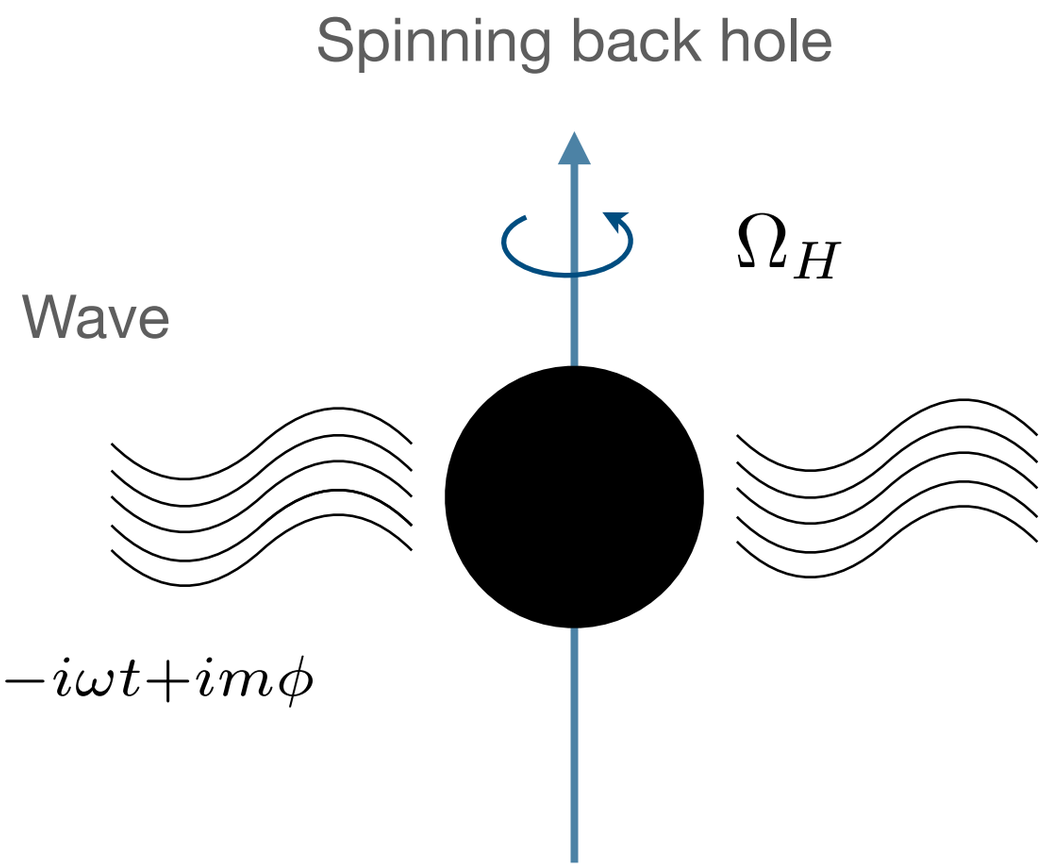

Superradiance condition:

Angular phase velocity of wave slower than angular velocity of BH horizon,

$$\omega/m < \Omega_{BH}$$

Zel'dovich; Starobinskii; Misner

Superradiance

Gravitational wave amplified when scattering from a rapidly rotating black hole

Numerical GR simulation by Will East

Superradiance

Waves bound near black hole repeat this process continuously: exponential growth of `gravitational atom'

Efficient for $\mu_a^{-1} \sim r_g$

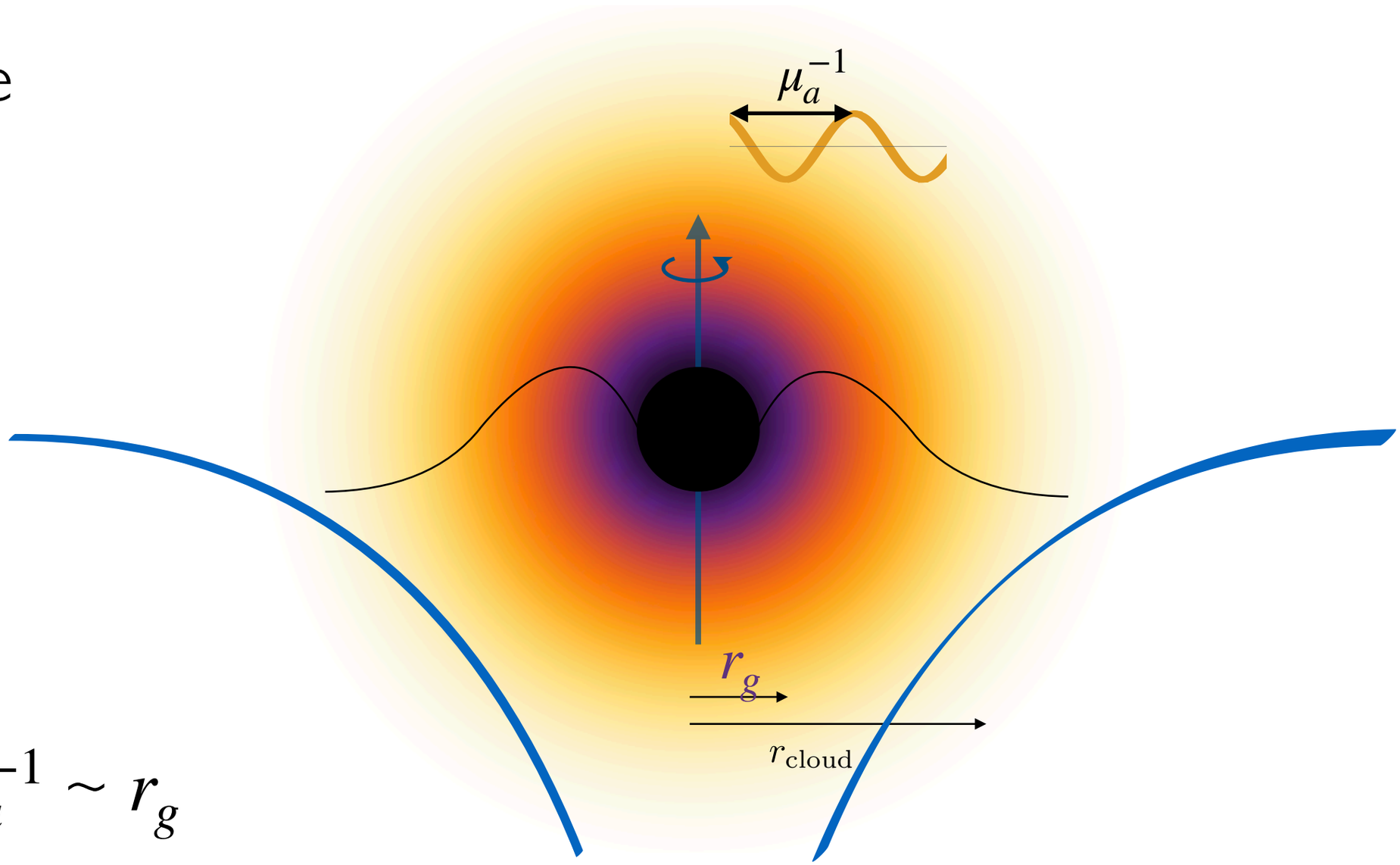

Zouros & Eardley'79; Damour et al '76; Detweiler'80; Gaina et al '78

Arvanitaki, Dimopoulos, Dubovsky, Kaloper, March-Russell 2009; Arvanitaki, Dubovsky 2010

Gravitational Atoms

Spin-0
Gravitational Atoms

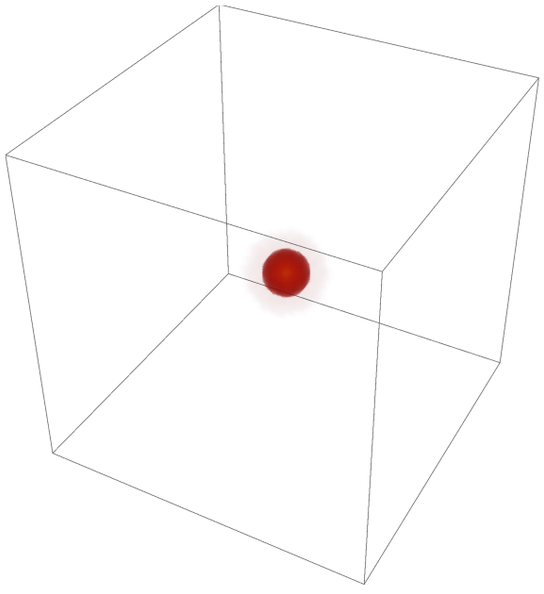

$n = 1, \ell = 0, m = 0$

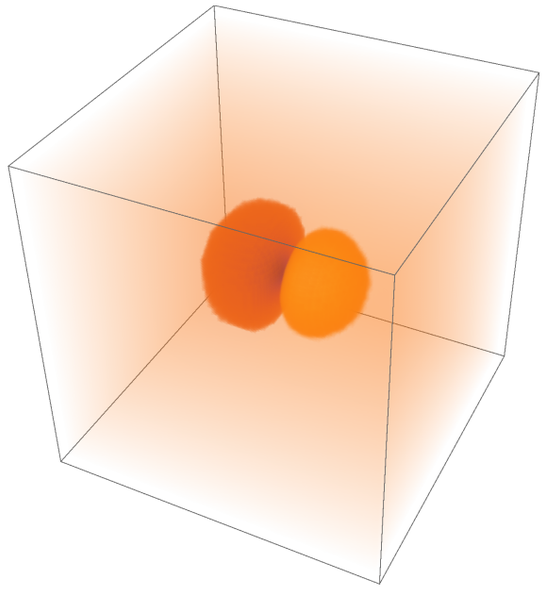

$n = 2, \ell = 1, m = 1$

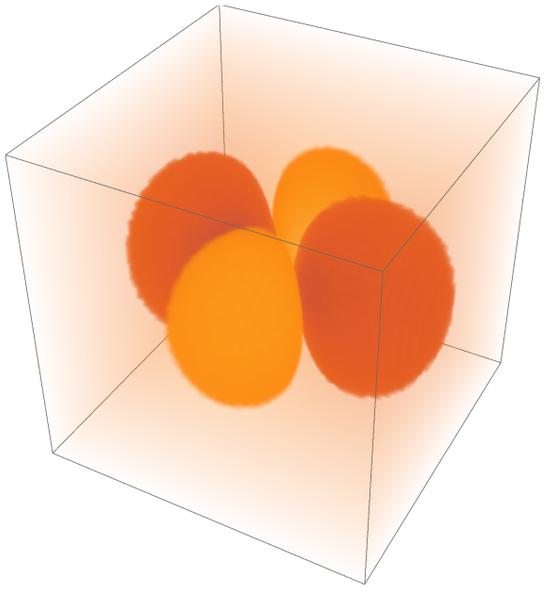

$n = 3, \ell = 2, m = 2$

Far from black hole,
`hydrogenic' potential a
good approximation

$$r \gg r_g \qquad V(r) = -\frac{G_{\rm N} M_{\rm BH} \mu_a}{r}$$

Gravitational Atoms

Spin-0
Gravitational Atoms

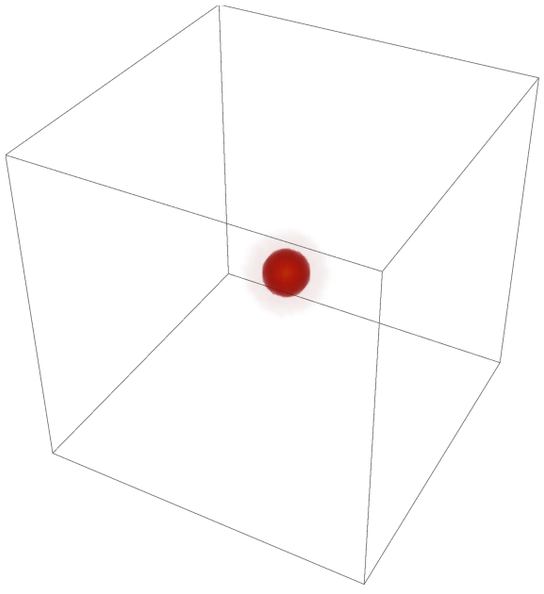

$n = 1, \ell = 0, m = 0$

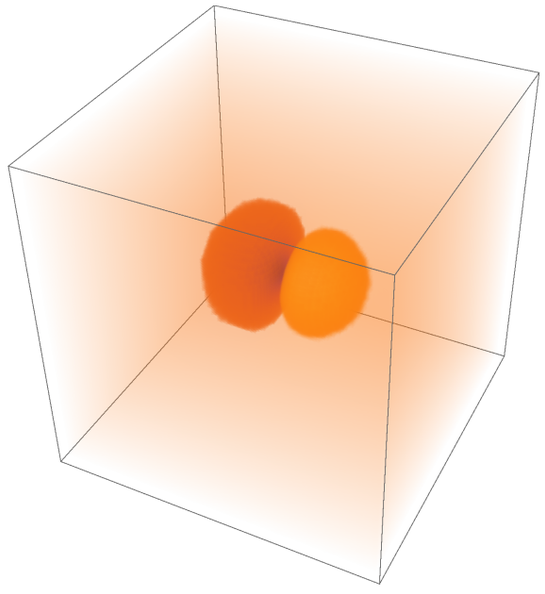

$n = 2, \ell = 1, m = 1$

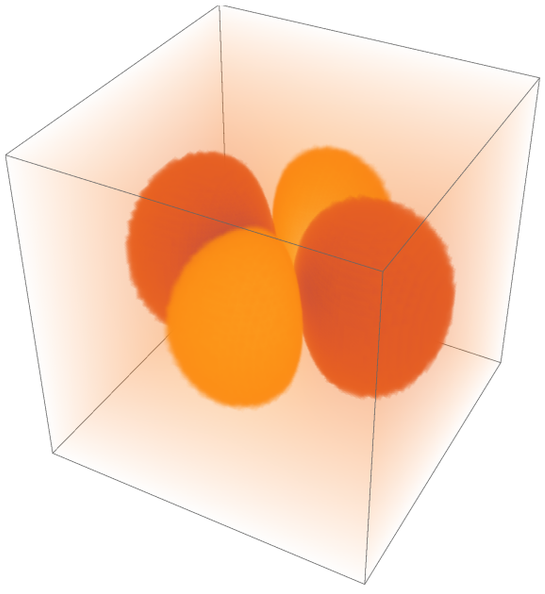

$n = 3, \ell = 2, m = 2$

Close to black hole, waves absorbed at the horizon

Ingoing boundary conditions give imaginary frequency: exponentially growing mode

$$E \simeq \mu \left(1 - \frac{\alpha^2}{2n^2} + i\Gamma_{\rm sr} \right)$$

Superradiance condition: angular frequency smaller than horizon angular frequency:

$$\frac{\mu_a}{m} < \Omega_{BH} \Rightarrow \Gamma_{sr} > 0$$

Gravitational Atoms: Spin-1

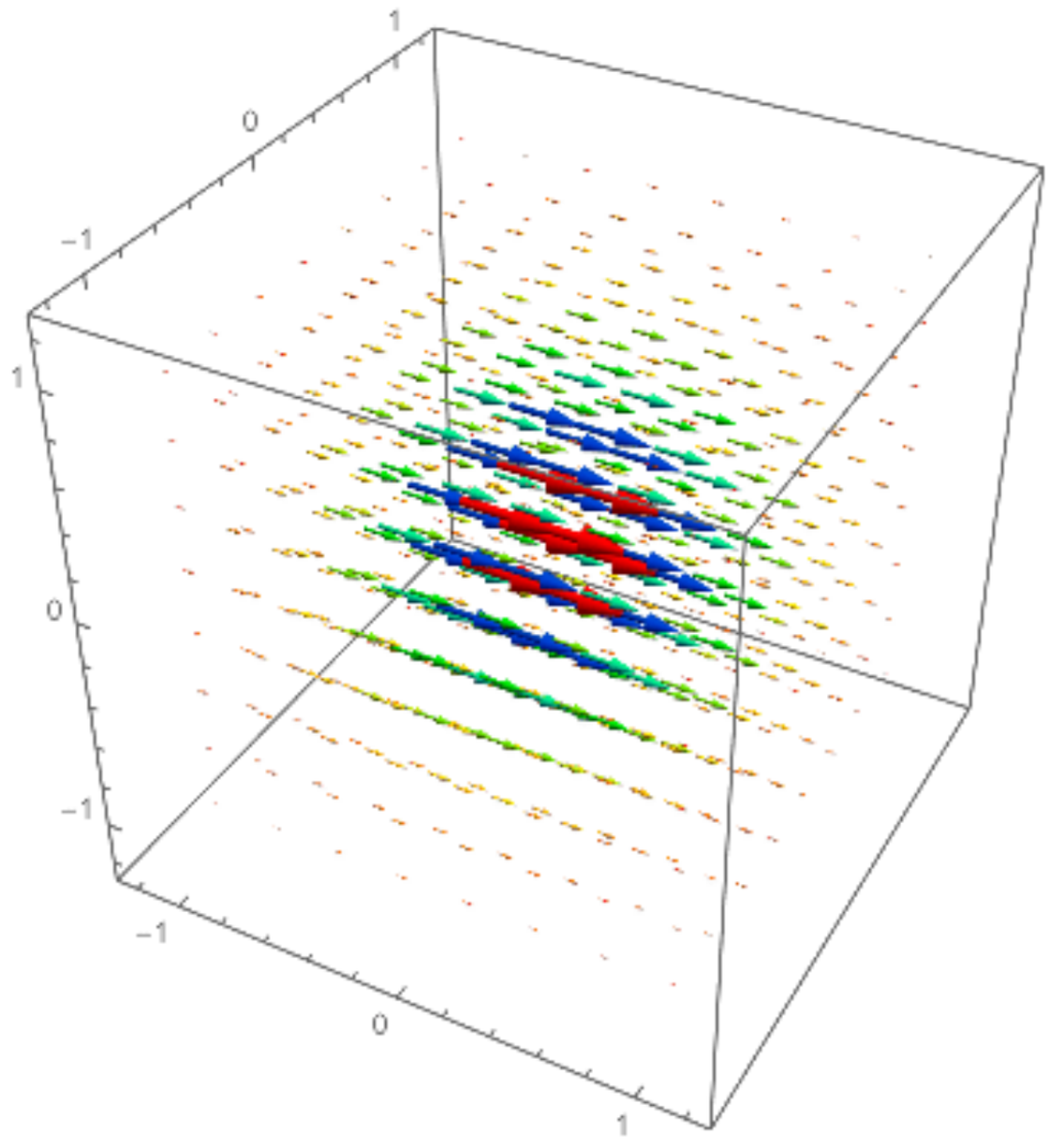

Mae Teo

Robert Lasenby

New massive vector fields (dark photons) can also superradiate: create different bounds states around the black hole

MB, R. Lasenby, M. Teo (2017)

Gravitational Atoms: Spin-1

Axion
Gravitational Atoms

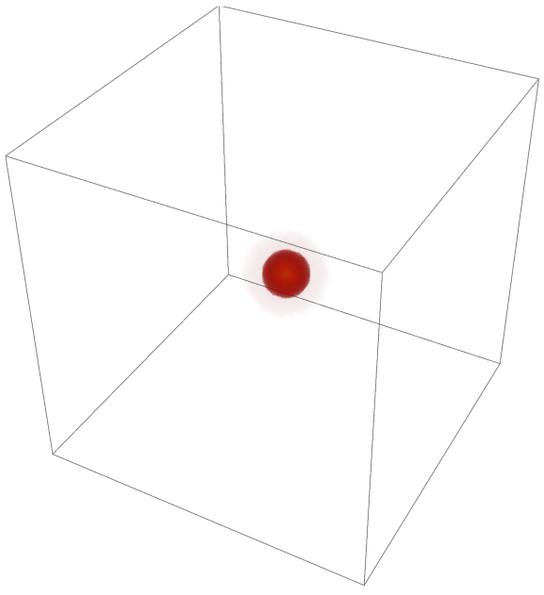

$n = 1, \ell = 0, m = 0$

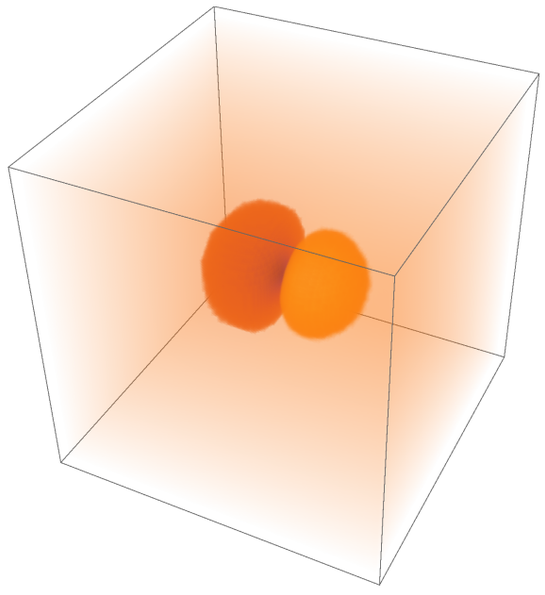

$n = 2, \ell = 1, m = 1$

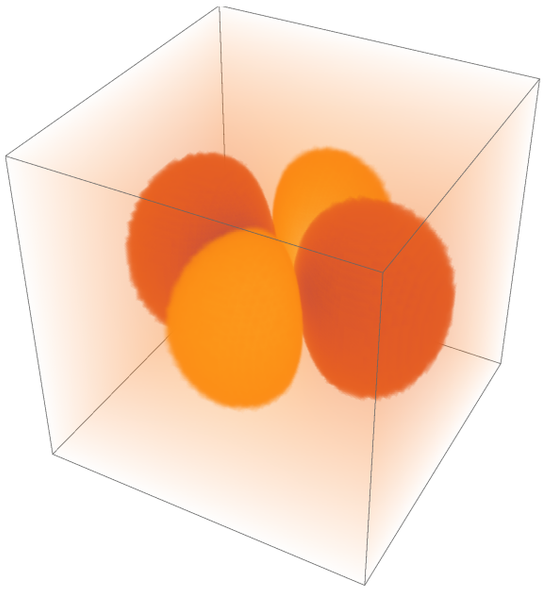

$n = 3, \ell = 2, m = 2$

Dark Photon
Gravitational Atoms

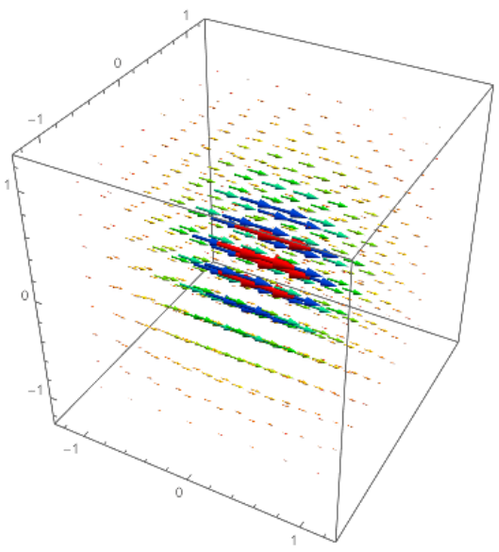

$n = 1, j = 1, \ell = 0, m = 1$

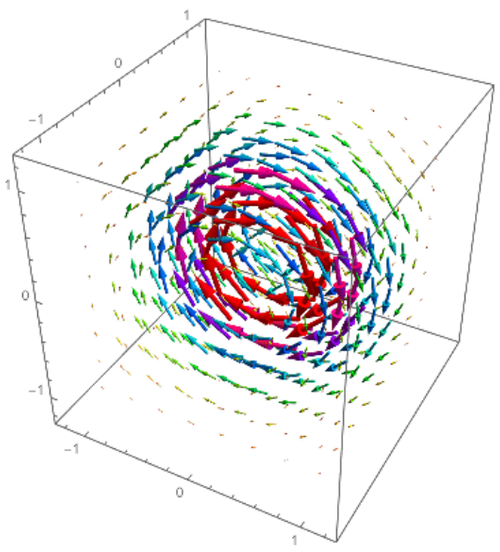

$n = 2, j = 1, \ell = 1, m = 1$

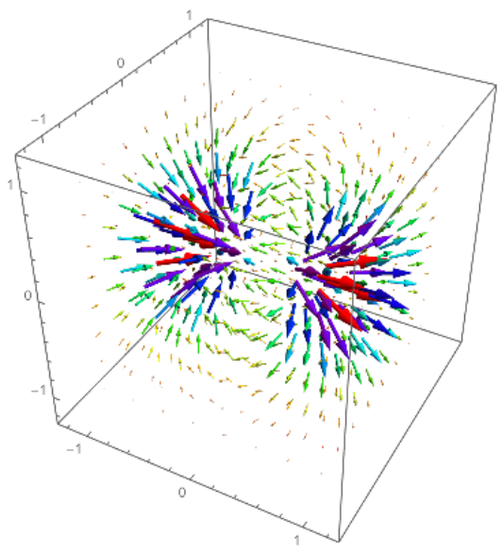

$n = 3, j = 1, \ell = 2, m = 1$

MB, R. Lasenby, M. Teo (2017)

Hydrogen-like radial profile, vector spherical harmonic angular:
localized closer to the black hole for the same total angular momentum

Black hole growing cloud

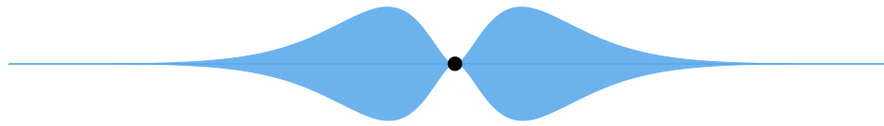

- BH spins down and fastest-growing level is formed
- Once BH angular velocity matches that of the level, growth stops

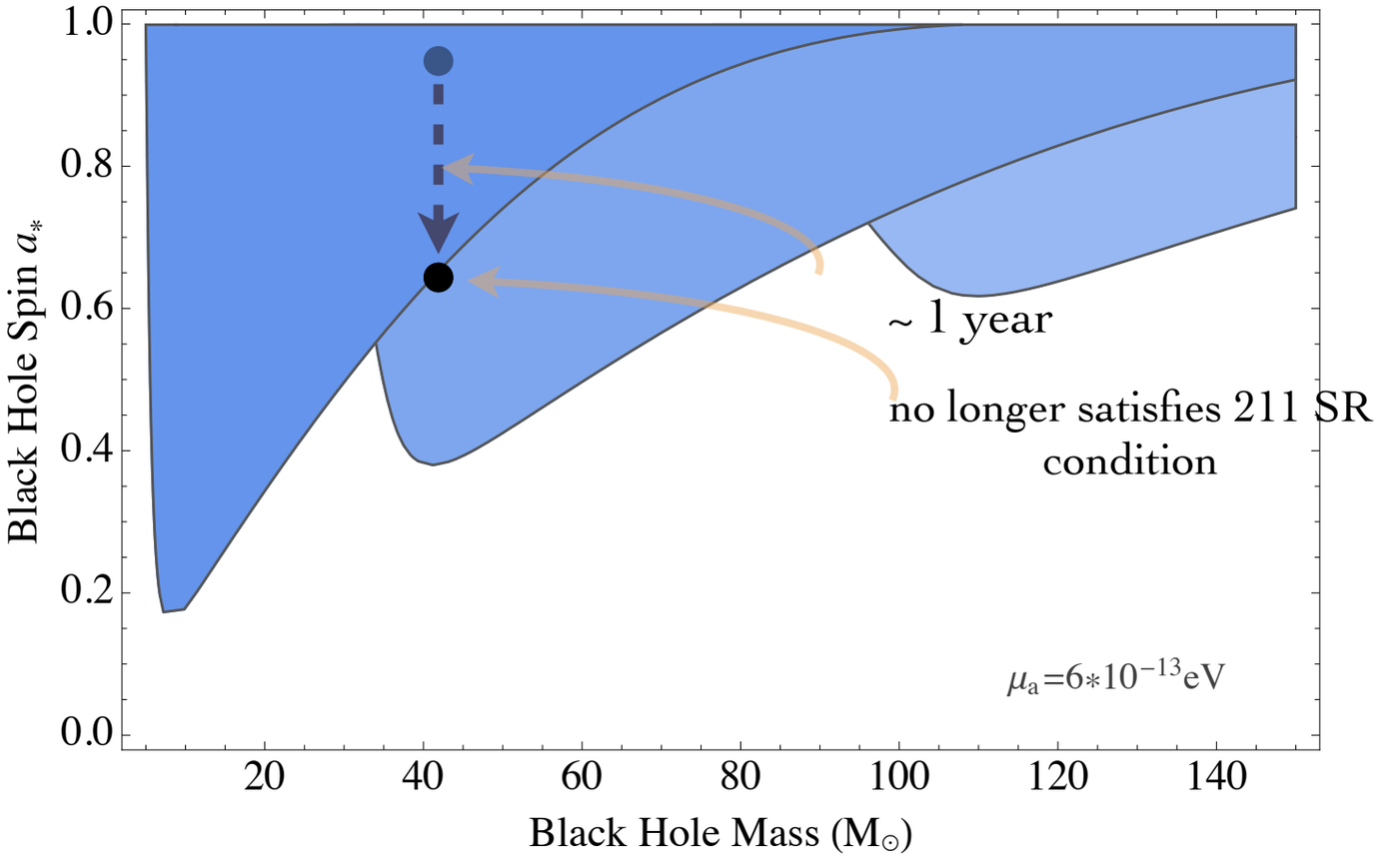

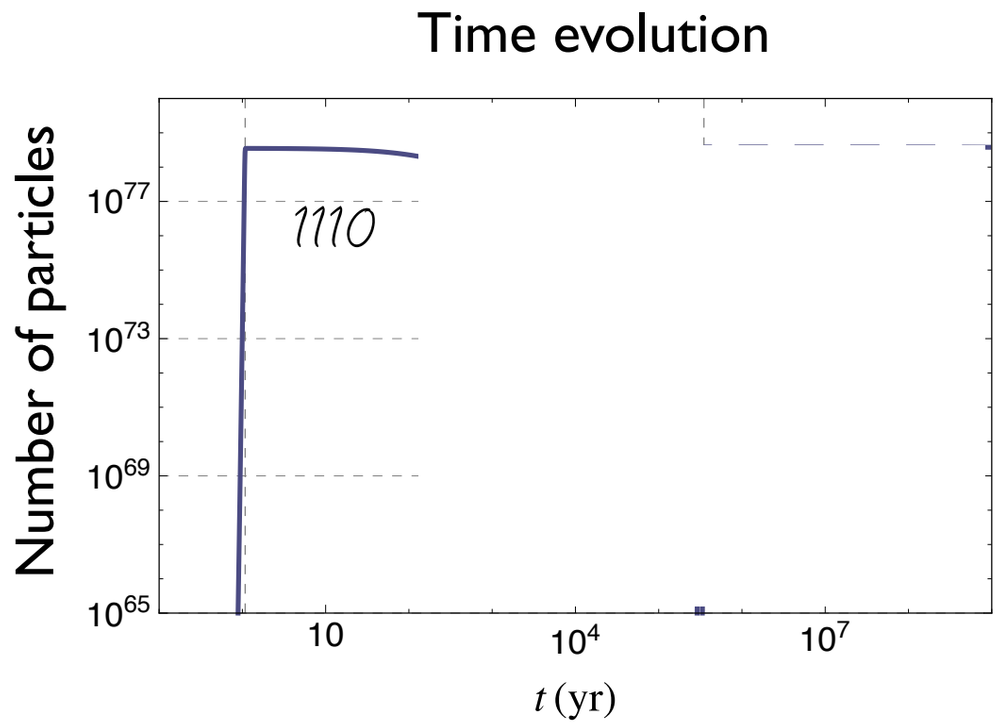

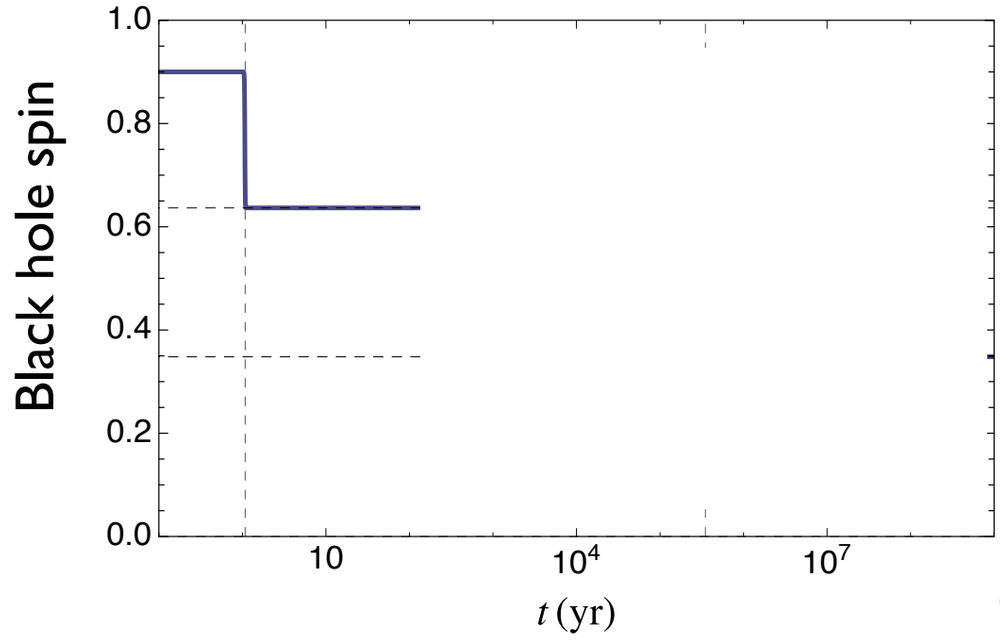

Black hole growing cloud

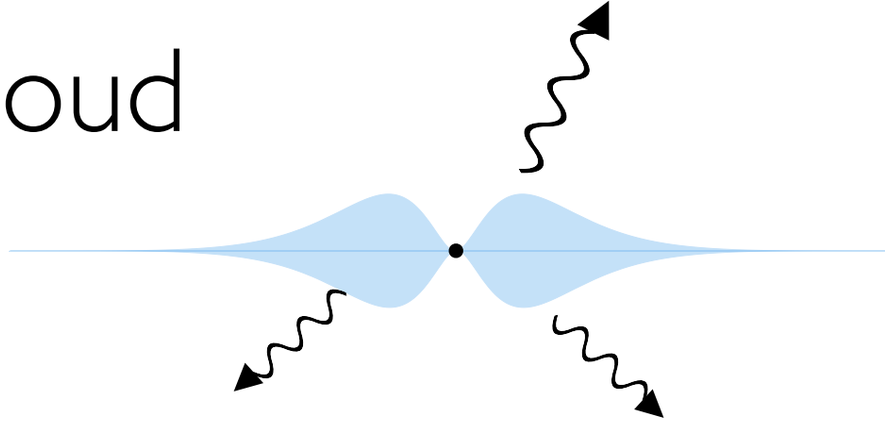

- Large energy density in the cloud, with time dependence set by the axion mass
- Annihilation to gravitational waves depletes the cloud on intermediate timescales

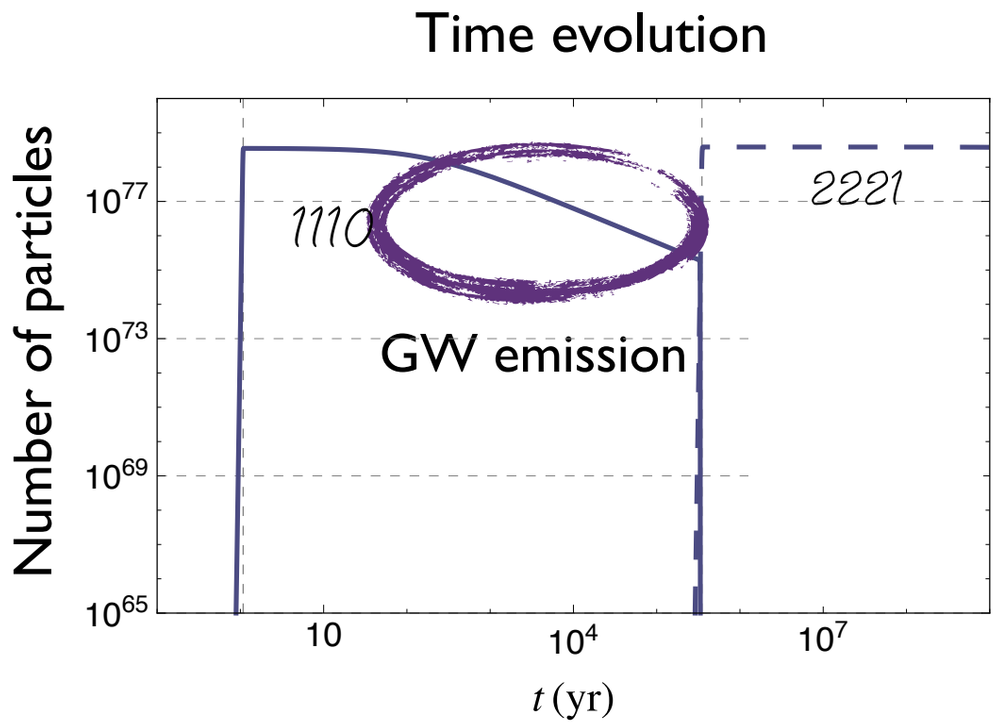

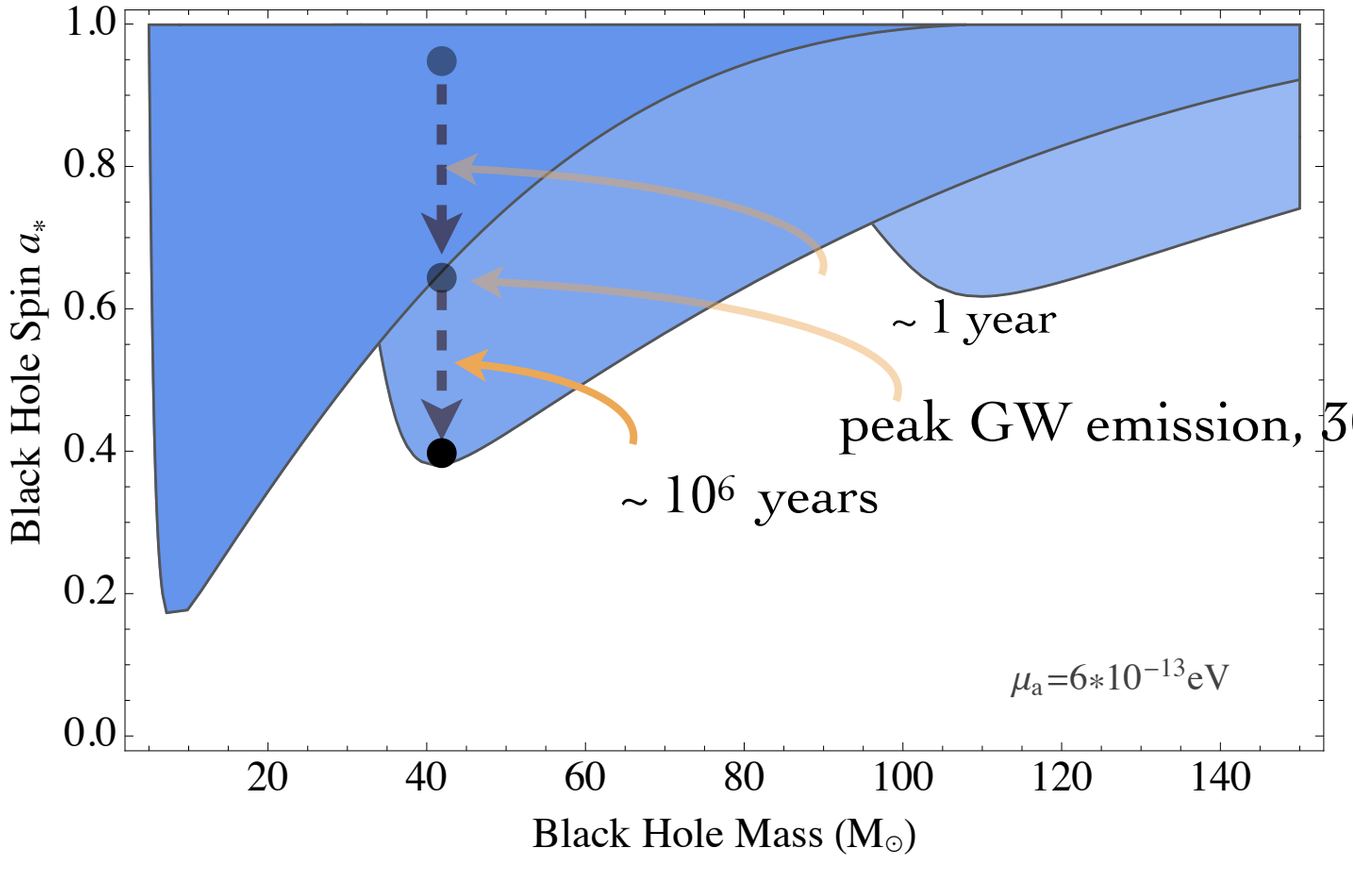

Gravitational Wave Signals

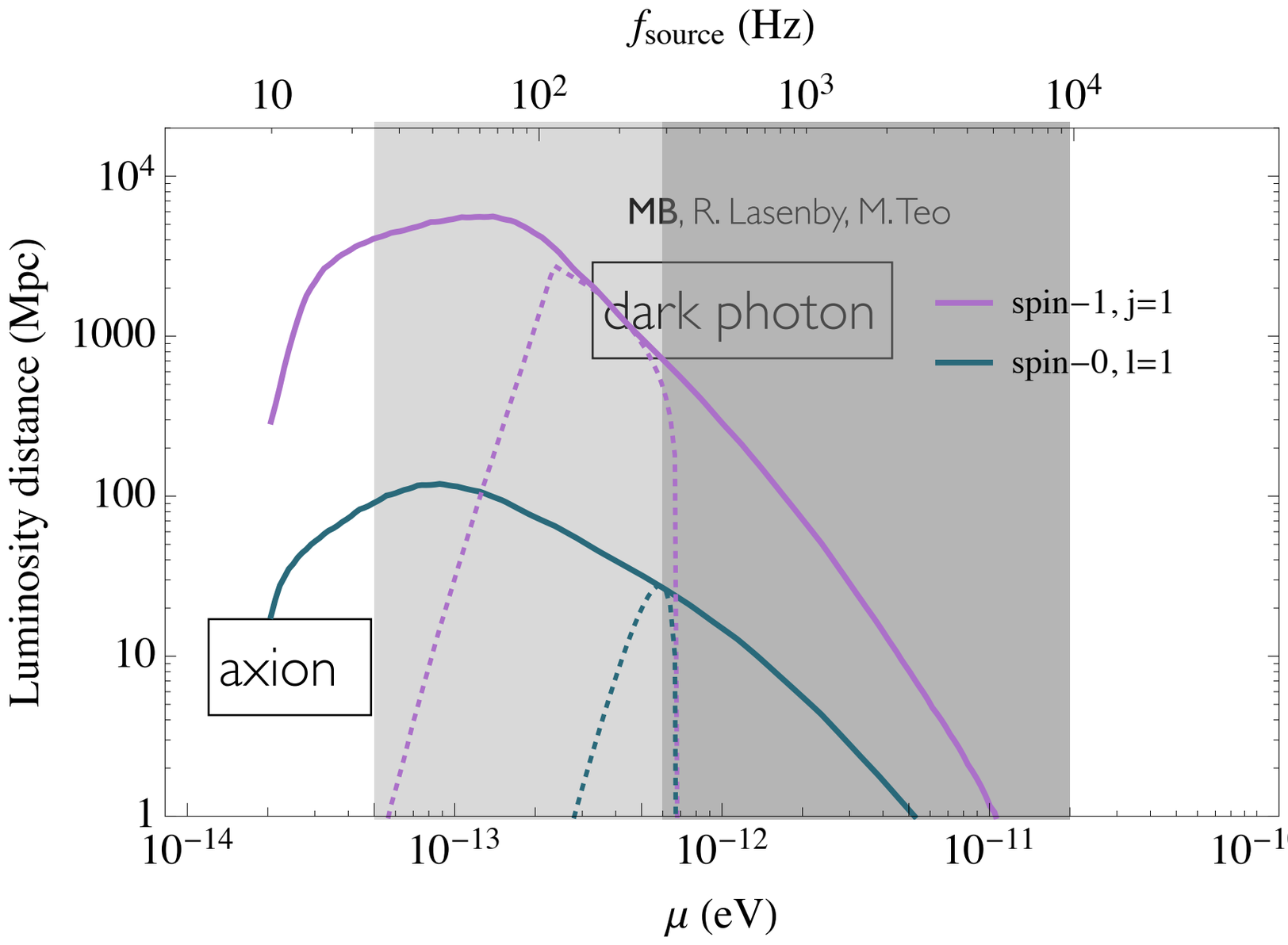

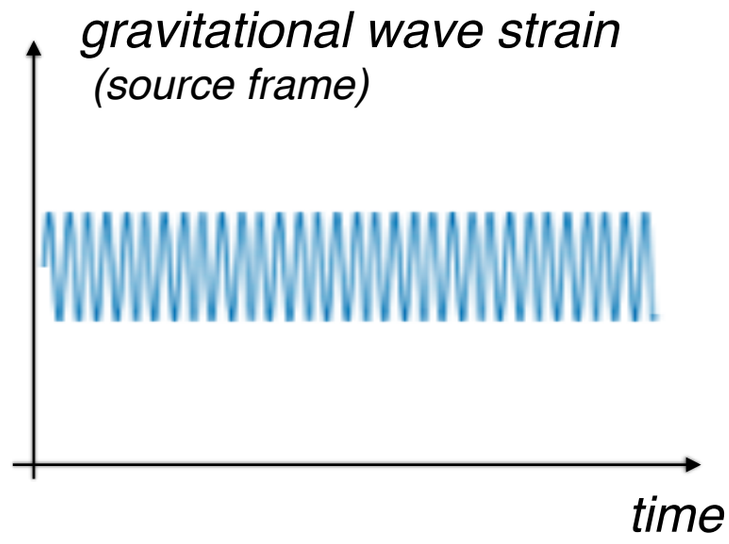

Time-varying energy density sources gravitational waves:
two bosons annihilating into gravitational waves

- coherent and monochromatic
- could be seen in follow-ups to mergers in the next LVK observing run

Mixed Superradiance

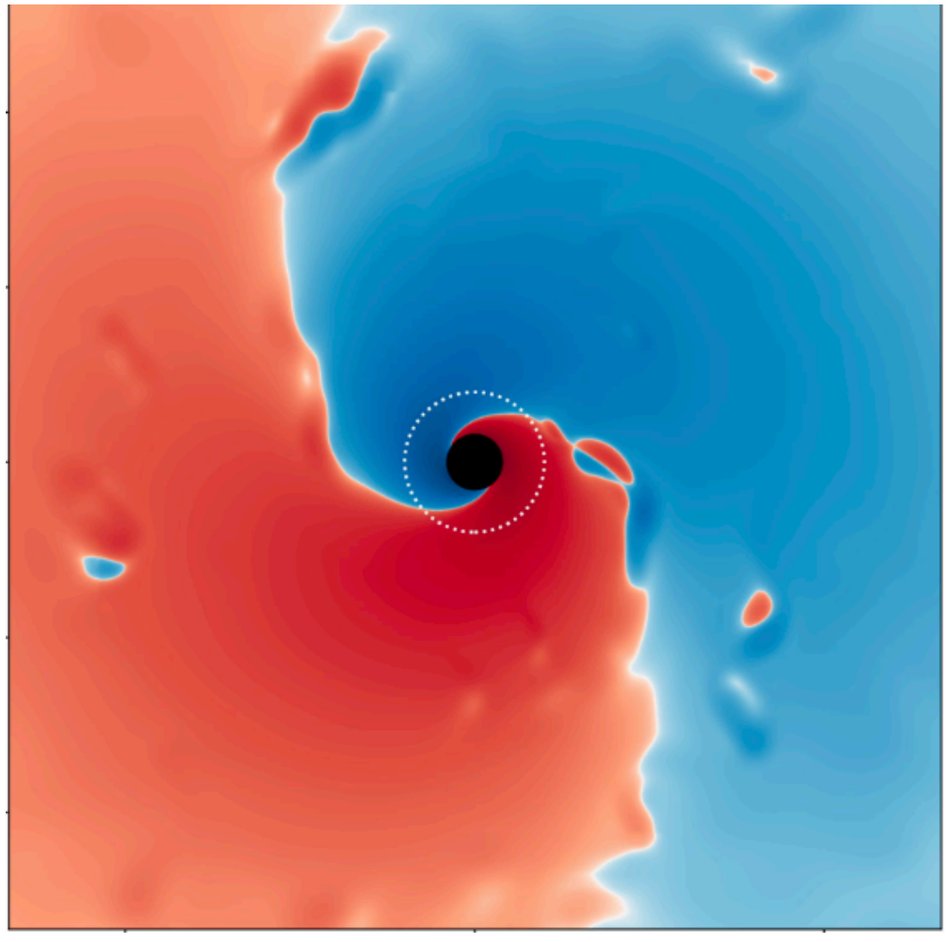

Nils Siemonsen

Cristina Mondino

Daniel Egana-Ugrinovich

Junwu Huang

Will East

Siemonsen, Mondino, Egaña-Ugrinovic, Huang, Baryakhtar, East, PRD **107**, 075025 2023

Superradiance sets up dark electromagnetic fields with density close to neutron star matter density

Can lead to new multimessenger signals in the presence of Standard Model coupling

(Not So) Dark Photons

- Dark photon

Kinetic mixing parameter

$$\mathcal{S} = \int \mathrm{d}^4x \left(-\frac{1}{4} F'^{\mu\nu} F'_{\mu\nu} - \frac{1}{2} \mu^2 A'_\mu A'^\mu + \epsilon F^{\mu\nu} F'_{\mu\nu} \right)$$

- Effects:
  - The dark photon gives rise to dark E&M fields
  - Dark E&M fields couple to electrons with a suppressed charge

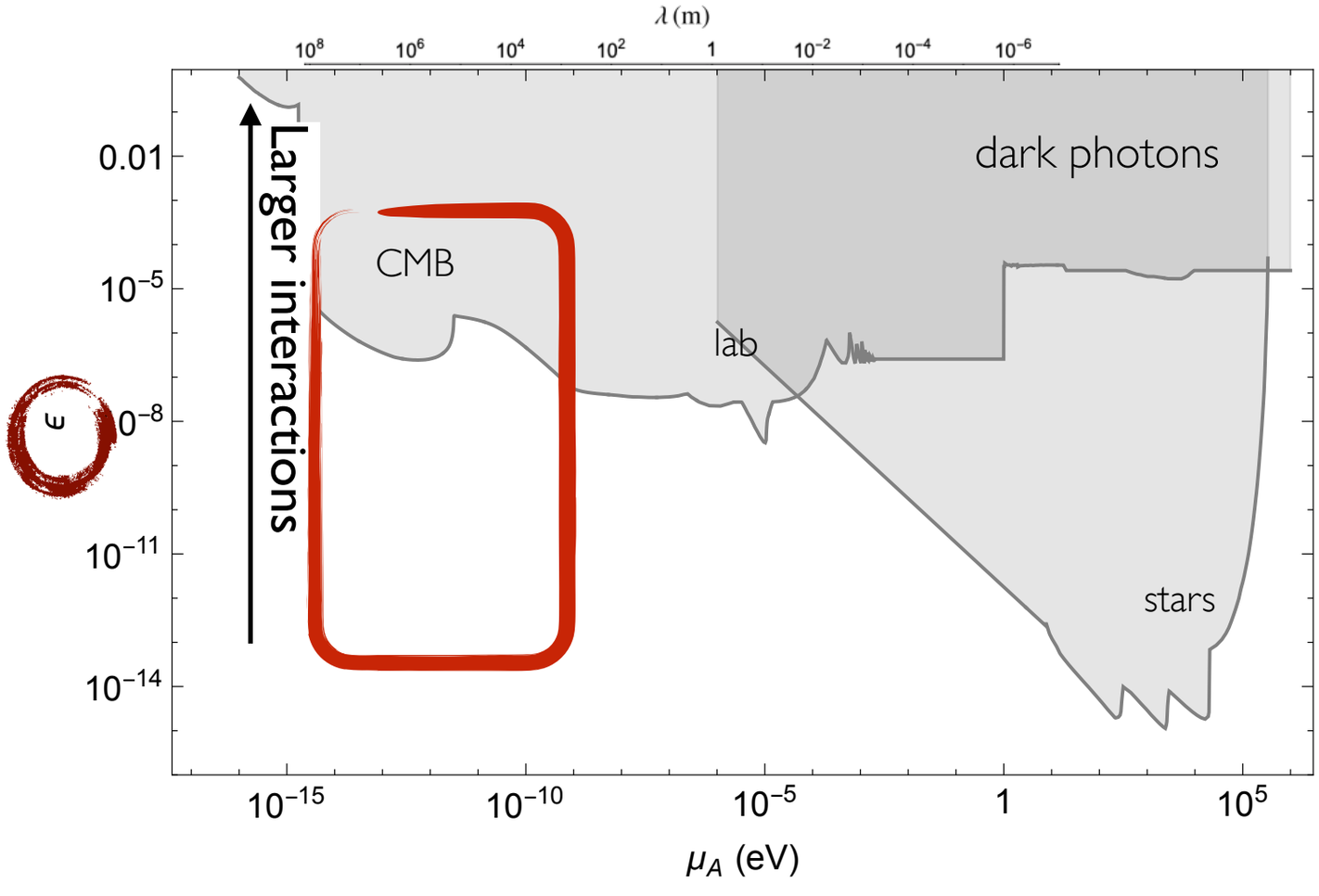

Okun 1982, Holdom 1985

Black Hole Generates Dark Photon Cloud

Large, rotating electric field

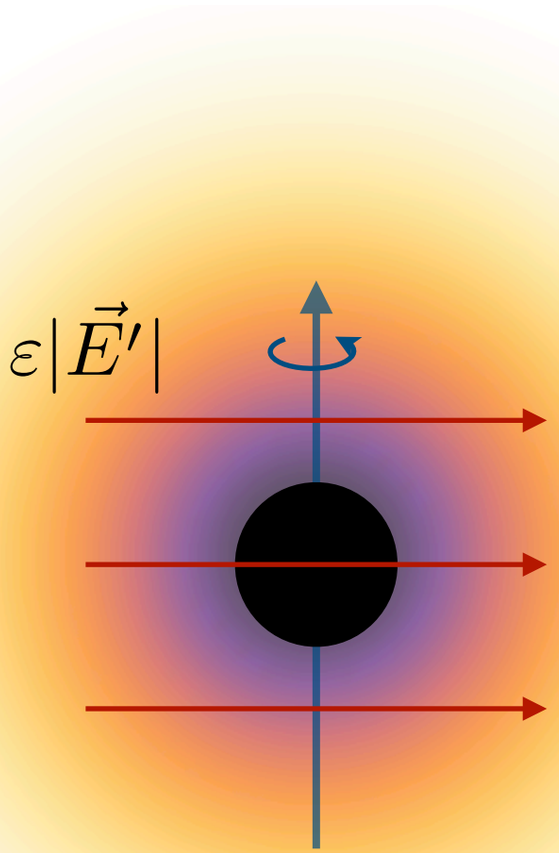

$$\epsilon E' = \epsilon B'/\alpha \approx (10\,\mathrm{keV})^2 \approx 10^{10}\,\mathrm{Gauss}\left(\frac{\epsilon}{10^{-6}}\right)\left(\frac{\alpha}{0.1}\right)^{5/2}$$

$$R_C = \frac{1}{\alpha\mu} = \frac{GM_{\mathrm{BH}}}{\alpha^2} \approx 150\,\mathrm{km}\left(\frac{M_{\mathrm{BH}}}{M_\odot}\right)$$

$$\epsilon E' \cdot R_C = 10^{10}\,\mathrm{GeV}$$

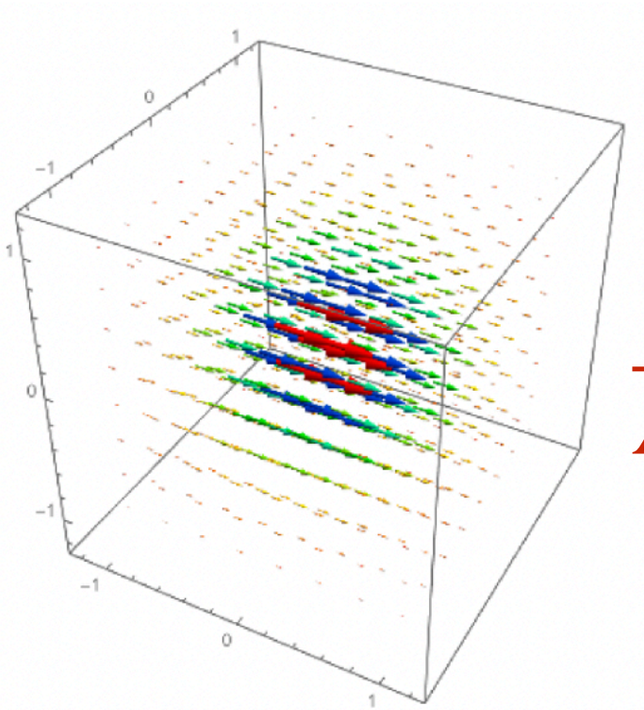

$\vec{A}'(\vec{x}, t)$

$$\vec{A}'(t) \to \vec{E}', \vec{B}' \to \begin{cases} \vec{E} = \epsilon\vec{E}', \\ \vec{B} = \epsilon\vec{B}' \end{cases}$$

Runaway particle production

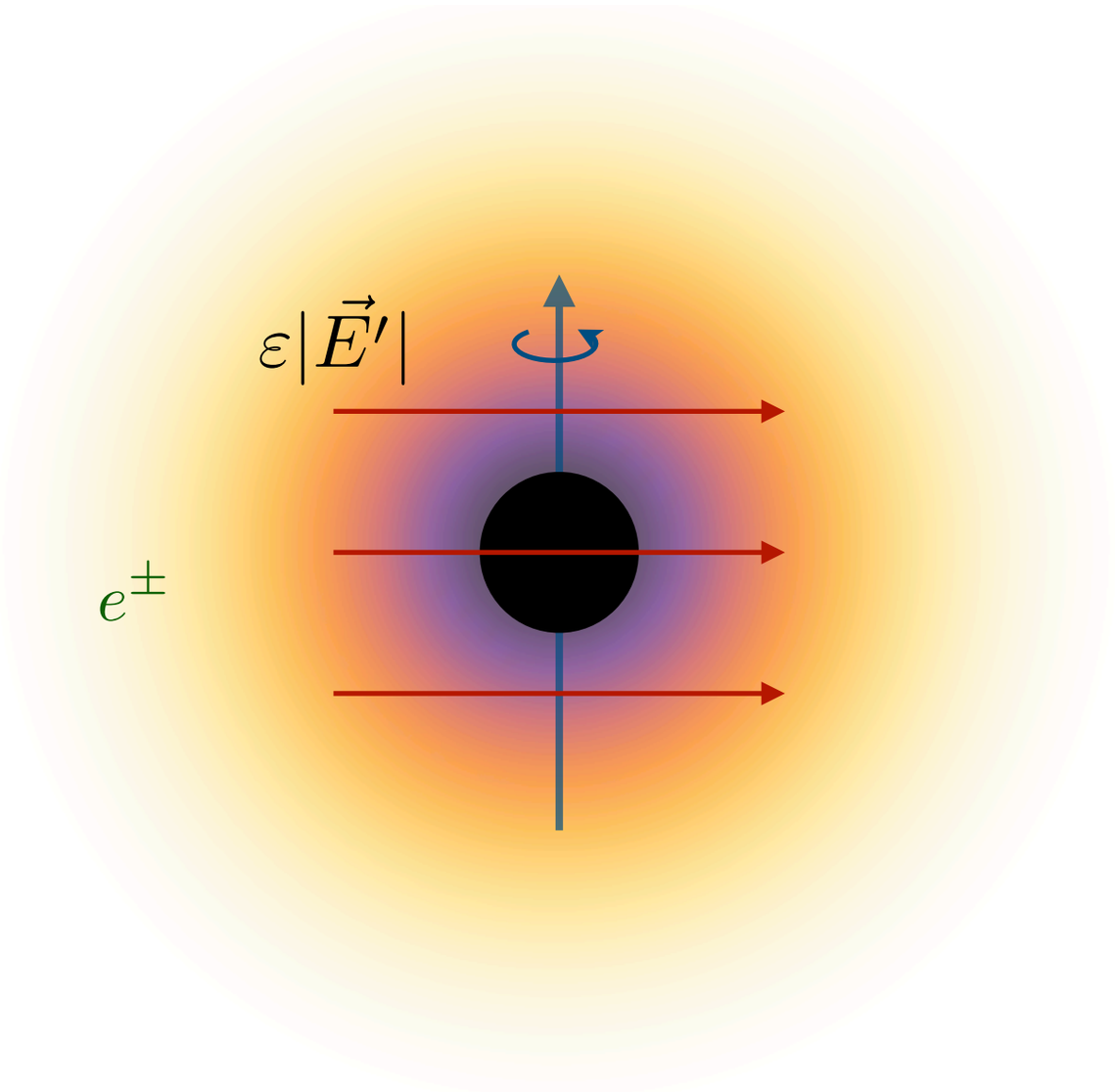

- As cloud grows, the electrons in the black hole neighborhood get accelerated to relativistic speeds and begin to radiate

Runaway particle production

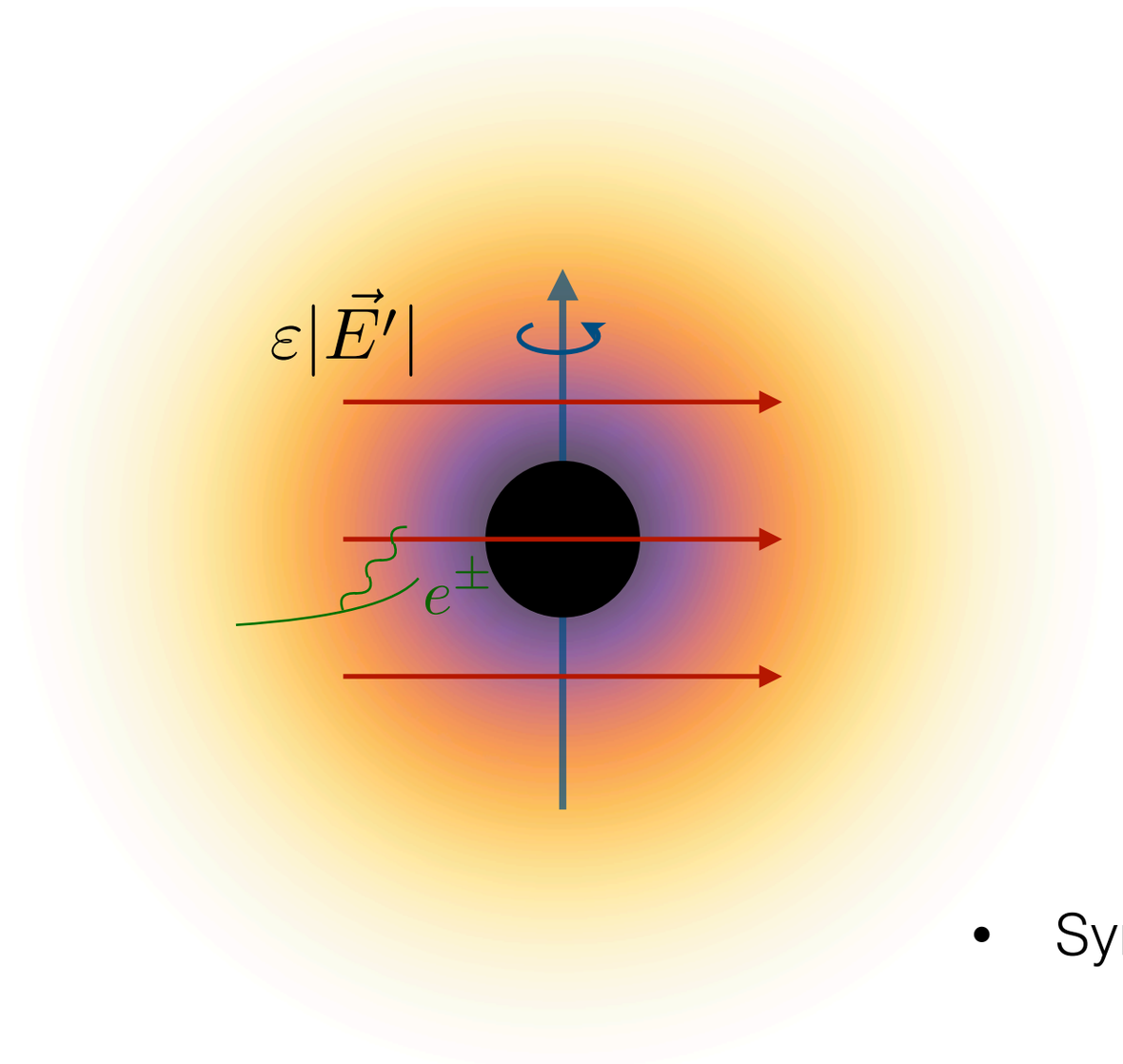

- As cloud grows, the electrons in the black hole neighborhood get accelerated to relativistic speeds and begin to radiate

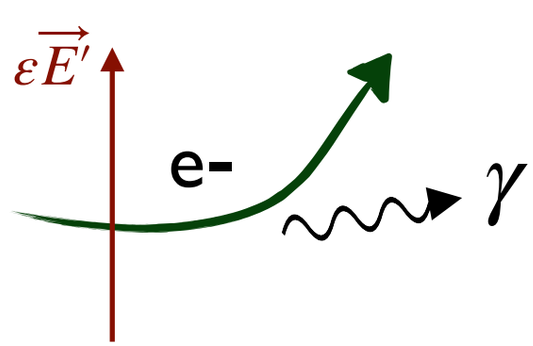

- Synchrotron

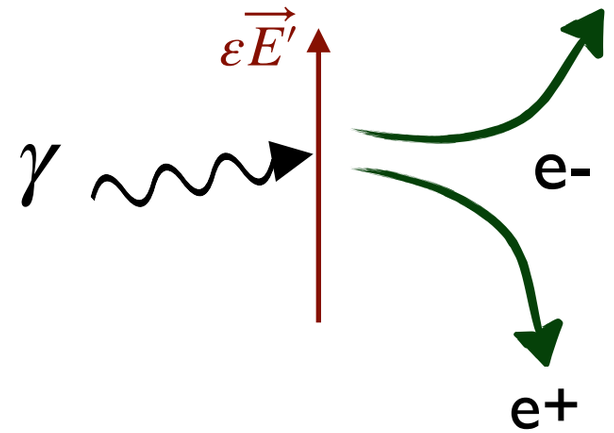

- Assisted Schwinger

Runaway particle production

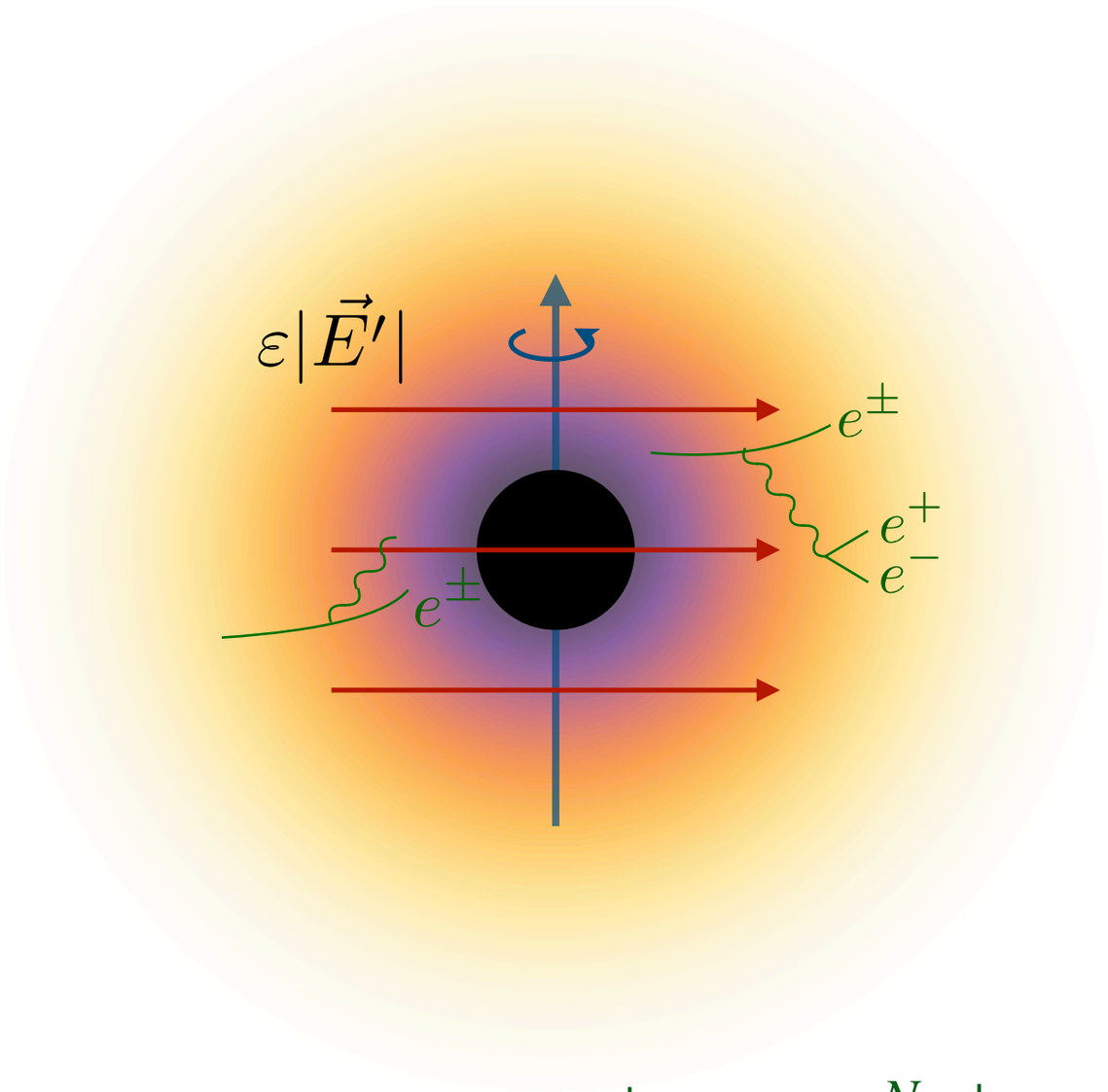

$$e^- \to e^-\gamma \to e^-e^+e^- \to 3^N e^{\pm}$$

- For large enough coupling, this results in a runaway cascade of particle production

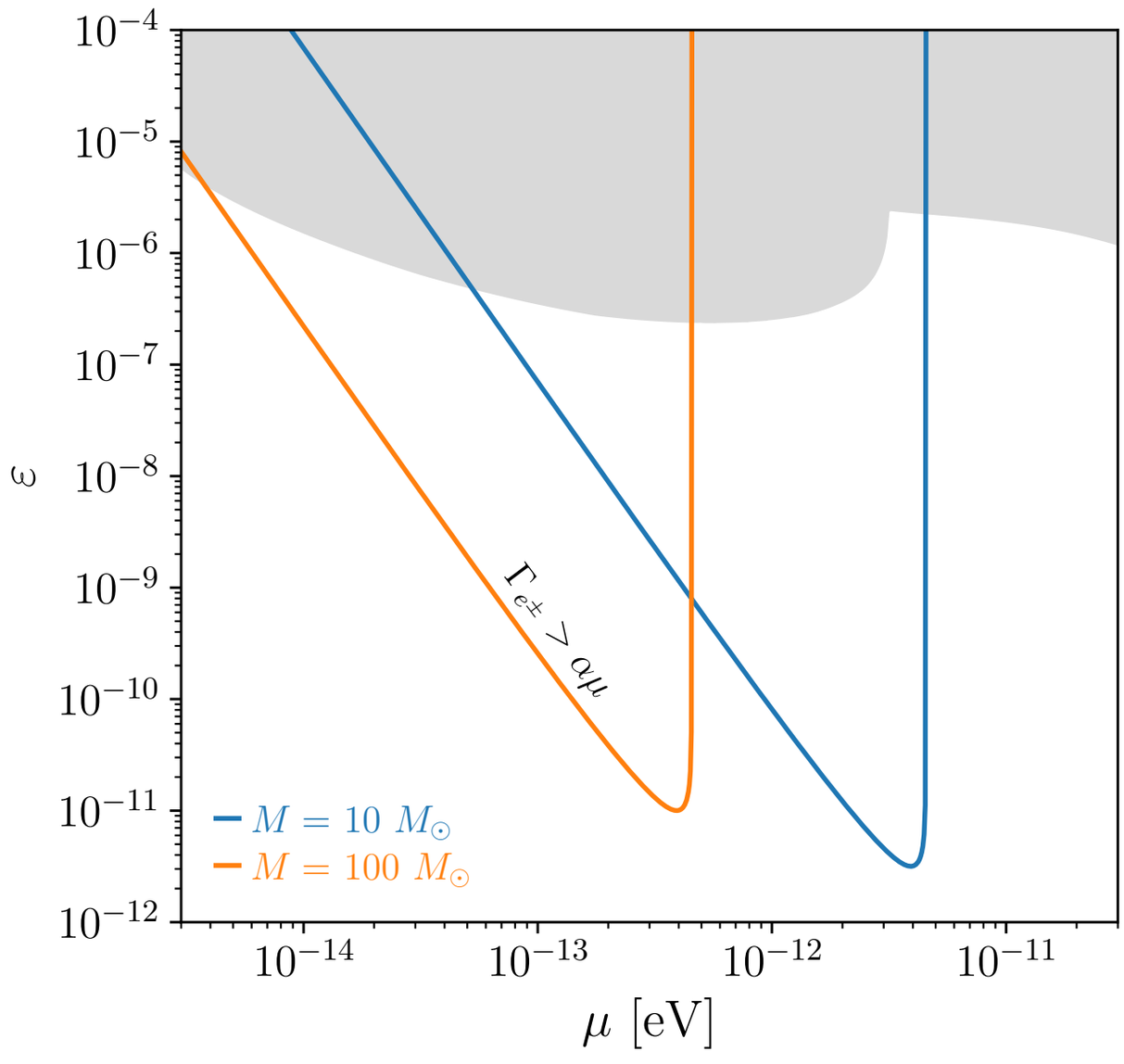

Large Plasma Density and Rotating Dipole Established

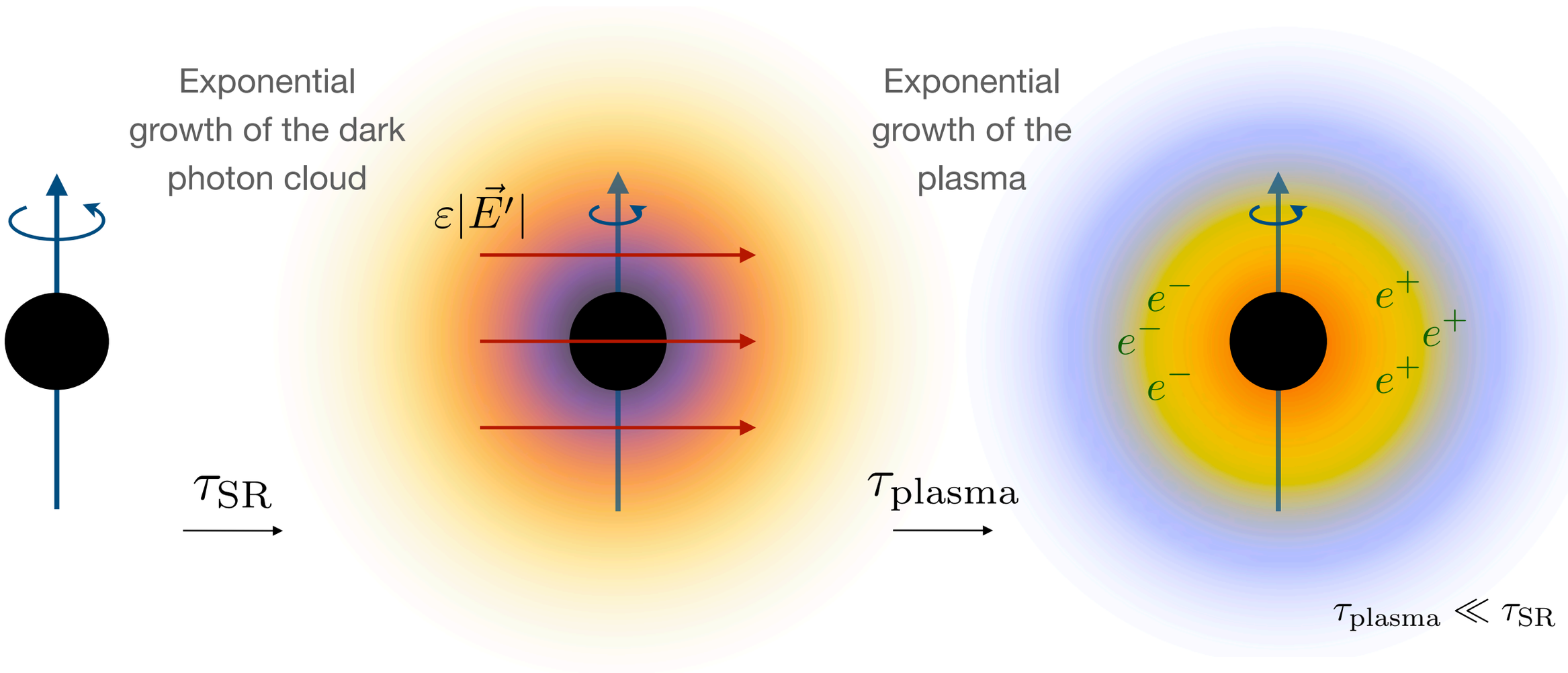

- As cloud grows, charged particles in the black hole neighborhood are accelerated to relativistic speeds and radiate
- For large enough coupling, get a cascade of particle production
- Charge density will try to screen the `visible' electric field, producing a rotating dipole $en_e \simeq \varepsilon \nabla \cdot \vec{E}'$

Comparison with a pulsar

Magnetosphere of neutron star pulsar

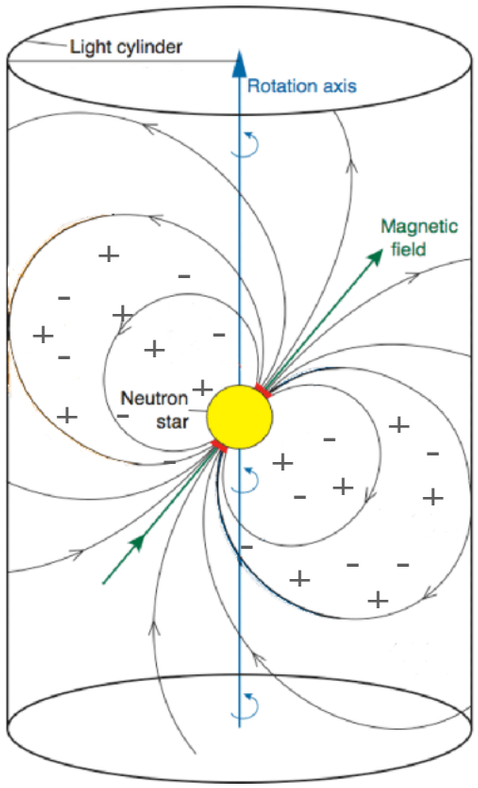

Black hole+dark photon cloud

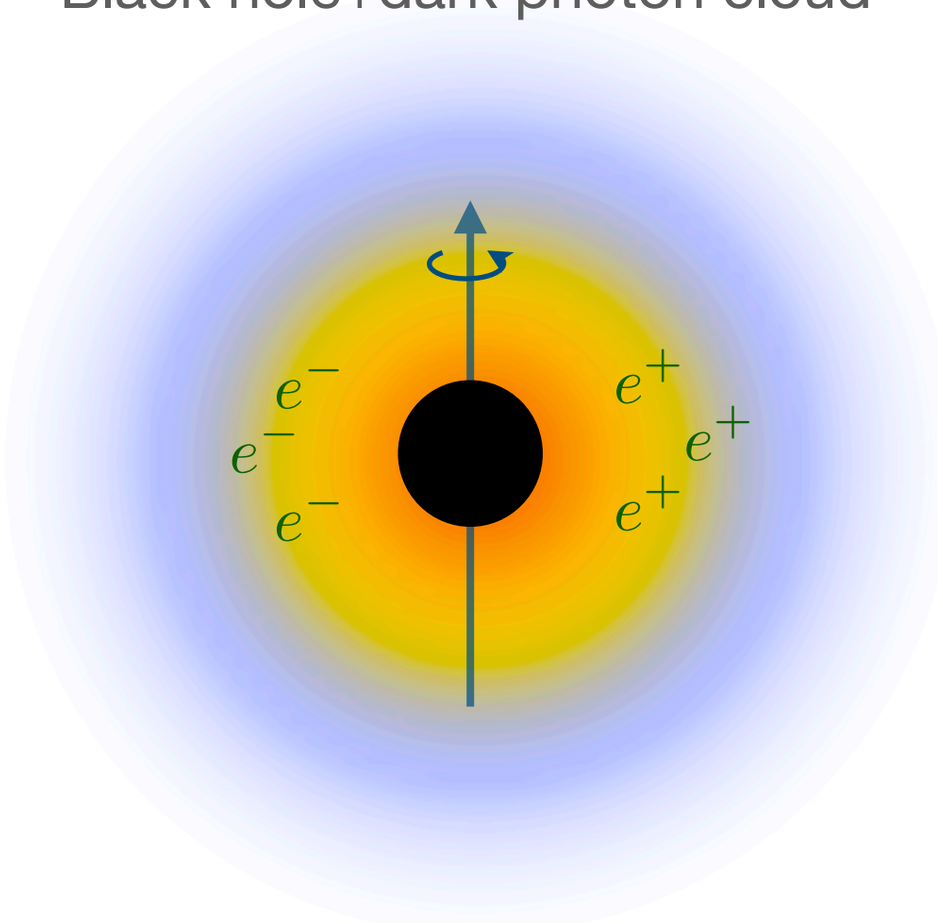

?

Comparison with a pulsar

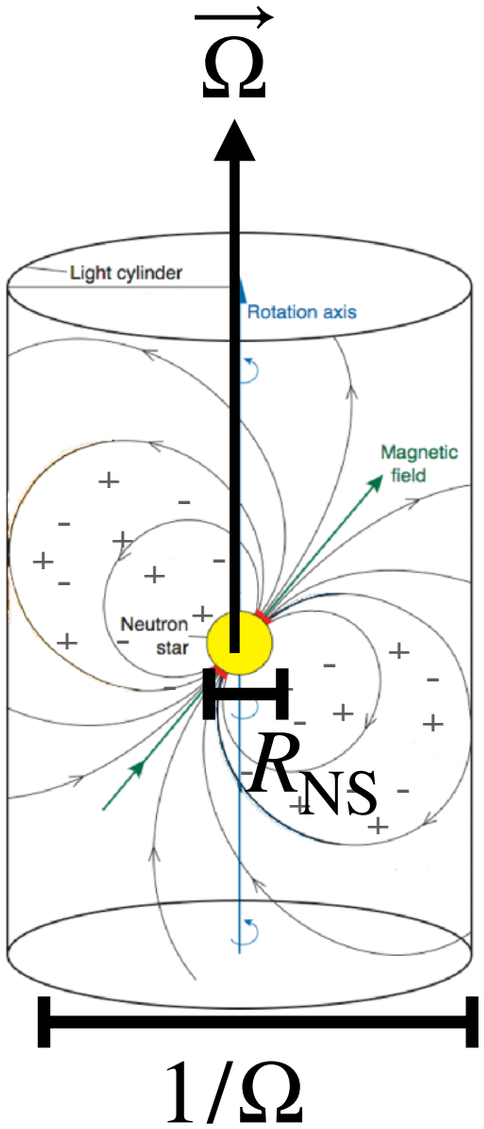

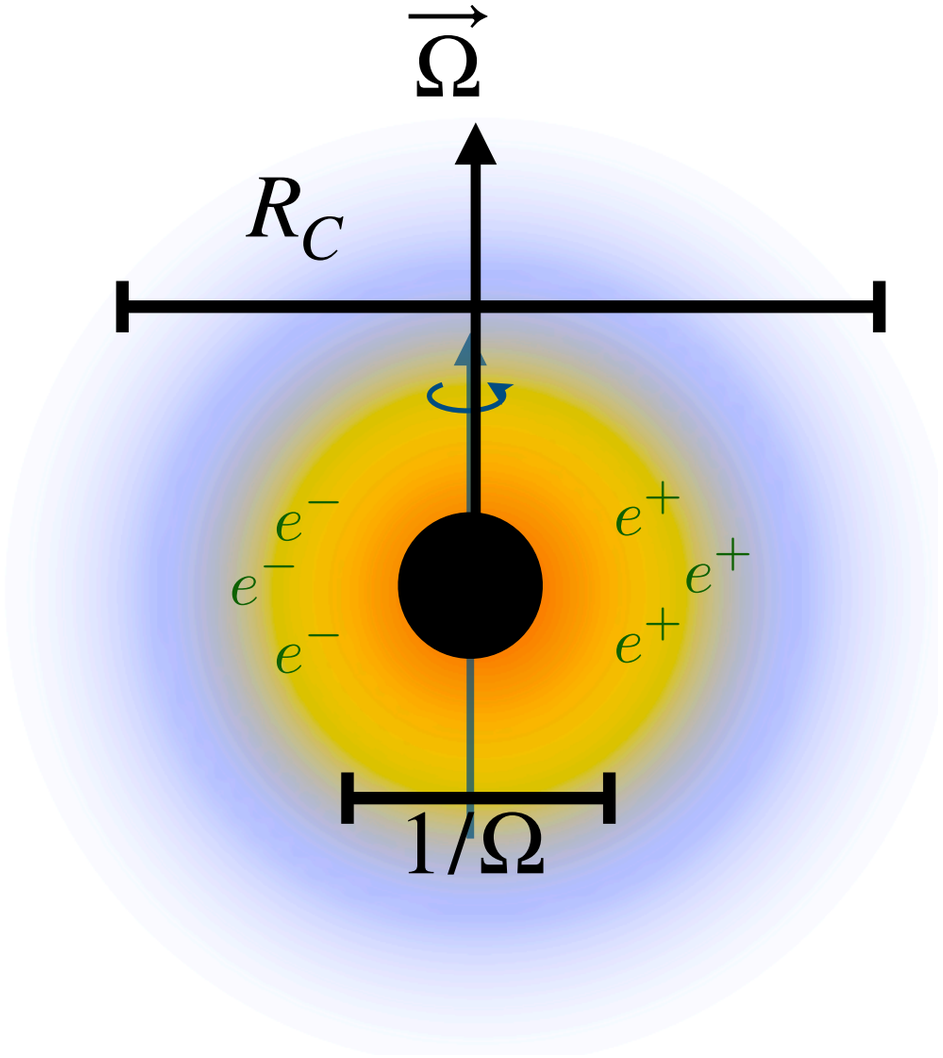

$\Omega \cdot R_{\rm NS} < 1$

$\Omega \cdot R_C = 1/\alpha > 1$

The black hole superradiance cloud is **larger** than the size of the light cylinder.

Comparison with a pulsar

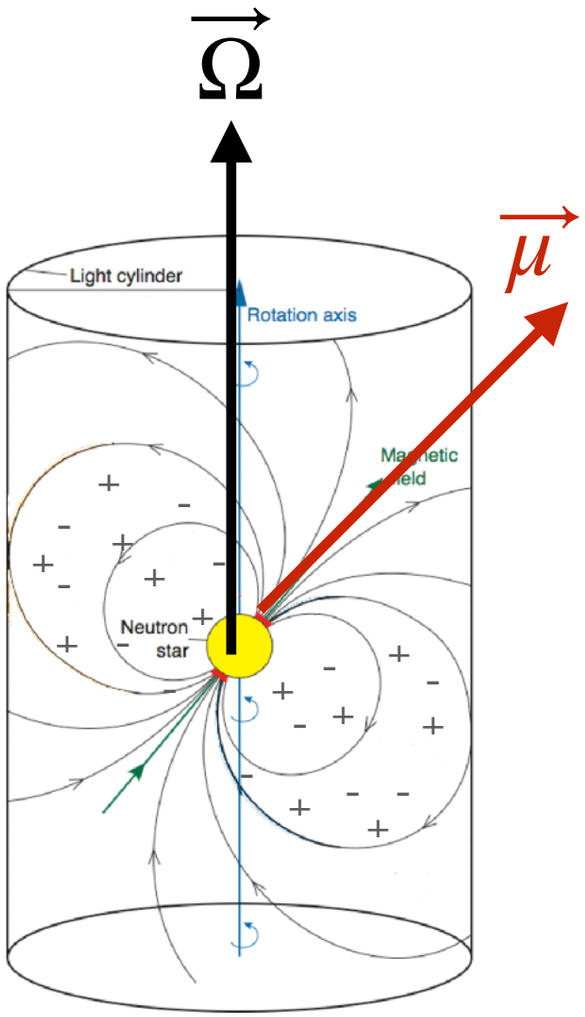

Magnetically dominated

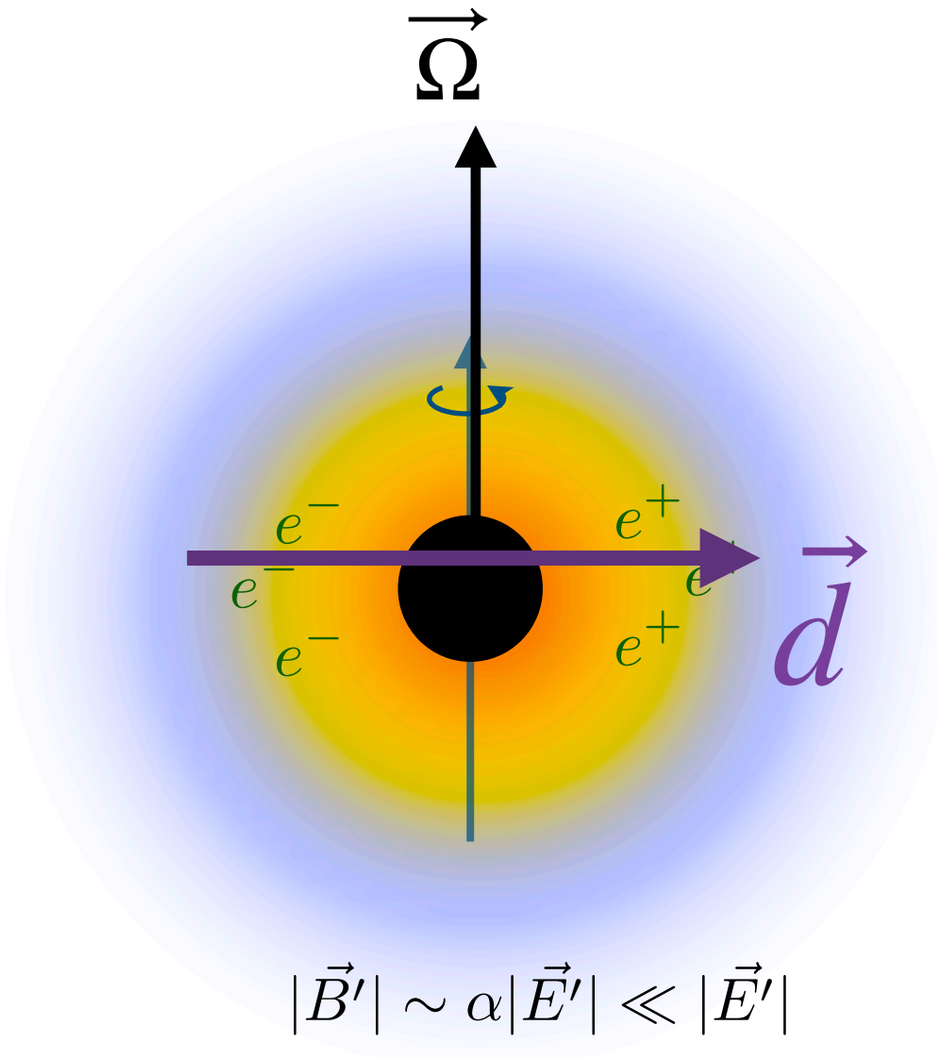

Electrically dominated

E field never vanishes → Dissipation is important

A new black hole `pulsar'

Adapt techniques from simulations of pulsar magnetospheres to simulate the electrodynamics of the dark photon cloud

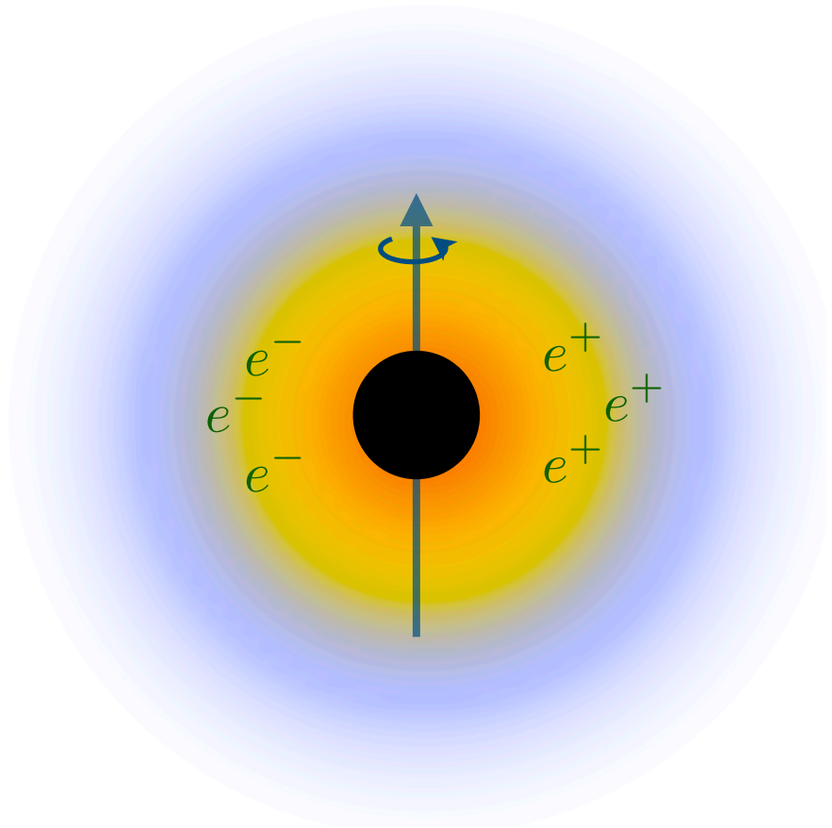

$$\partial_t \vec{B} = -\nabla \times \vec{E}$$

$$\partial_t \vec{E} = \nabla \times \vec{B} - \vec{J} - \epsilon\mu^2 \vec{A}'$$

Superradiance field (source)

Ohm's law $\vec{J} = \sigma(\vec{E} + \vec{v} \times \vec{B})$

- Solve equations for the E, B fields
- Compute EM energy emitted for $\sigma \gg \mu$ ($\sigma \to \infty$)

Nils Siemonsen

Full resistive magnetohydrodynamics simulation in Kerr BH background

Simulation: energy dissipation

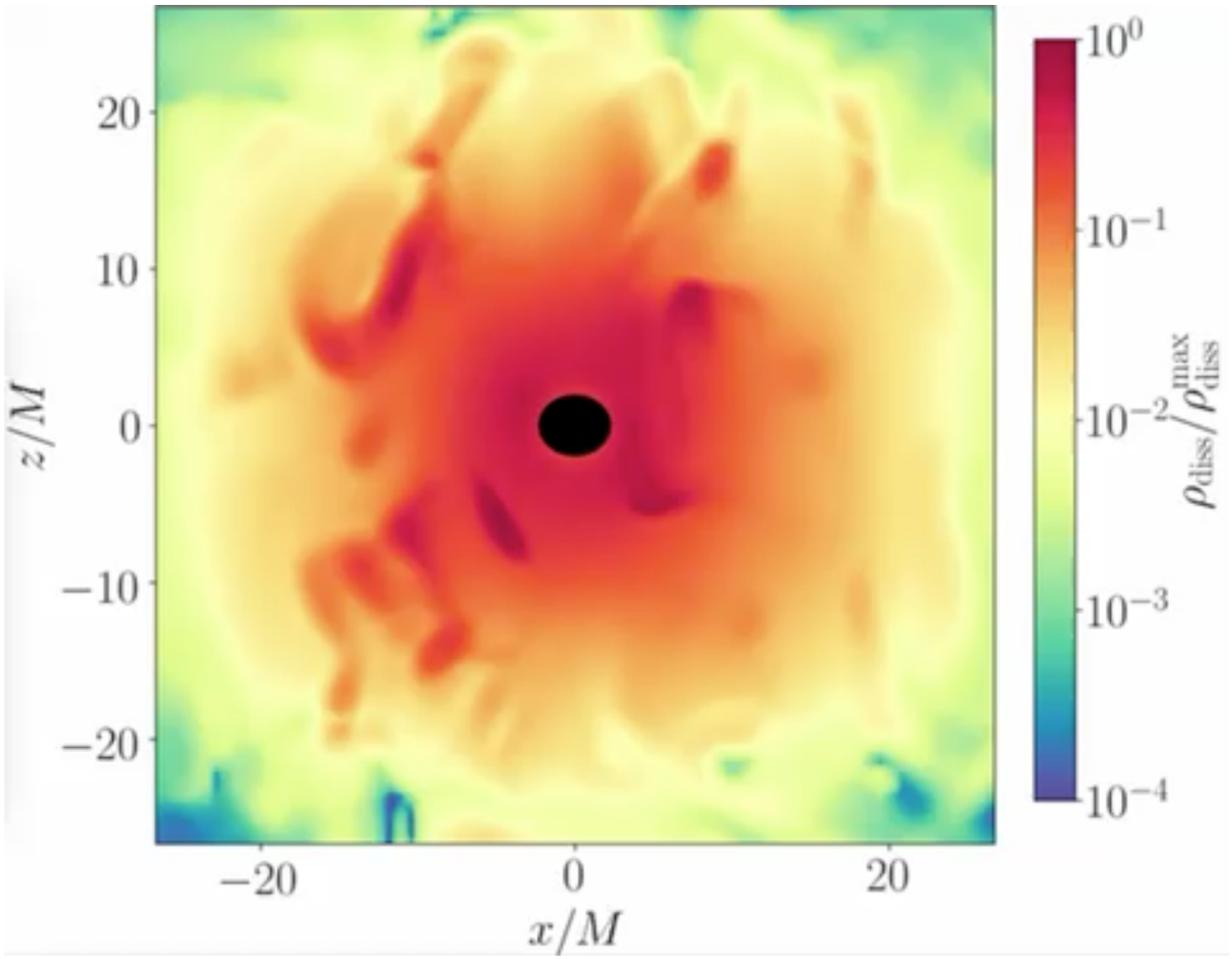

$$\rho_{\rm diss} = \vec{E} \cdot \vec{J}$$

Turbulent structure in the dissipative energy density!

Simulation: energy dissipation

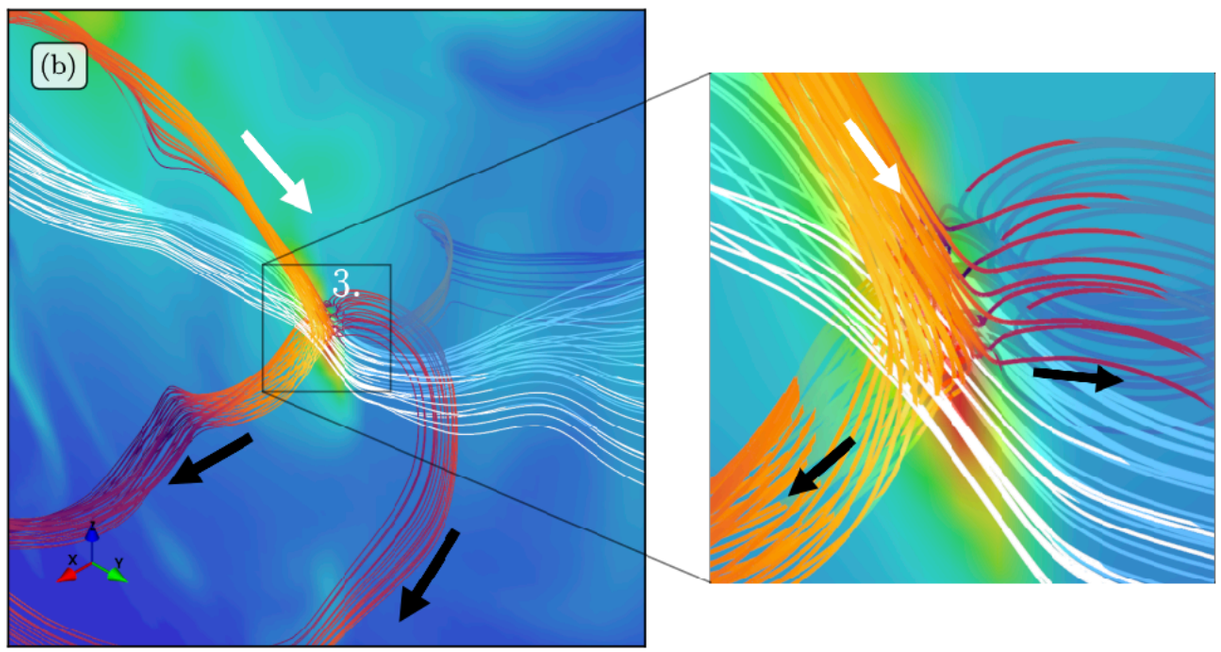

The dissipative energy density is maximal in the regions of magnetic field lines reconnection.

Field energy dissipated into particle acceleration and high energy emissions

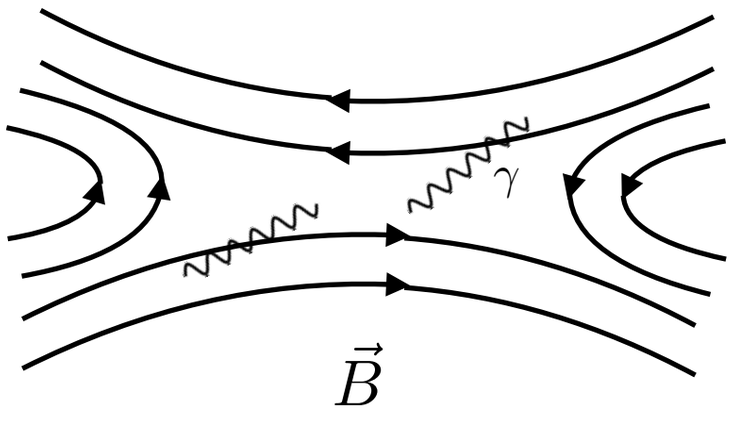

- Discontinuity in the magnetic field lines
- In a **neutron star pulsars** it happens on the equatorial plane (2d structures “current sheets”)

Simulation: luminosity

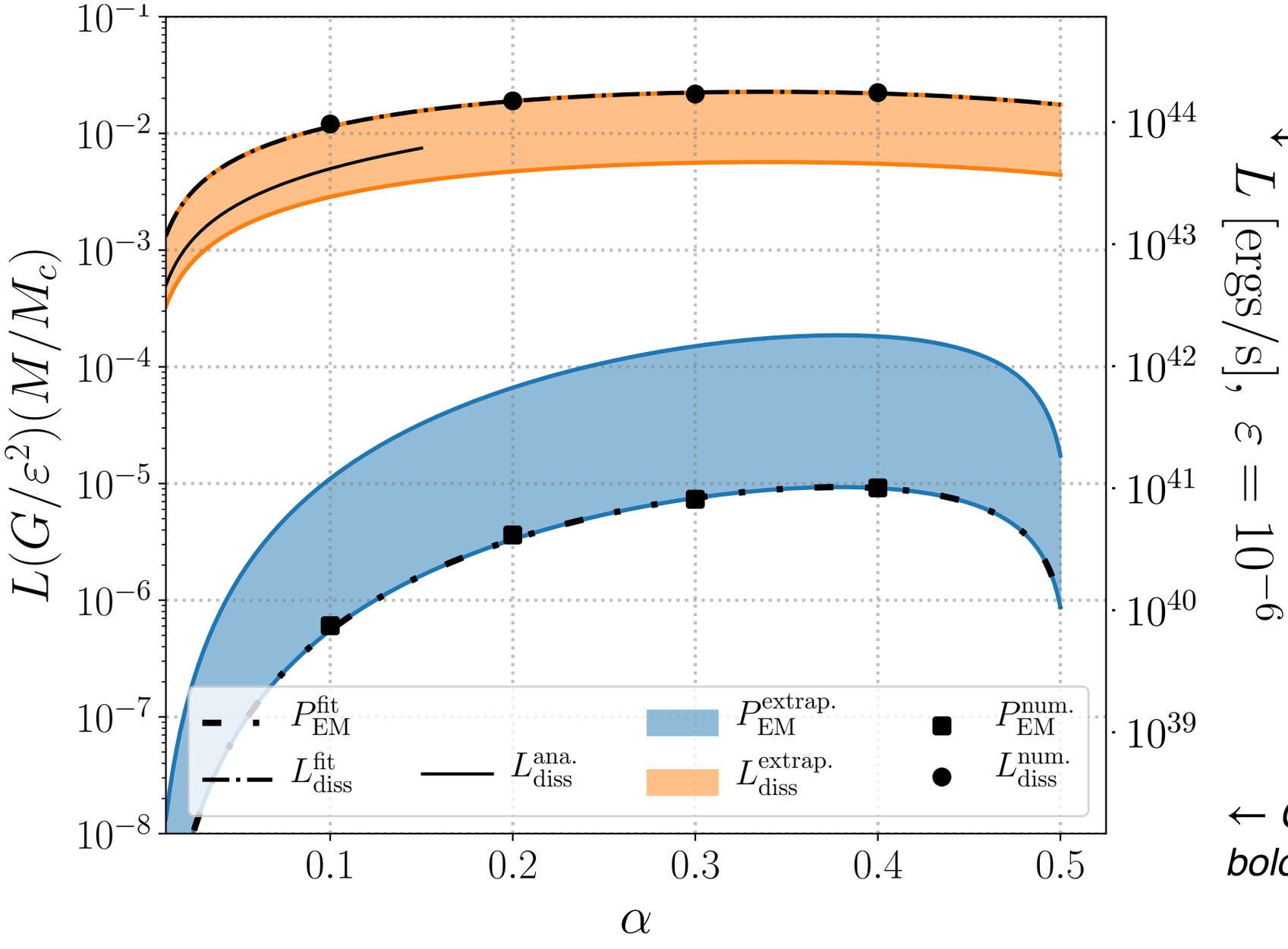

- Power output in electromagnetic flux and **resistive heating and particle production**
- **Synchrotron emission of highly boosted particles ~ few keV to MeV**

Simulation: periodicity?

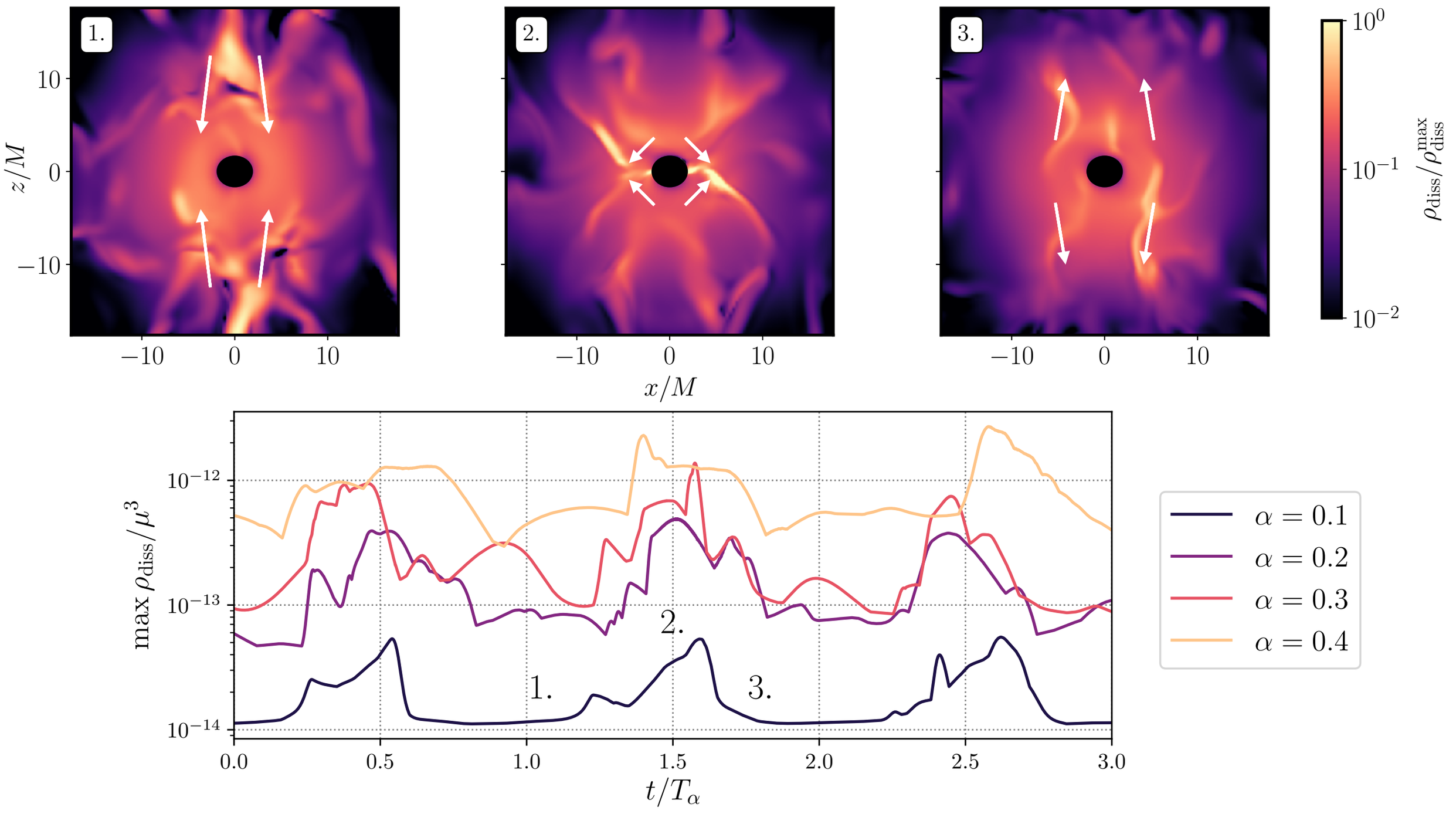

- Periodicity at the particle mass expected in electromagnetic signal from recently formed, (initially) rapidly rotating black holes

A New Pulsar?

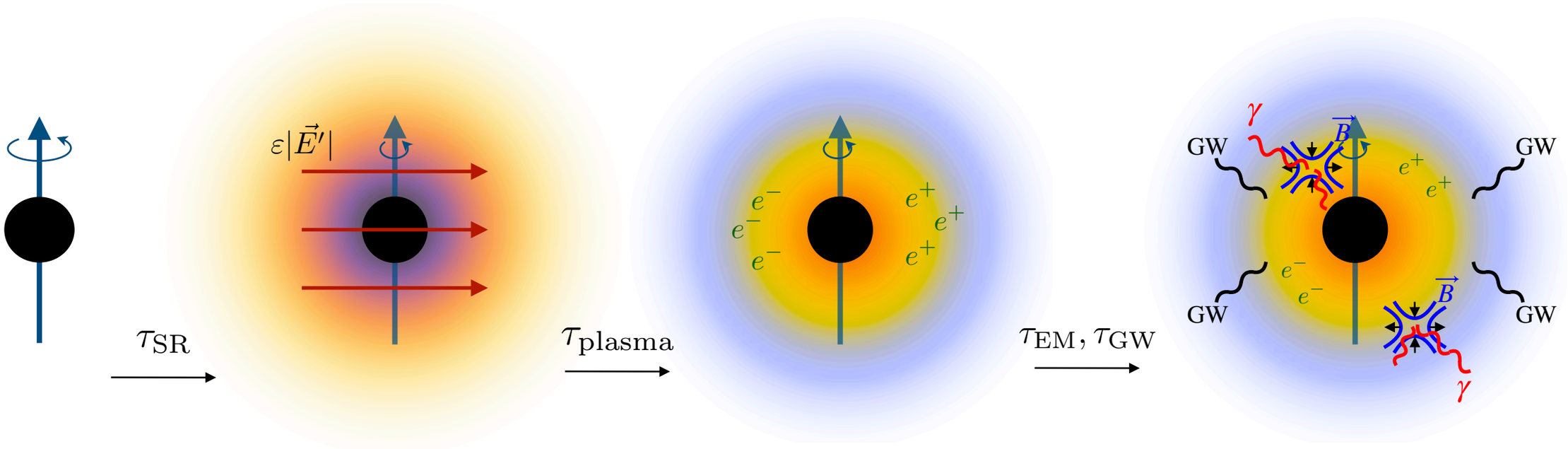

Decay of the superradiance cloud through gravitational wave and EM emissions: **multimessenger signals**

Cristina Mondino

EM follow-up of BH mergers

A signal from viable dark photon parameter space could be hiding in existing observations!

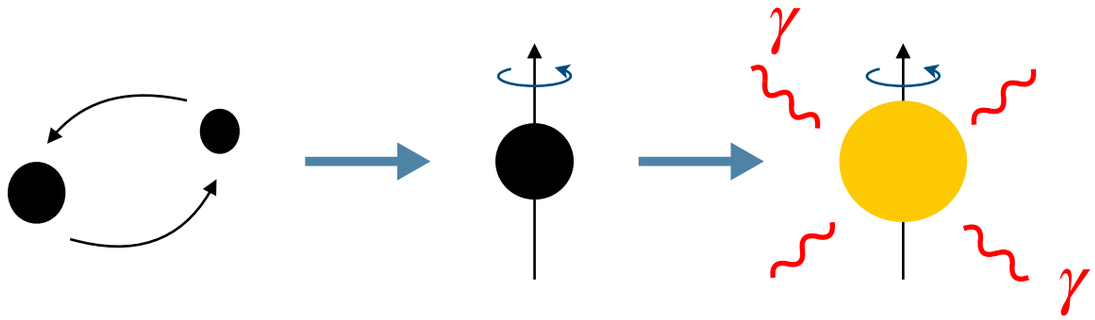

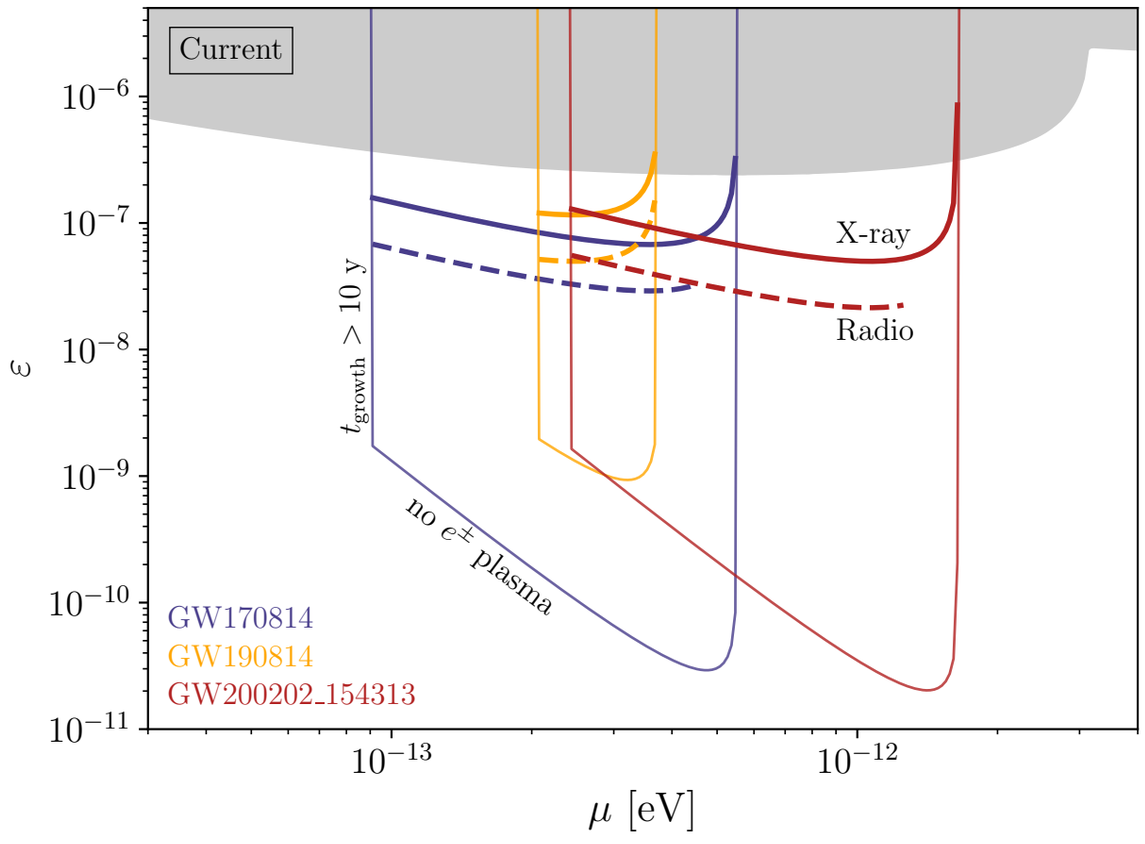

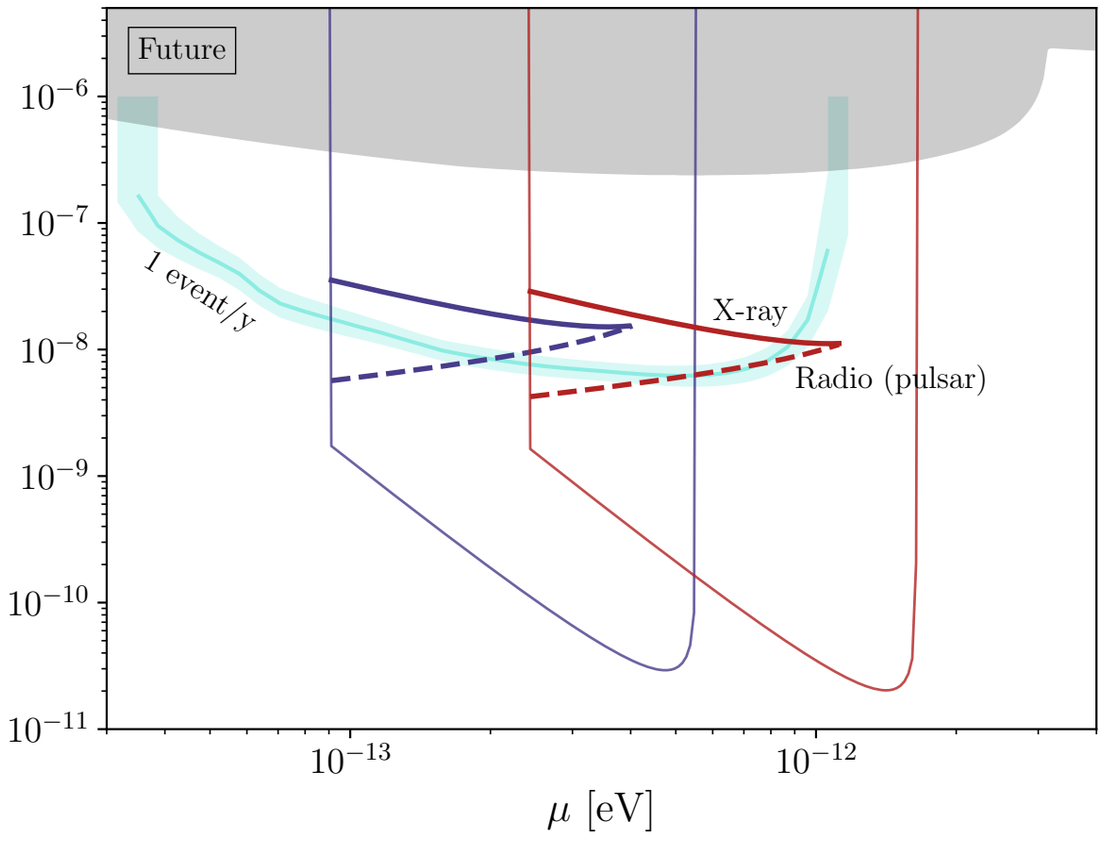

GW follow-up of anomalous pulsars

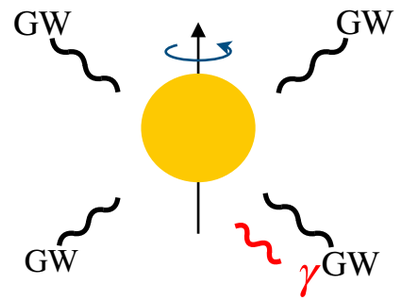

Existing all-sky searches

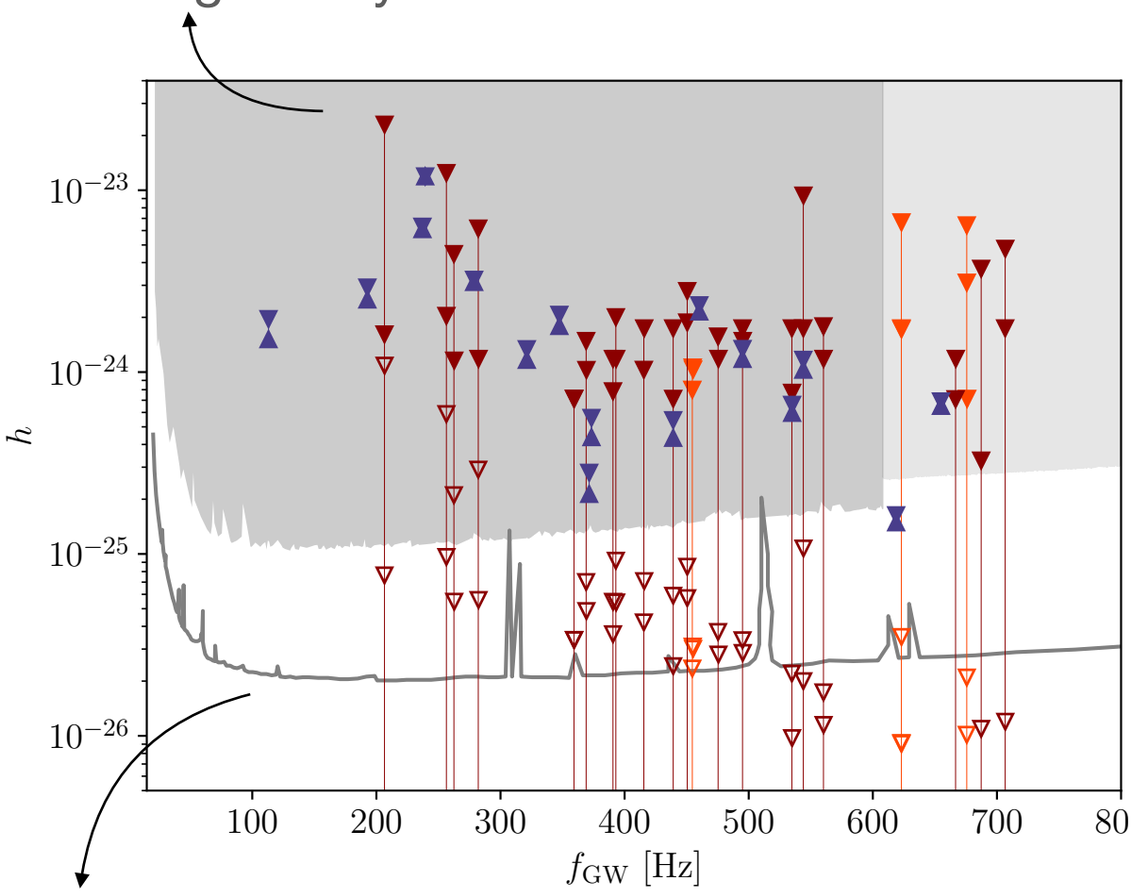

Targeted search

Observed frequency doublets of triplets

Observed pulsars with $\dot{f}_{\rm obs} > 0$

(with spin-up rate due to GW emissions)

- Some of the observed pulsating sources could be old BHs with radiating SR cloud

Dark Photons and Black Holes

- Rotating black holes produce`clouds' of weakly coupled bosons through **superradiance**
- Dark photons with Standard Model mixing will lead to dramatic dynamics around the black hole: perhaps, a new `pulsar'!

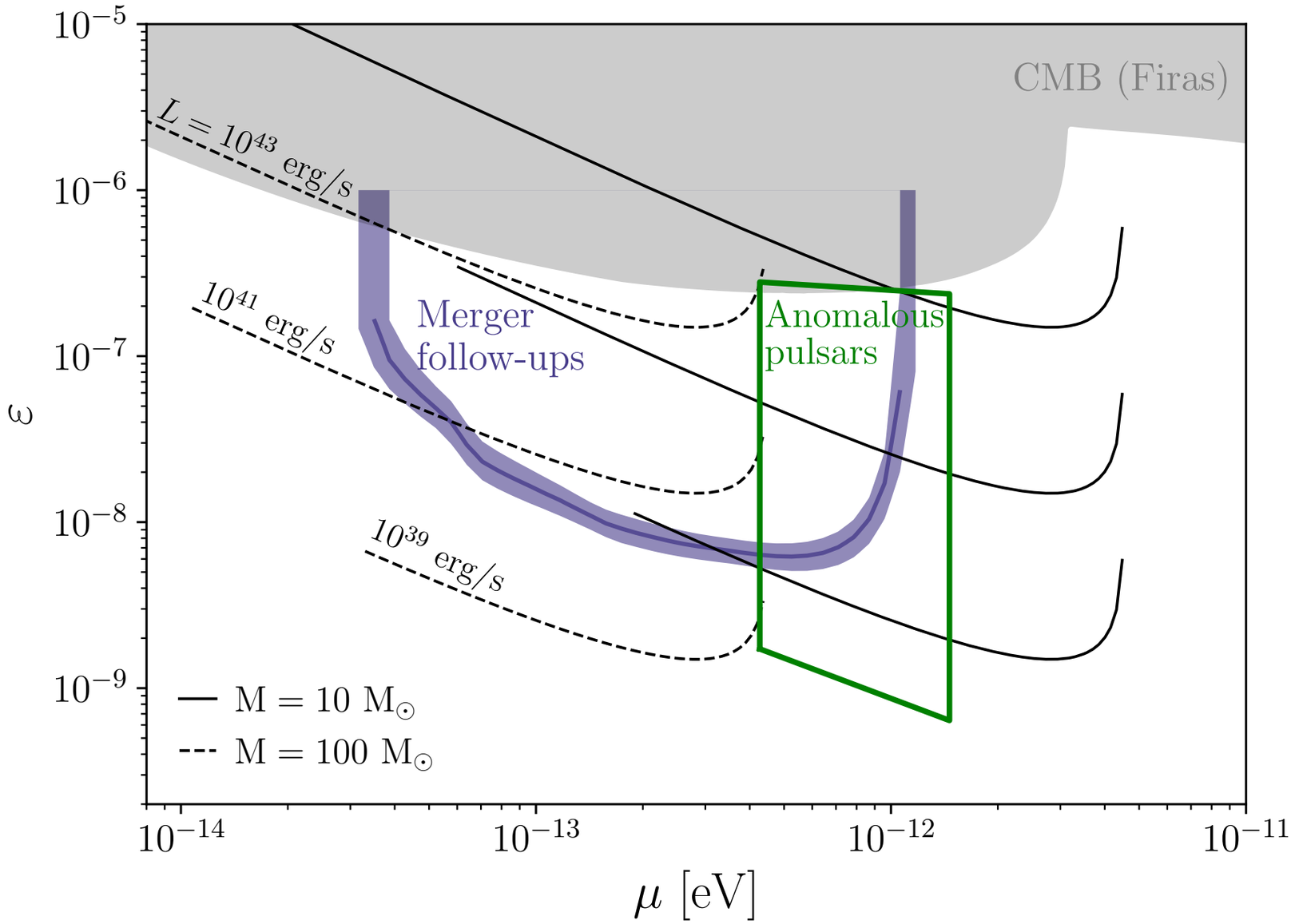

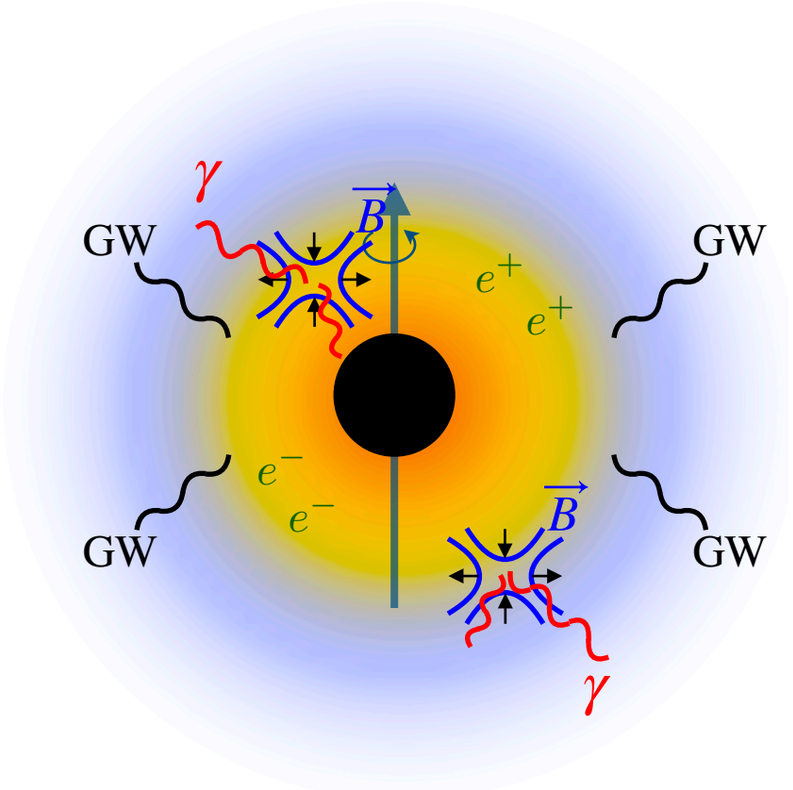

Neutron star pulsar

Magnetosphere of neutron star pulsar

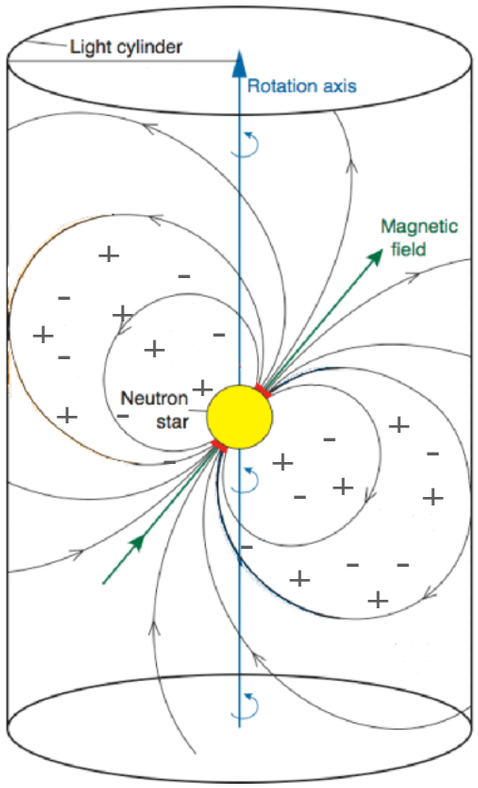

1) $$\partial_t \vec{B} = -\nabla \times \vec{E}$$
$$\partial_t \vec{E} = \nabla \times \vec{B} - \vec{J}$$

2) $$\rho\vec{E} + \vec{J} \times \vec{B} = 0 \qquad (\rho = \nabla \cdot \vec{E}\ )$$

"Force-free" plasma (perfect conductor)

$$\vec{J} = f(\vec{E}, \vec{B})$$

- Solve equations for the E, B fields
- Compute EM energy emitted

SR cloud + plasma

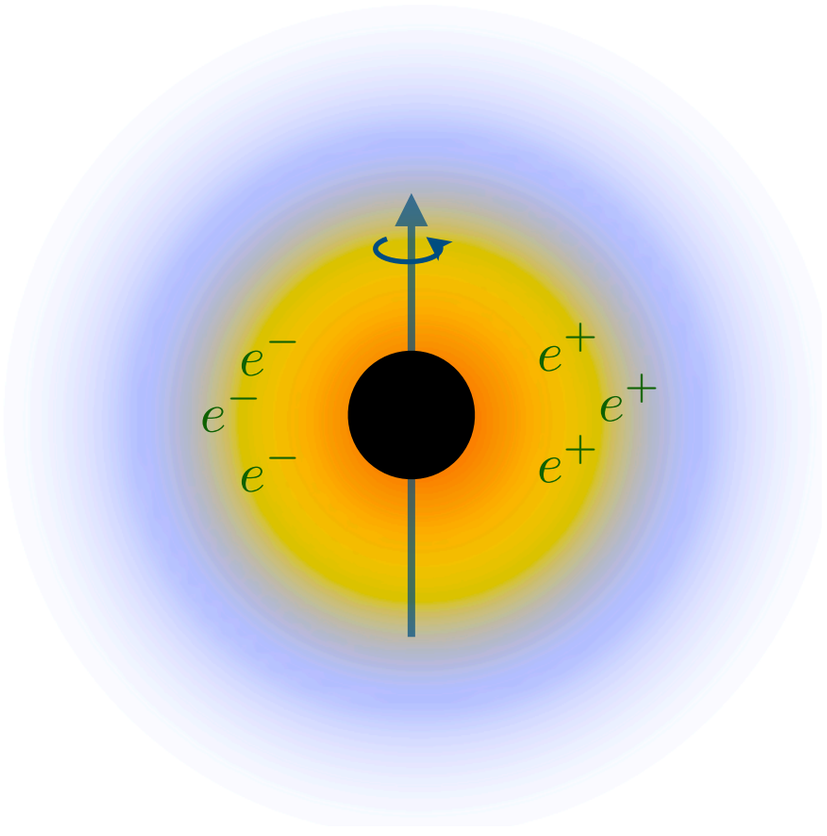

Superradiance field (source)

$$\partial_t \vec{B} = -\nabla \times \vec{E}$$

$$\partial_t \vec{E} = \nabla \times \vec{B} - \vec{J} - \epsilon\mu^2 \vec{A}'$$

Ohm's law $\vec{J} = \sigma(\vec{E} + \vec{v} \times \vec{B})$

- Solve equations for the E, B fields
- Compute EM energy emitted for $\sigma \gg \mu$ ($\sigma \to \infty$)

Simulation: E field

Vacuum (no screening)

$$\vec{E} = \epsilon \vec{E}_{\rm SR}$$

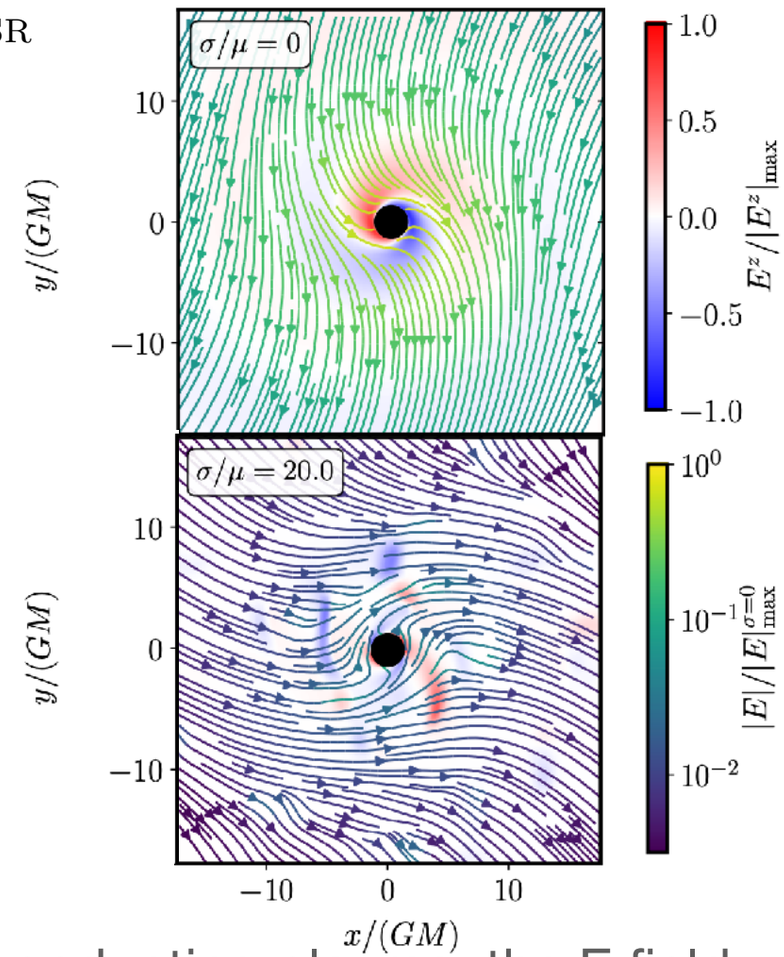

Highly conducting plasma: the E field is screened

Charge density

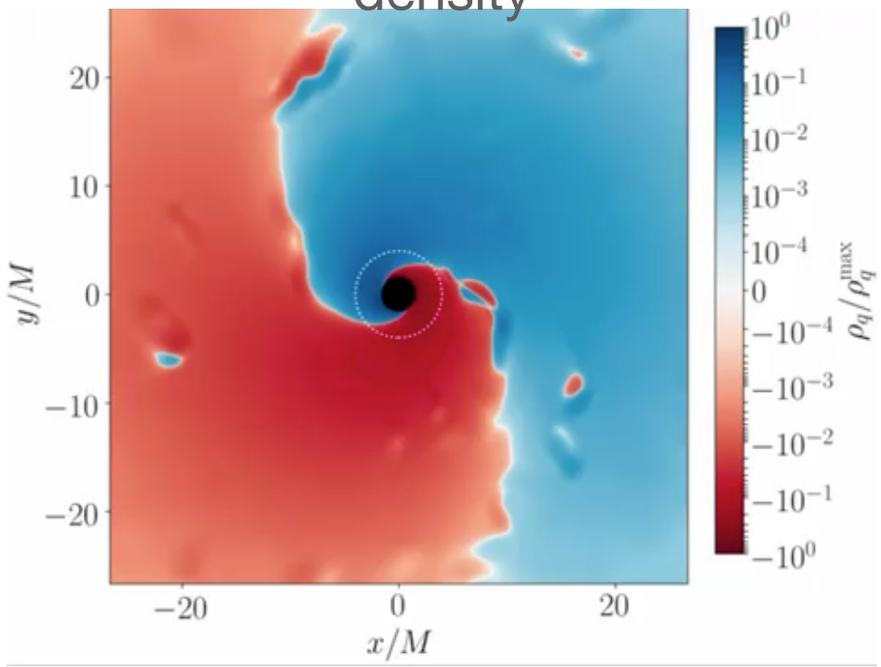

Rotating dipole

Simulation: B field

Vacuum $\vec{B} = \epsilon \vec{B}_{\rm SR}$

$\vec{B}$ determined by plasma dynamics

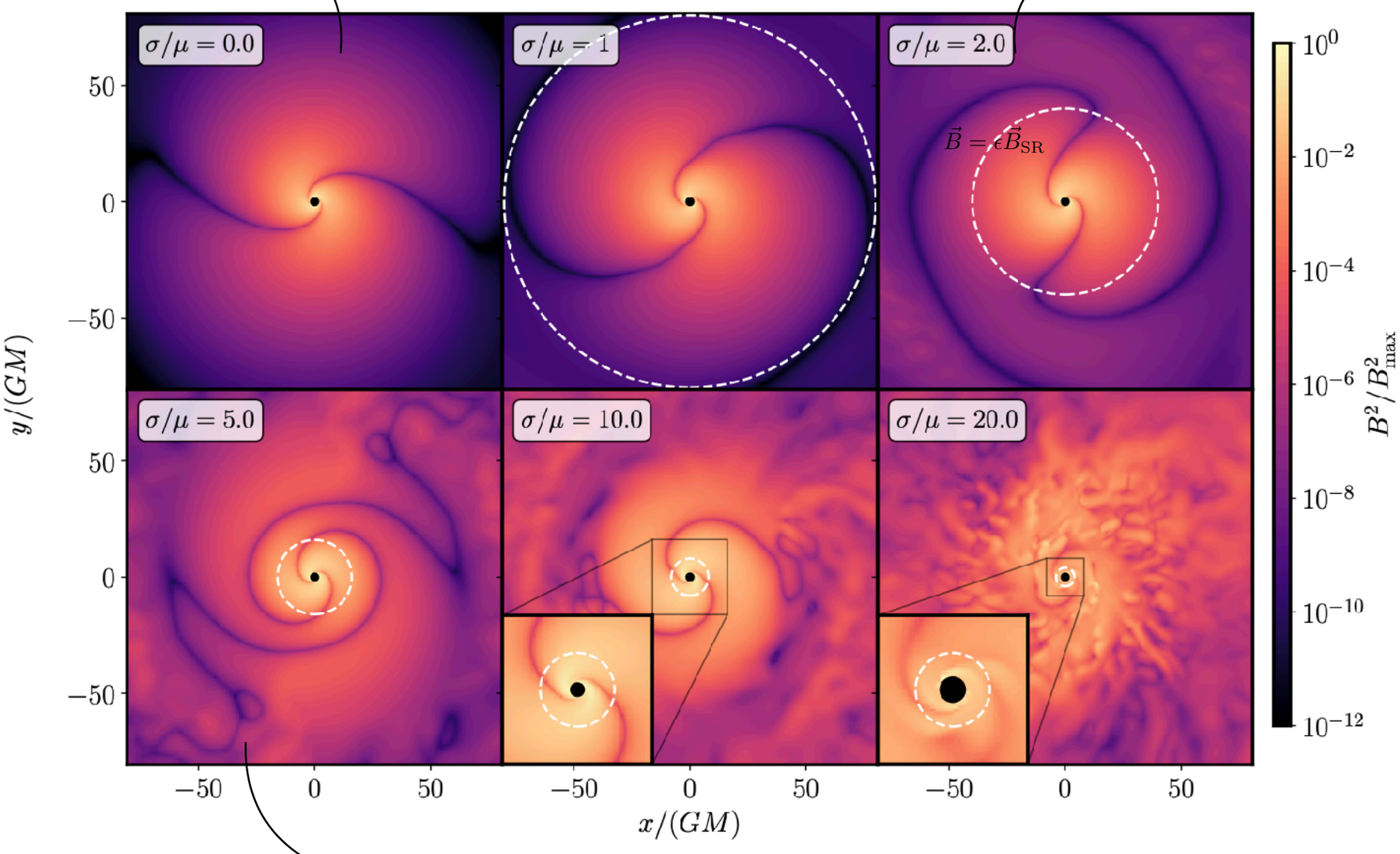

Twisting of the magnetic field lines

Far from the BH, the plasma cannot keep up with field rotation at frequency $\sim \mu$

Turbulent field structure!

Plasma production

Schwinger pair production:

$$\Gamma_{e^\pm} = \frac{\alpha_{\rm EM}}{2\pi}\frac{e\varepsilon|\vec{E}'|}{m_e}\exp\left(-\frac{4m_e^6\mu^2}{(e\varepsilon|\vec{E}'|)^4}\right)$$

Size of the superradiance cloud:

$$r_{\rm cloud} = \frac{1}{\alpha\mu}$$

Efficient pair production if

$$\Gamma_{e^\pm} \gg \alpha\mu \qquad (\alpha \equiv \mu G M)$$

→ Cascade production of charged particles until the electric field is screened

$$en_e \simeq \varepsilon\nabla\cdot\vec{E}'$$

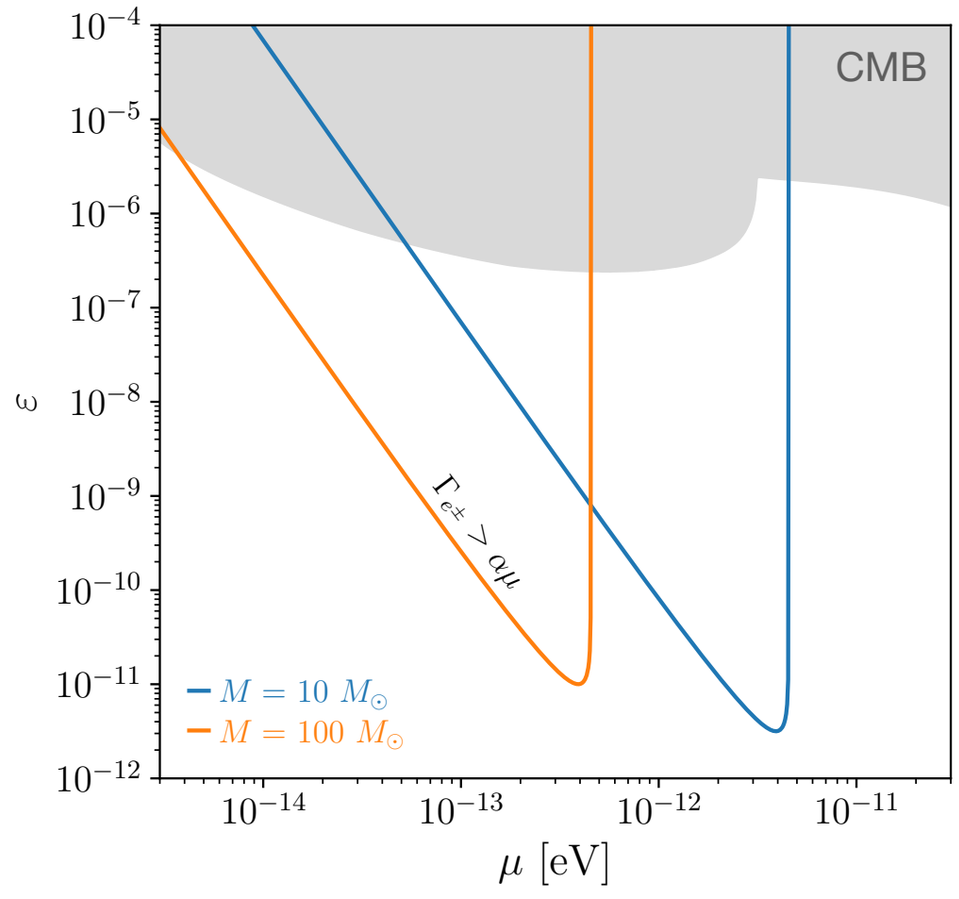

Important timescales

$$\tau_{\rm SR} \simeq \frac{1}{4 a_* \alpha^6 \mu}$$

$$\tau_{\rm plasma} \simeq \frac{1}{\Gamma_{e^\pm}}$$

$$\tau_{\rm plasma} \ll \tau_{\rm SR}$$

Plasma production keeps up with growth of the SR cloud.

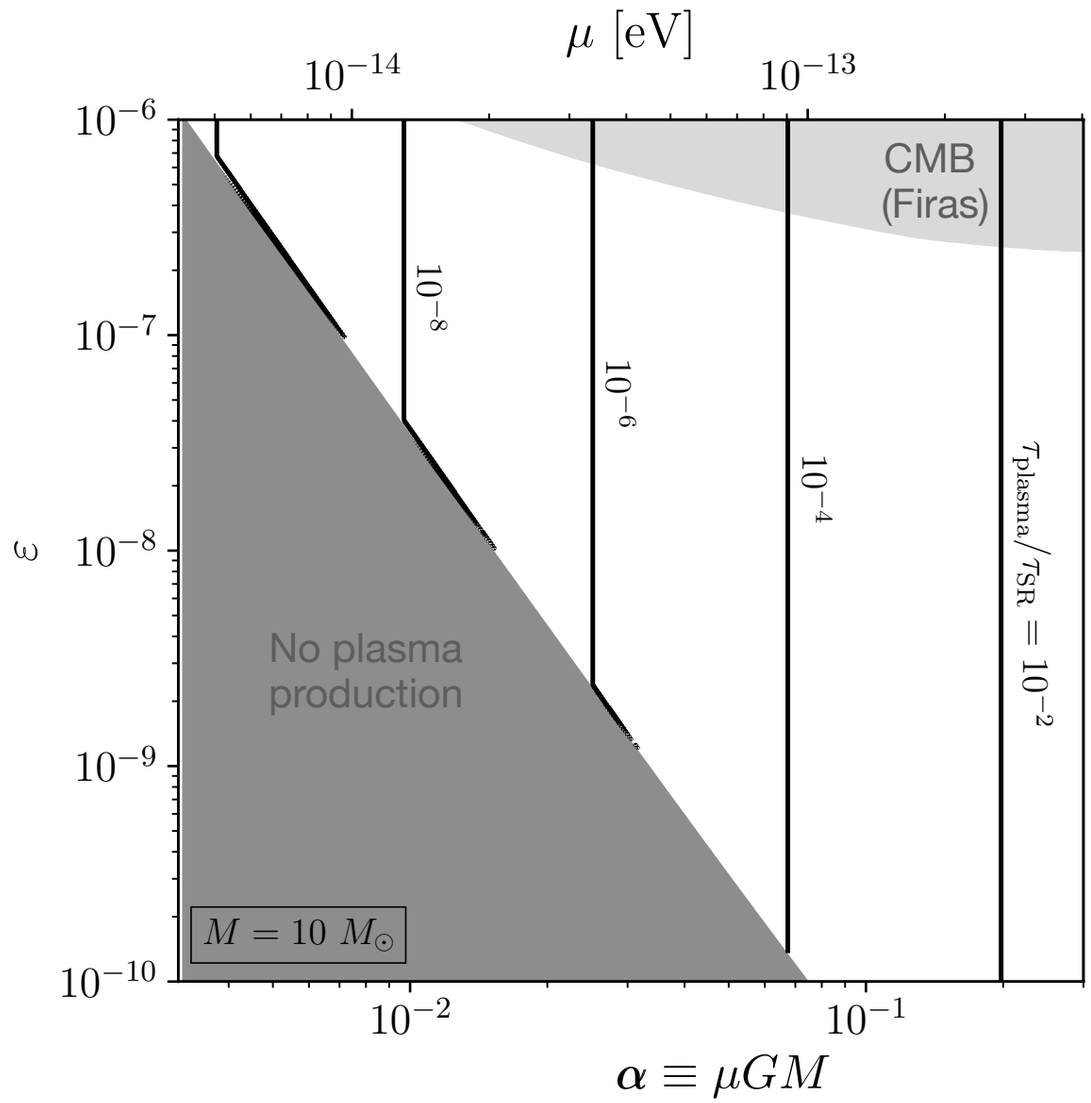

Observations: time evolution

- Signal period ($T = 2\pi/\mu$)
- Signal rise time ($\Gamma_{SR} \sim \alpha^6 \mu$)
- Signal decay time ($\Gamma_{GW} \sim \alpha^{12} \mu$)

$$\tau_{\rm GW} \approx \frac{GM}{17\alpha^{11}\Delta a_*}$$

$$\tau_{\rm EM} \approx \frac{GM \ln 2}{\varepsilon^2 F(\alpha)}$$

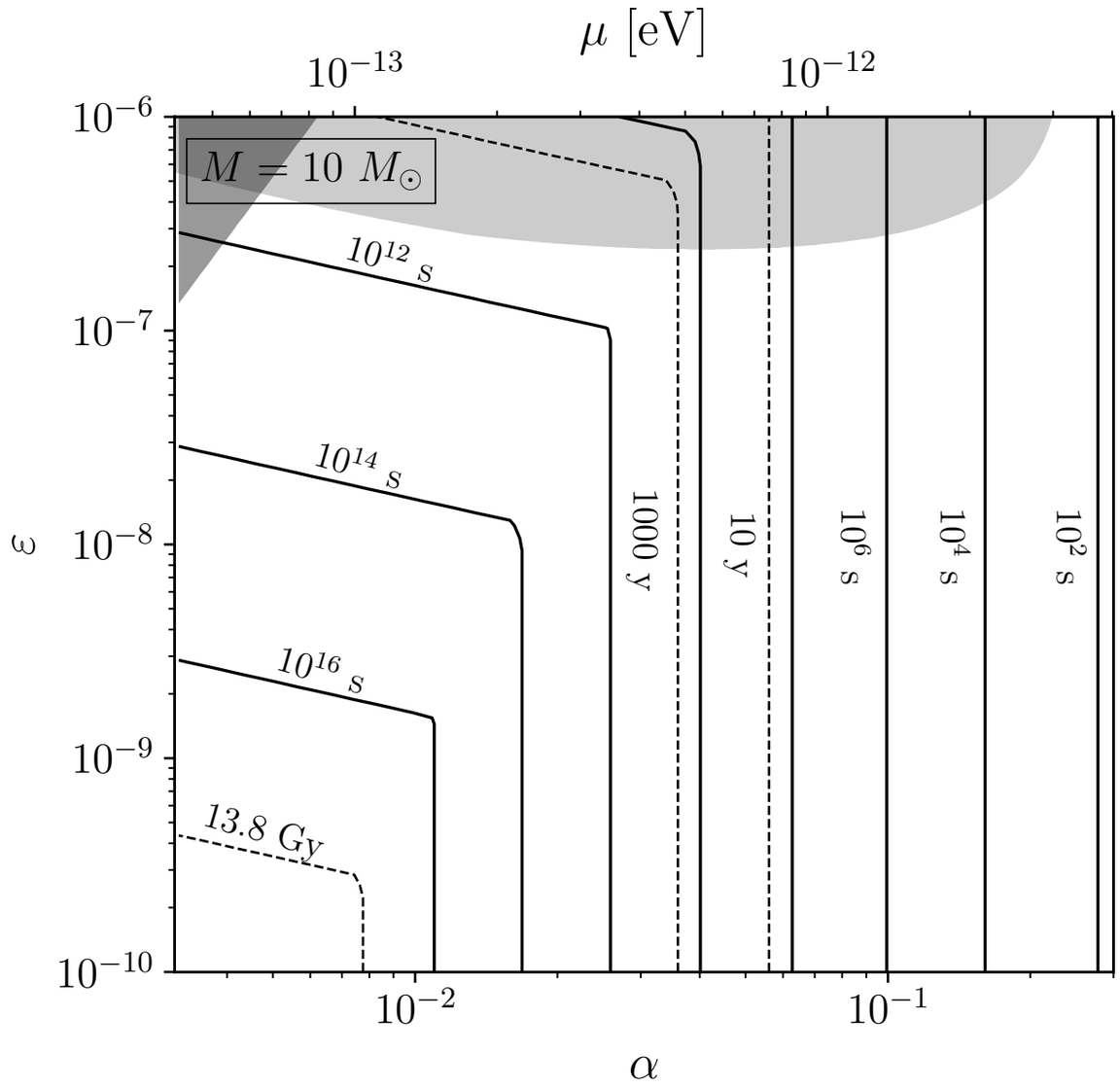

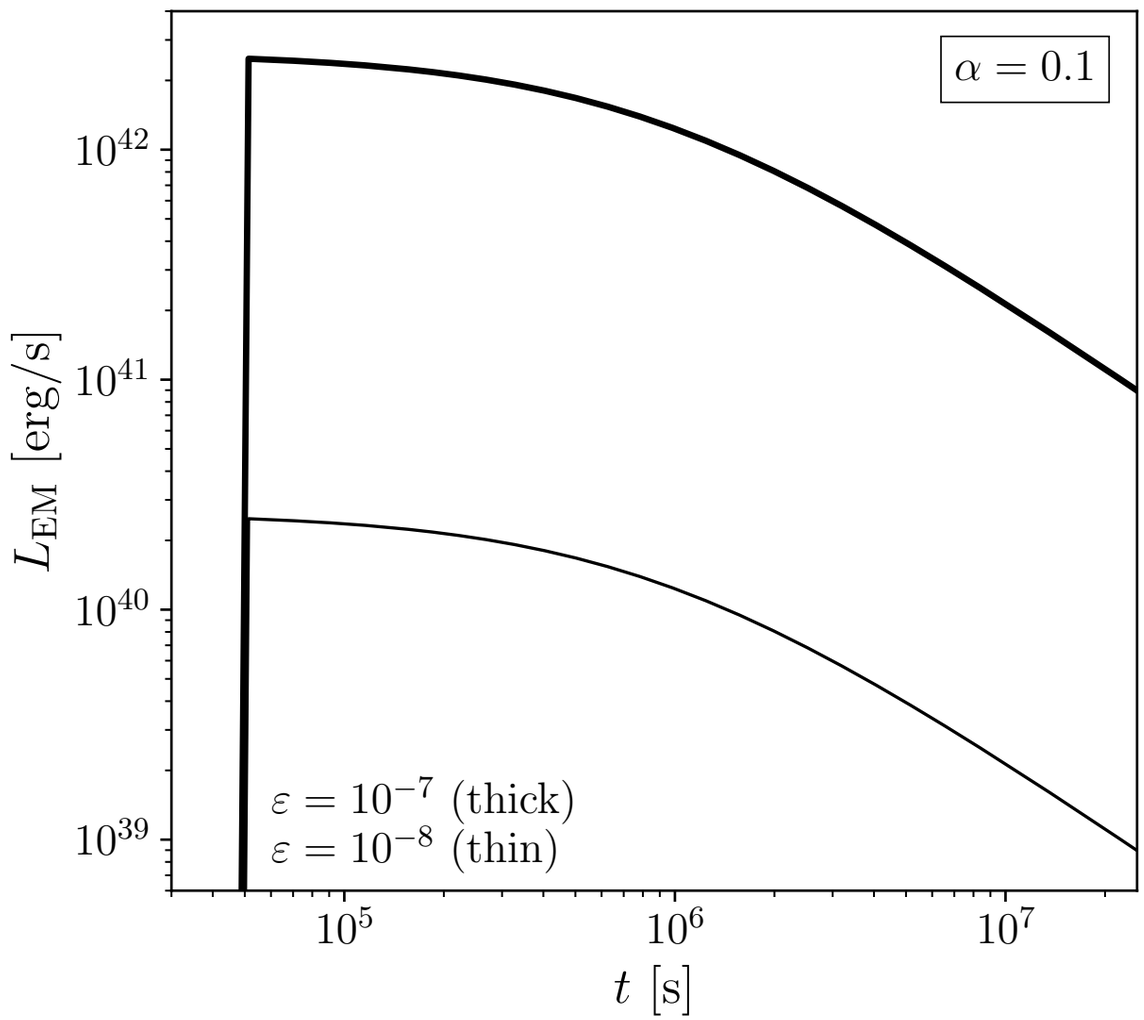

EM emissions

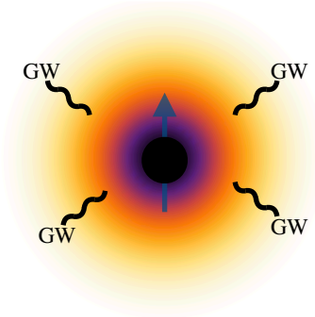

Luminosity of the dark photon superradiance cloud

$$L_{\rm fit} = \varepsilon^2 F(\alpha) \frac{M_c(t)}{GM}$$

$$M_c(t) = \frac{M_c(t_0)}{1 + (t - t_0)/\tau_{\rm GW}}$$

Time evolution

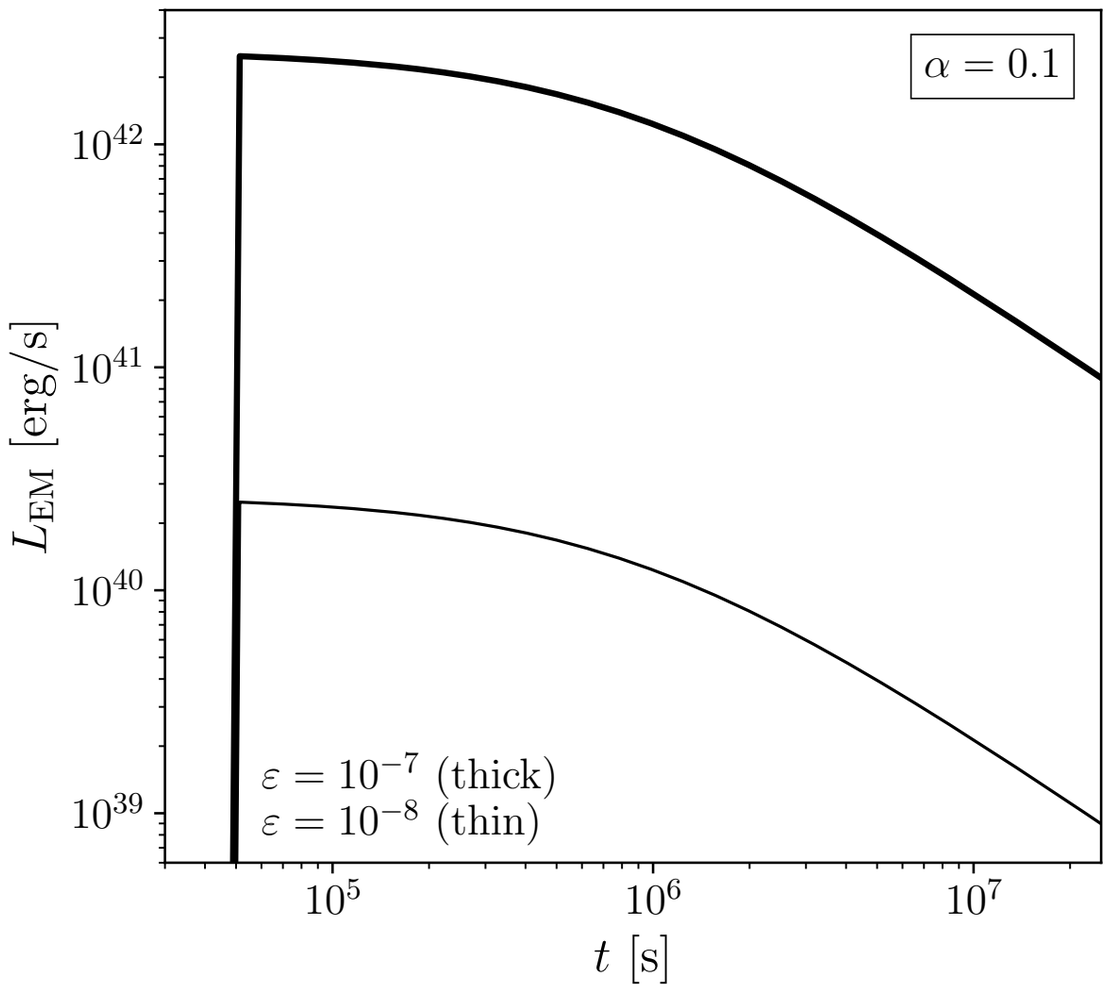

Simulation: power output

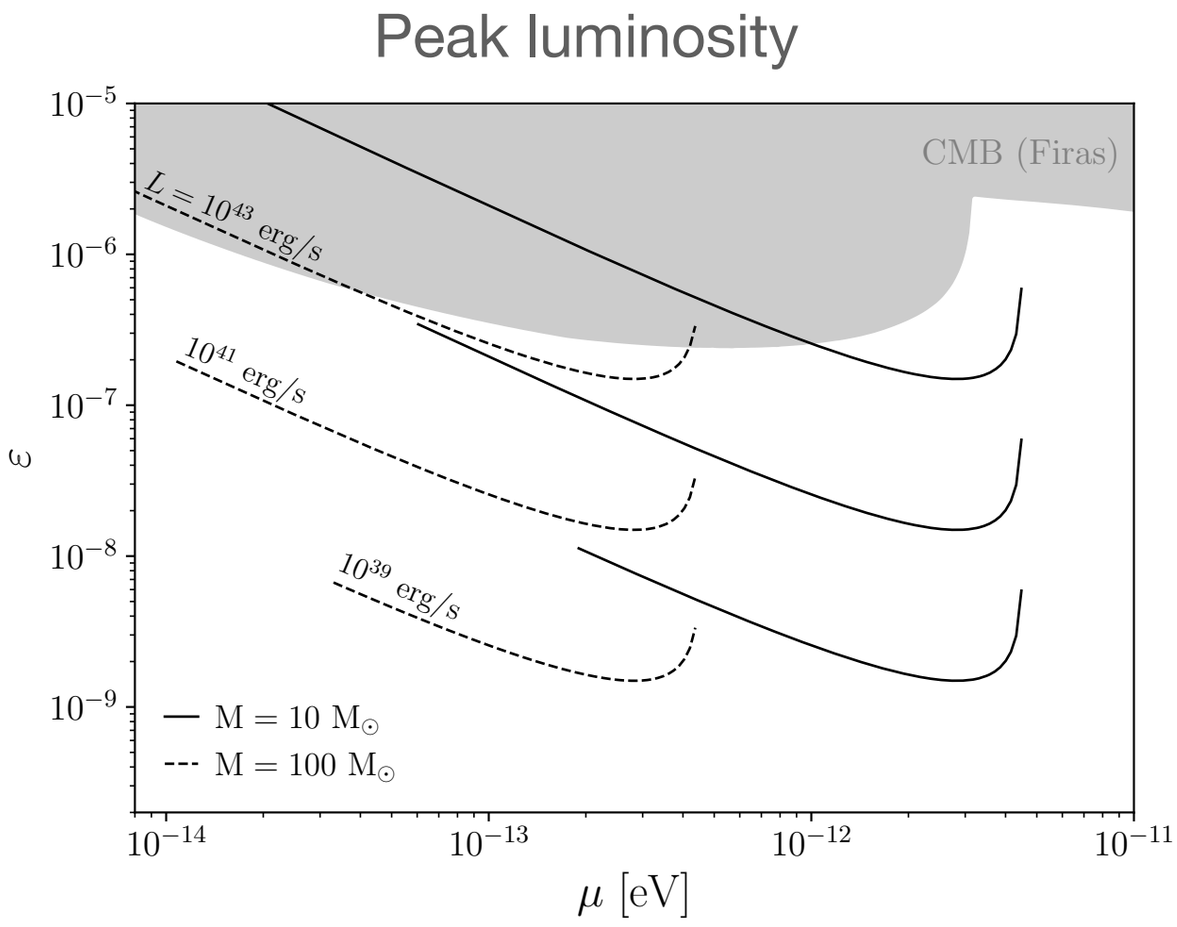

$$L_{\rm fit} = \varepsilon^2 F(\alpha) \frac{M_c}{GM}$$

Crab pulsar $L_{\rm crab} \simeq 10^{38}$ erg/s

Supernova $L_{\rm SN} \simeq 10^{43} - 10^{45}$ erg/s

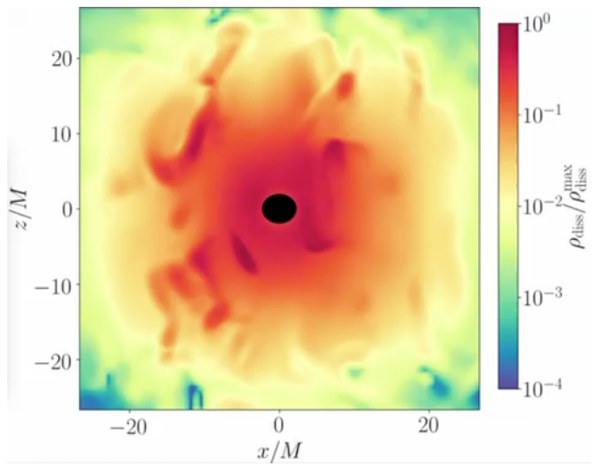

Neutron star pulsar

Magnetosphere of neutron star pulsar

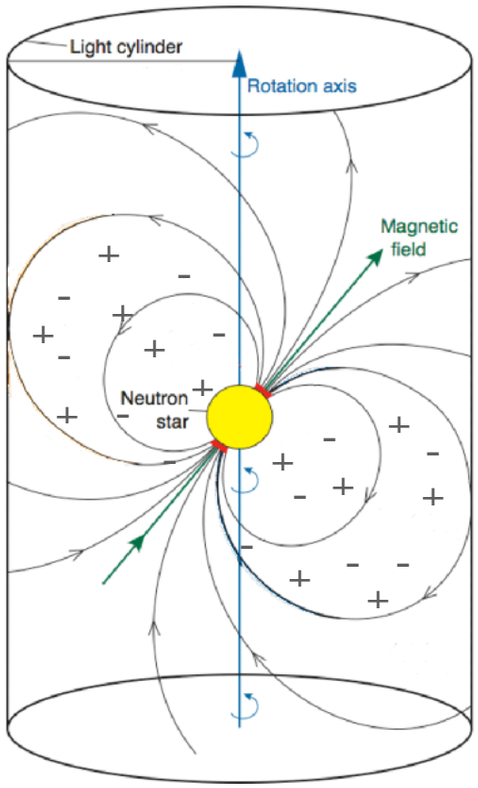

1) $$\partial_t \vec{B} = -\nabla \times \vec{E}$$
$$\partial_t \vec{E} = \nabla \times \vec{B} - \vec{J}$$

2) $$\rho\vec{E} + \vec{J} \times \vec{B} = 0 \qquad (\rho = \nabla \cdot \vec{E}\ )$$

“Force-free” plasma (perfect conductor)

Neutron star pulsar

Magnetosphere of neutron star pulsar

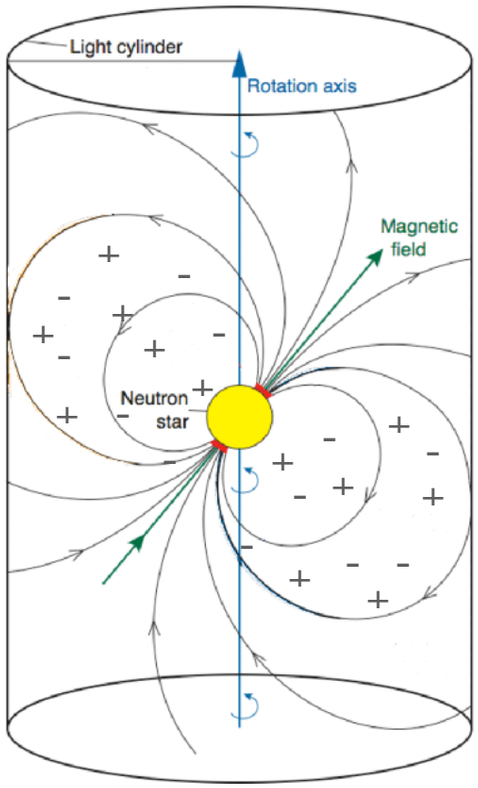

1) $$\partial_t \vec{B} = -\nabla \times \vec{E}$$
$$\partial_t \vec{E} = \nabla \times \vec{B} - \vec{J}$$

2) $$\rho\vec{E} + \vec{J} \times \vec{B} = 0 \qquad (\rho = \nabla \cdot \vec{E}\ )$$

"Force-free" plasma (perfect conductor)

$$\vec{J} = f(\vec{E}, \vec{B})$$

- Solve equations for the E, B fields
- Compute EM energy emitted

SR cloud + plasma

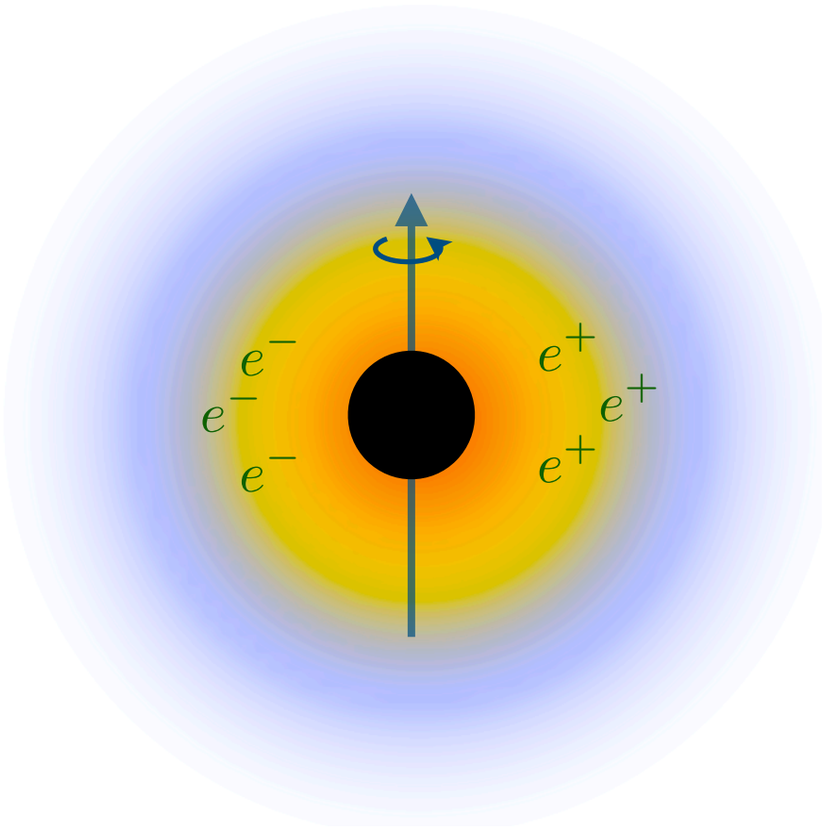

Superradiance field (source)

$$\partial_t \vec{B} = -\nabla \times \vec{E}$$

$$\partial_t \vec{E} = \nabla \times \vec{B} - \vec{J} - \epsilon\mu^2 \vec{A}'$$

Ohm's law $\vec{J} = \sigma(\vec{E} + \vec{v} \times \vec{B})$

- Solve equations for the E, B fields
- Compute EM energy emitted for $\sigma \gg \mu$ ($\sigma \to \infty$)

A new black hole `pulsar'

Adapt techniques from simulations of pulsar magnetospheres to simulate the electrodynamics of the dark photon cloud

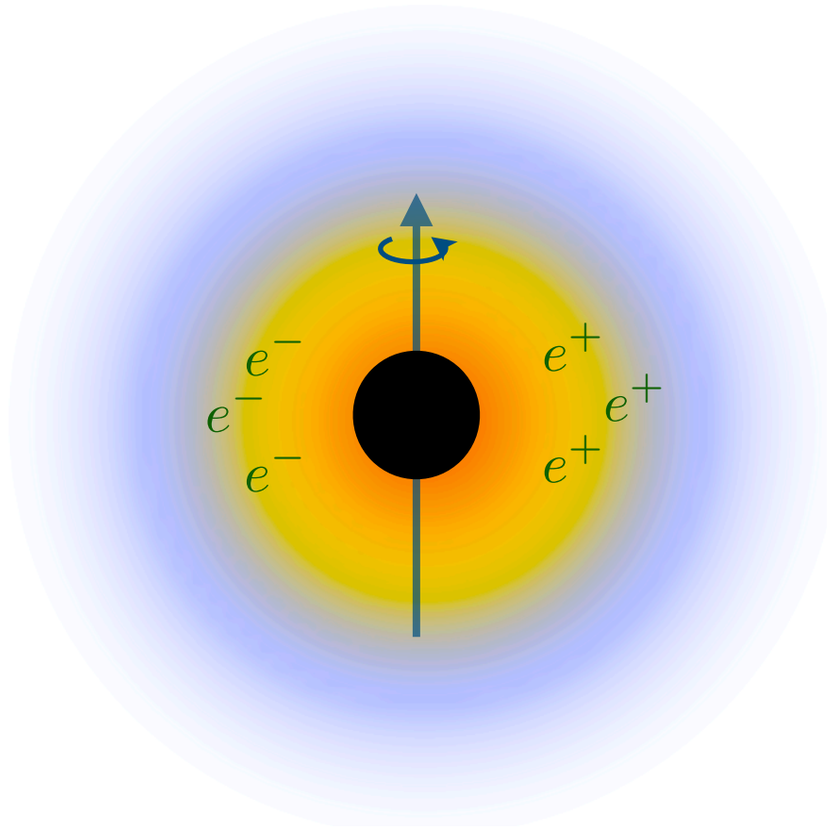

$$\partial_t \vec{B} = -\nabla \times \vec{E}$$

$$\partial_t \vec{E} = \nabla \times \vec{B} - \vec{J} - \epsilon\mu^2 \vec{A}'$$

Superradiance field (source)

Ohm's law $\vec{J} = \sigma(\vec{E} + \vec{v} \times \vec{B})$

- Solve equations for the E, B fields
- Compute EM energy emitted for $\sigma \gg \mu$ ($\sigma \to \infty$)

Nils Siemonsen

Full resistive magnetohydrodynamics simulation in Kerr BH background

Simulation: E field

Vacuum (no screening)

$$\vec{E} = \epsilon \vec{E}_{\rm SR}$$

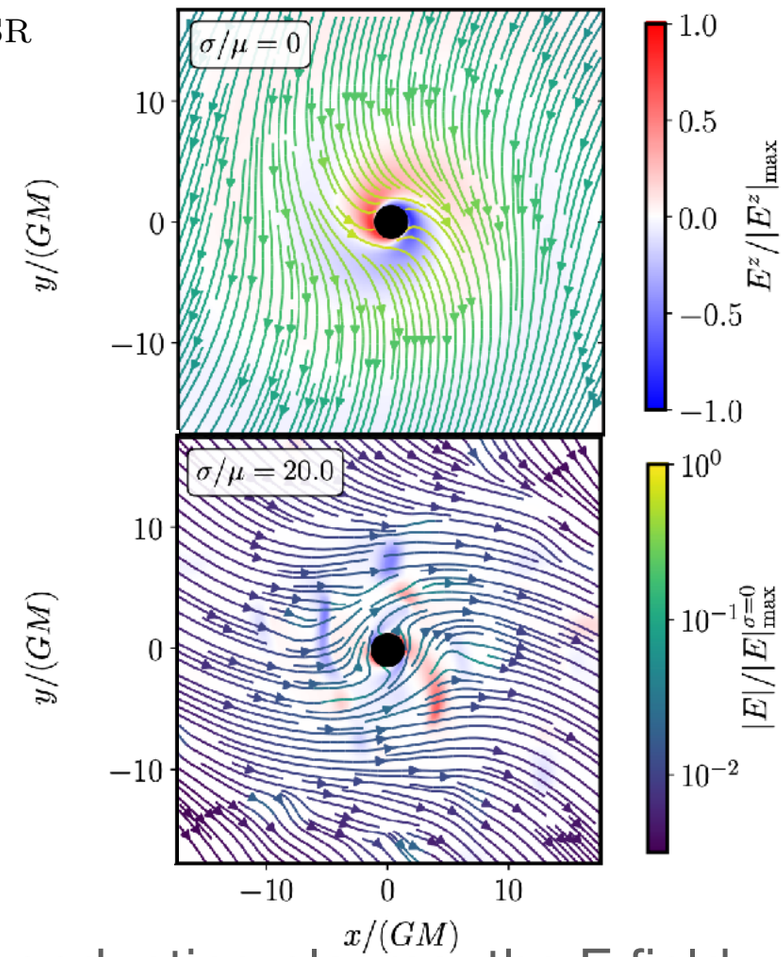

Highly conducting plasma: the E field is screened

Charge density

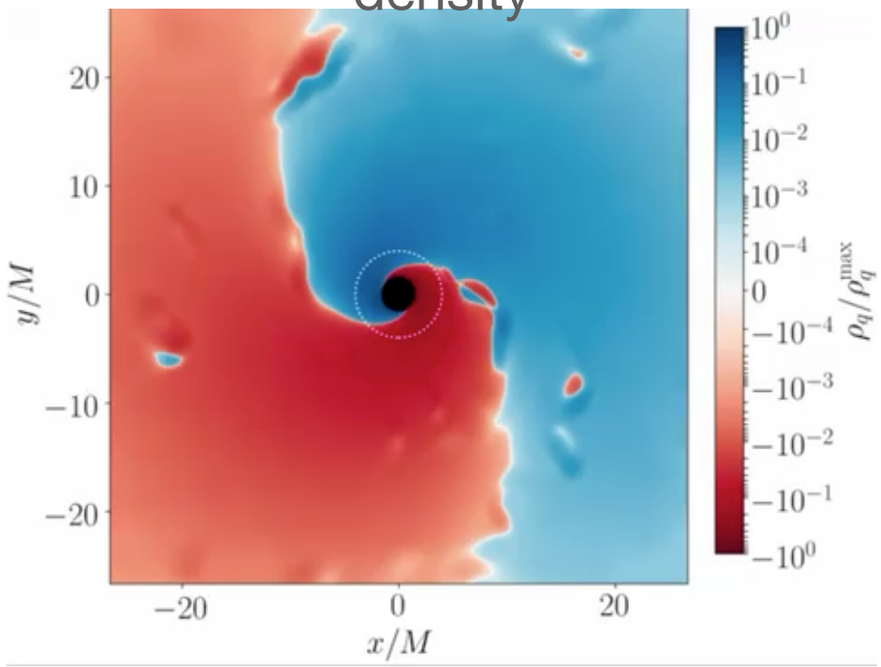

Rotating dipole

Simulation: B field

Vacuum $\vec{B} = \epsilon \vec{B}_{\rm SR}$

$\vec{B}$ determined by plasma dynamics

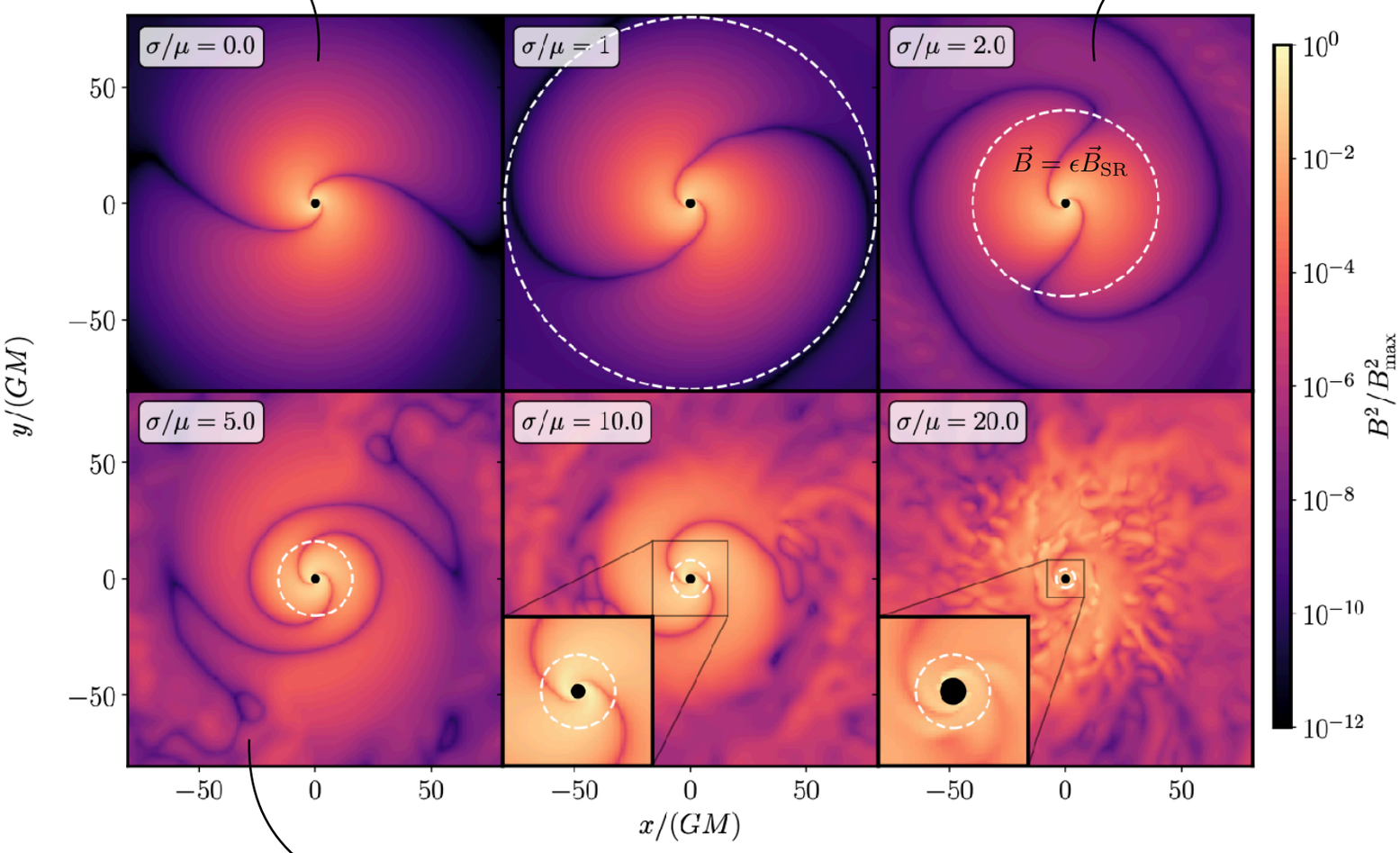

Twisting of the magnetic field lines

Far from the BH, the plasma cannot keep up with field rotation at frequency $\sim \mu$

Turbulent field structure!

Simulation: energy dissipation

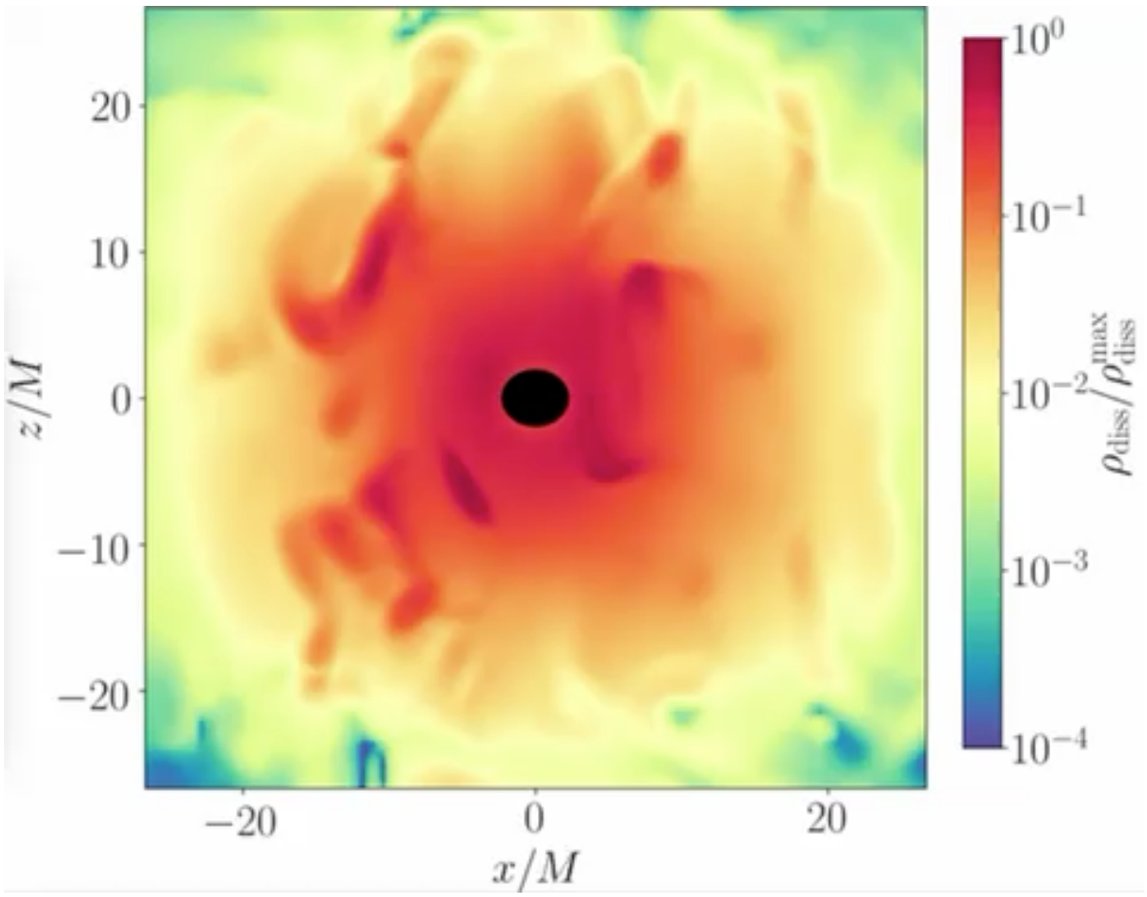

$$\rho_{\rm diss} = \vec{E} \cdot \vec{J}$$

Turbulent structure in the dissipative energy density!

Simulation: energy dissipation

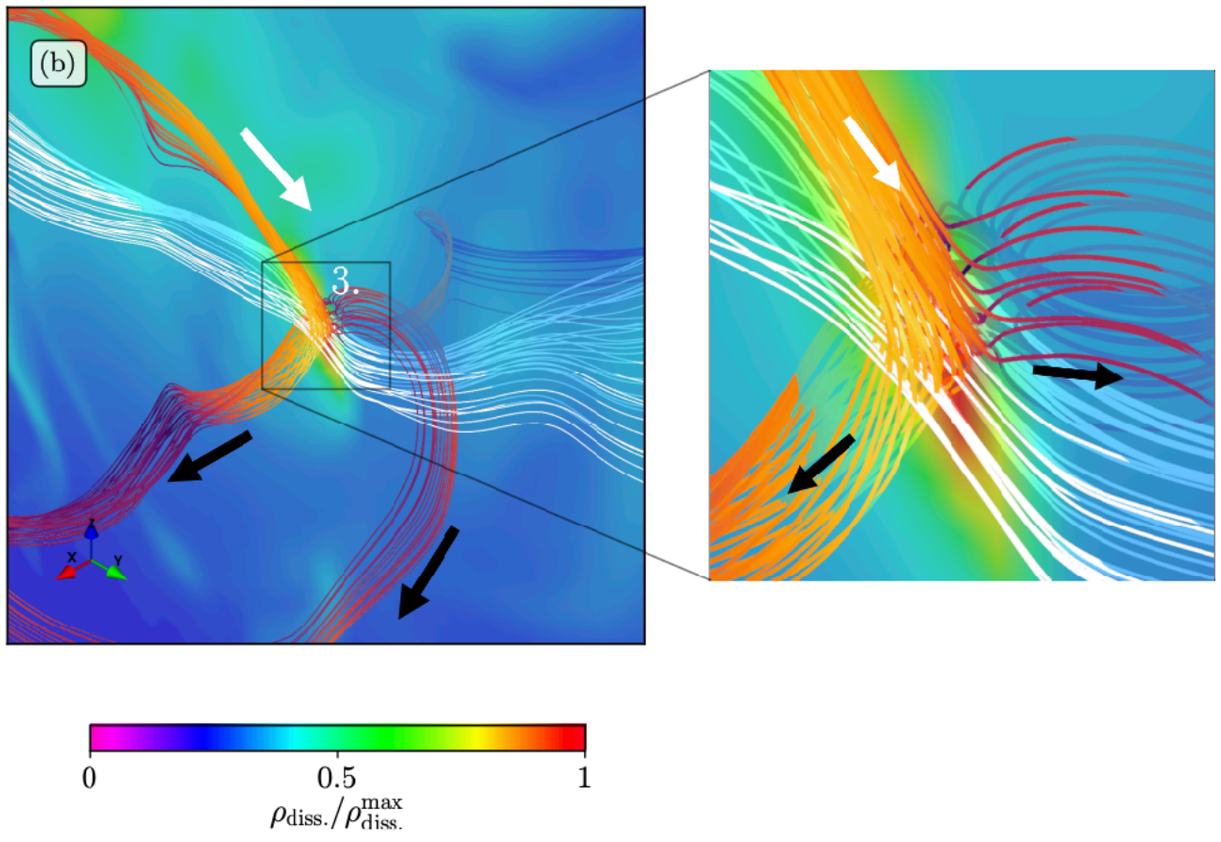

The dissipative energy density is maximal in the regions of magnetic field lines reconnection.

Magnetic reconnection?

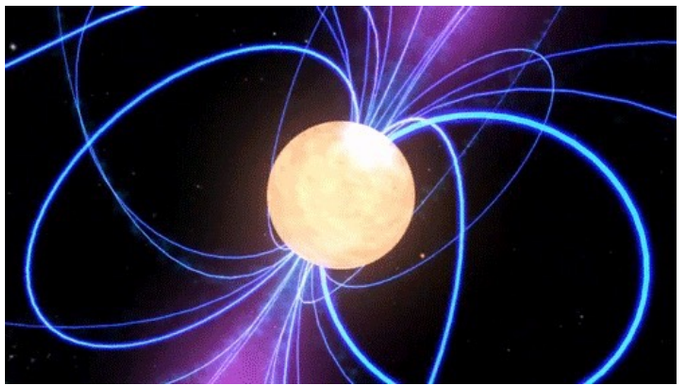

- Discontinuity in the magnetic field lines
- In a **neutron star pulsars** it happens on the equatorial plane (2d structures “current sheets”)

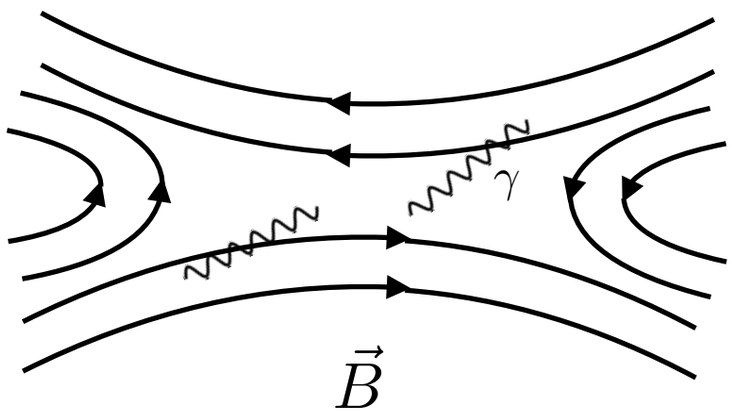

Field energy dissipated into particle acceleration and high energy emissions

Simulation: power output

Numerical solutions and fit

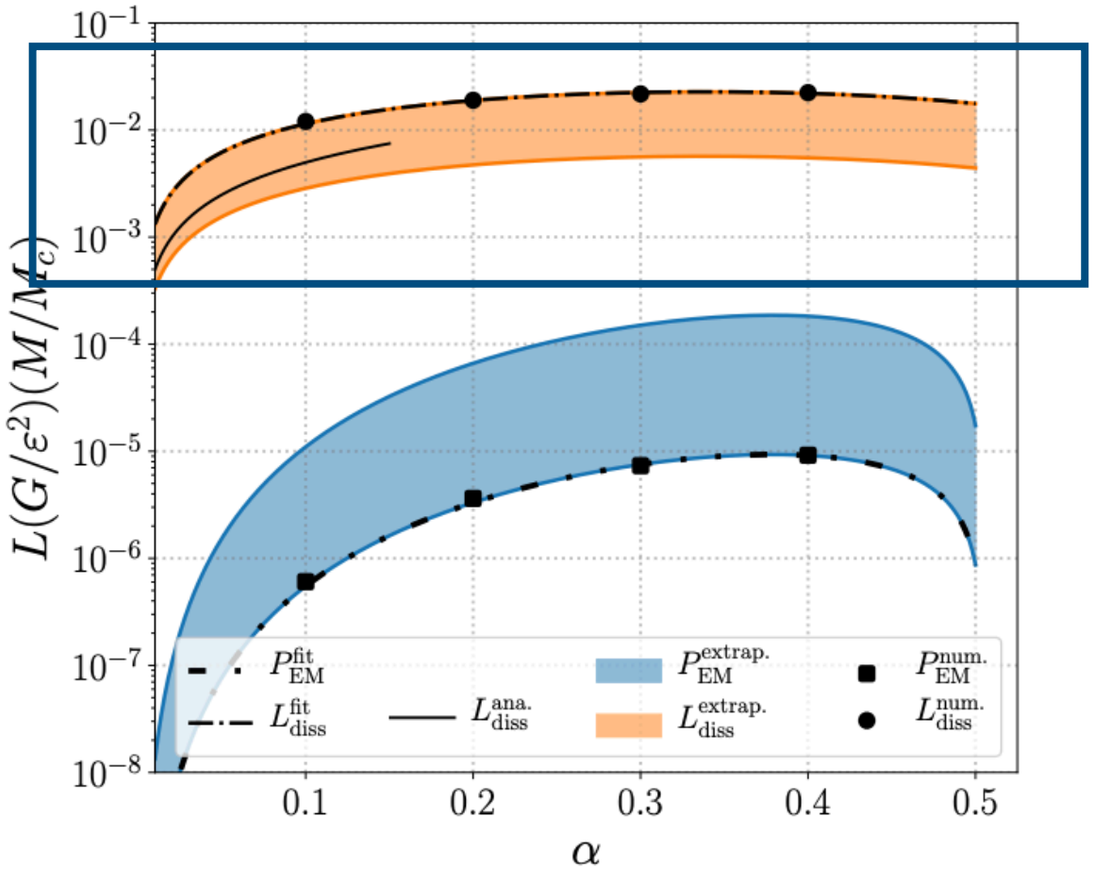

- Poynting flux

$$P_{\rm EM} = \oint dS\ \vec{r}\cdot(\vec{E}\times\vec{B})$$

- Dissipative losses

$$L_{\rm diss} = \int dV\, \vec{E}\cdot\vec{J}$$

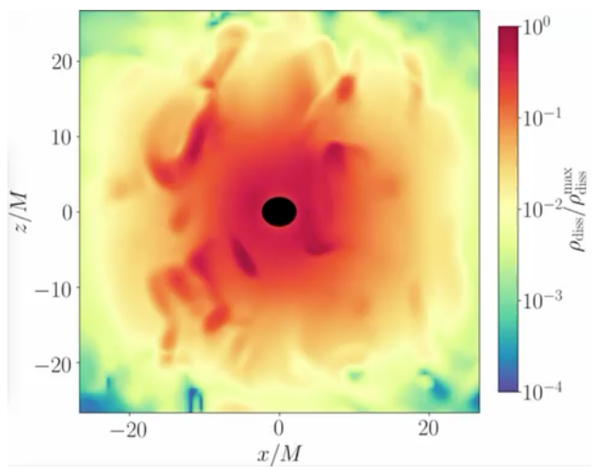

Simulation: power output

Numerical solutions and fit

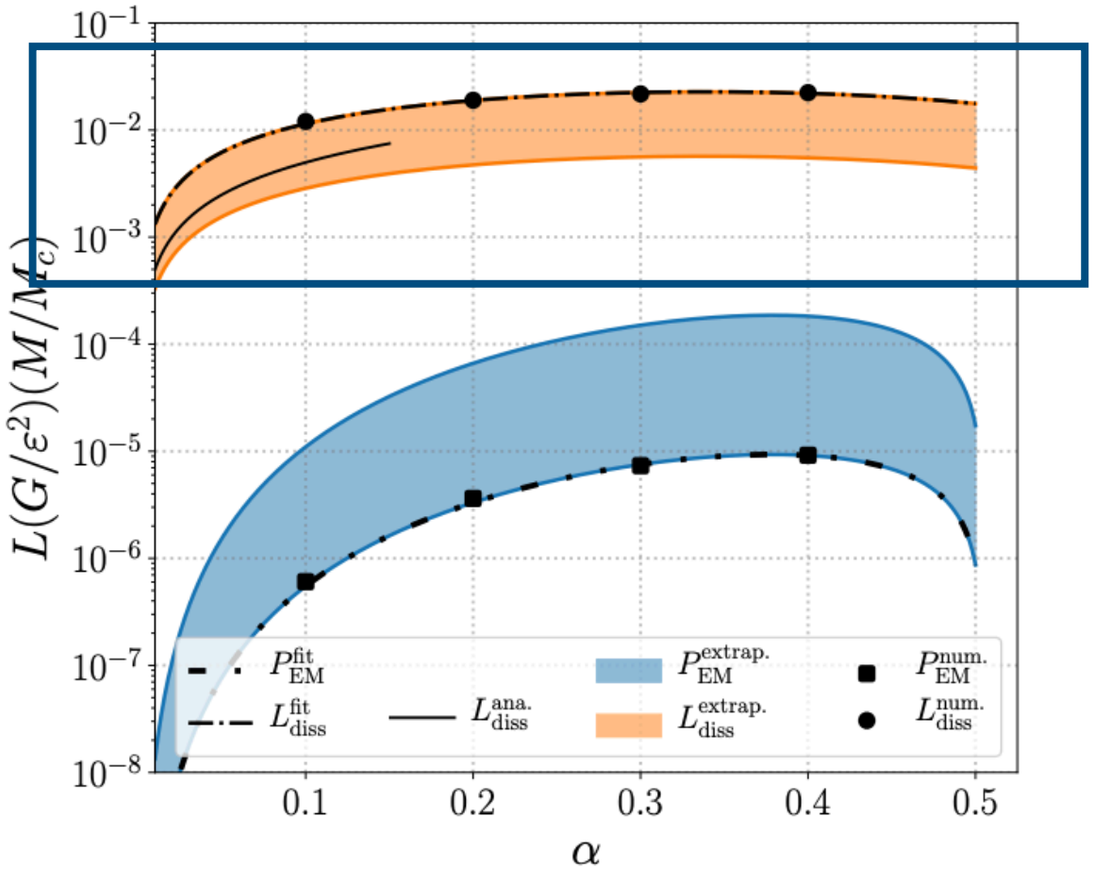

- Dissipative losses

$$L_{\rm diss} = \int dV \vec{E} \cdot \vec{J}$$

$$L_{\rm fit} = \varepsilon^2 F(\alpha) \frac{M_c}{GM}$$

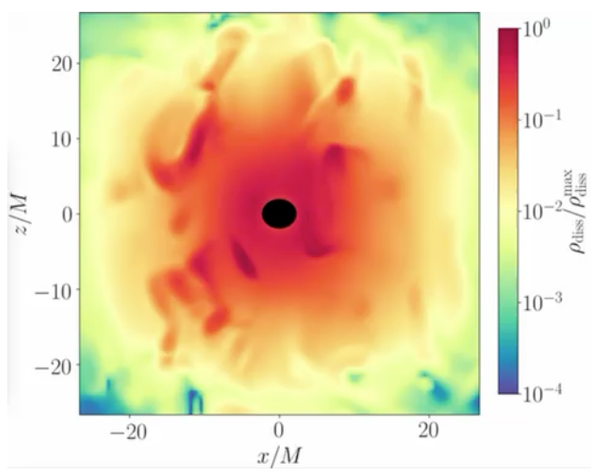

Simulation: power output

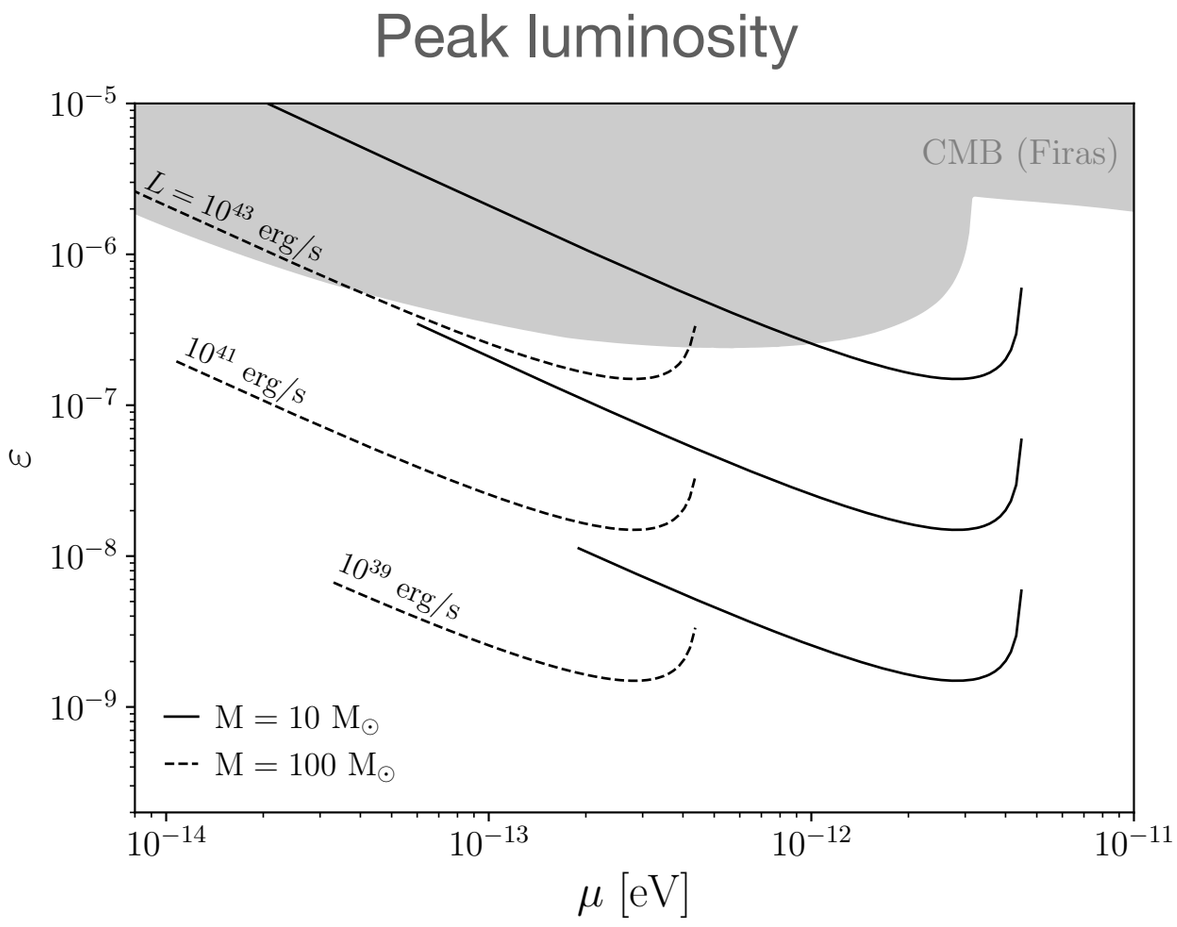

$$L_{\rm fit} = \varepsilon^2 F(\alpha) \frac{M_c}{GM}$$

Crab pulsar $L_{\rm crab} \simeq 10^{38}$ erg/s

Supernova $L_{\rm SN} \simeq 10^{43} - 10^{45}$ erg/s

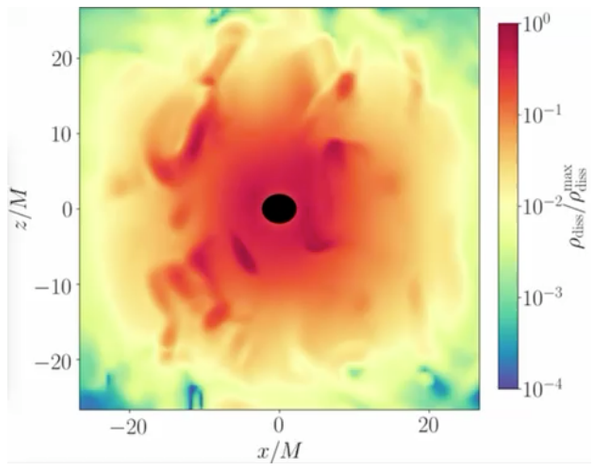

Simulation: periodicity?

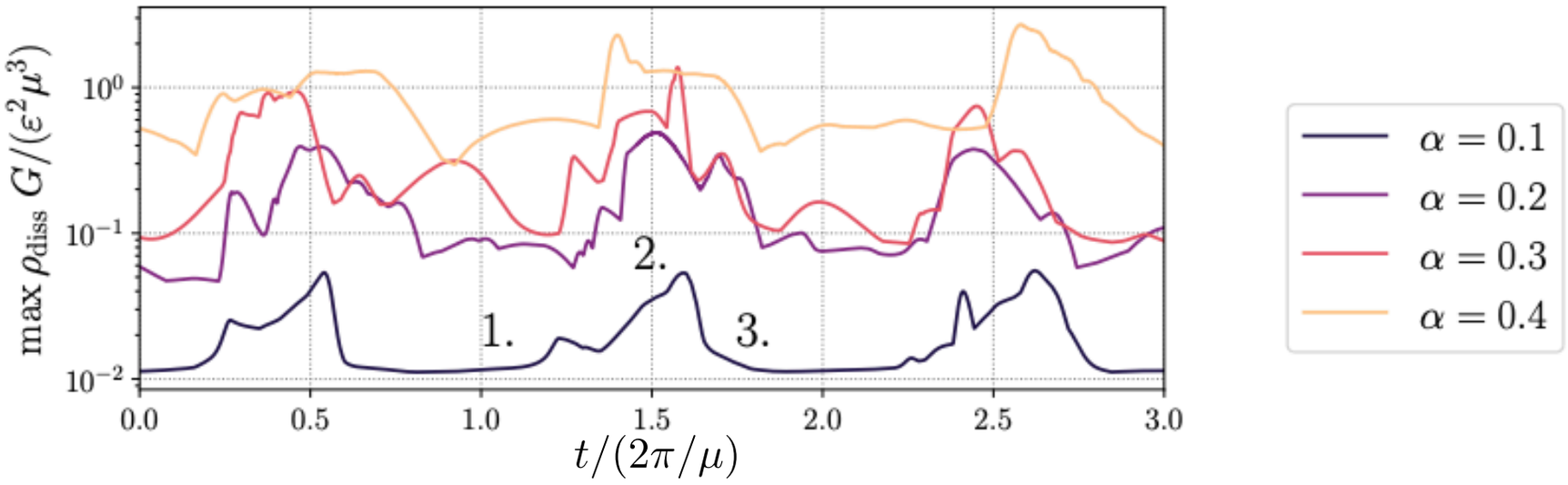

- Fundamental time scale of the system $2\pi/\mu$
- Weak evidence of periodicity from our simulation
- Pulsar analogy

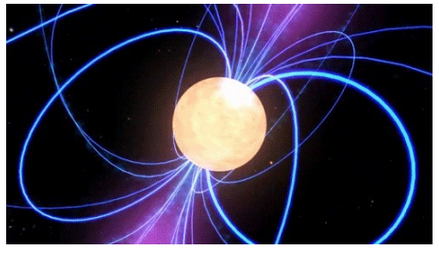

Theory

QCD Axion: Strong-CP problem

- Solve the problem by promoting θ to a dynamical field, the **axion *a*:**

$$V \supset \frac{\alpha_s}{8\pi}\theta\, G\tilde{G} \quad \rightarrow \quad V \supset \frac{\alpha_s}{8\pi}\left(\frac{a}{f} - \theta\right) G\tilde{G}$$

- Nonperturbative QCD effects create potential for the axion

$$V(a) = -m_\pi^2 f_\pi^2 \sqrt{1 - \frac{4 m_u m_d}{(m_u + m_d)^2} \sin^2\left(\frac{a}{2f_a}\right)}$$

- At the minimum the strong-CP problem is solved ($\theta \sim 0$) and the axion acquires a small mass

$$m_a = 5.70(6)(4)\,\mu\text{eV}\left(\frac{10^{12}\text{GeV}}{f_a}\right)$$

The QCD axion
in string theory

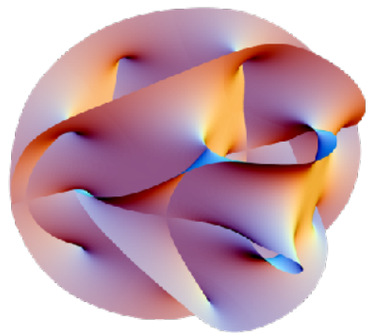

- 4D axions appear as zero modes of gauge fields compactified in extra dimensions

- Nonperturbative gravity effects generate a mass, exponentially suppressed:

$$\mu^4 e^{-S}\left(1-\cos\left(\frac{\phi}{f}\right)\right)$$

- Requiring string theory to produce the QCD axion puts an upper bound on the size of these corrections

$$\mu^4 e^{-S} \ll \Lambda^4$$

- Complex string compactifications produce multiplicity of light string axions

Kallosh, Linde, Linde, Susskind [9502069]
Svrcek , Witten [0605206]
Arvanitaki, Dimopoulos, Dubovsky, Kaloper, March-Russell [0905.4720]

Axion dark matter

- Cosmological evolution analogous to damped harmonic oscillator with frequency given by the mass and damping by Hubble friction:

$$\ddot{a} + 3H\dot{a} + m^2 a = 0$$

- Early on, H >> m: frozen by Hubble friction

- When H < m: begins to oscillate; energy density dilutes as nonrelativistic matter

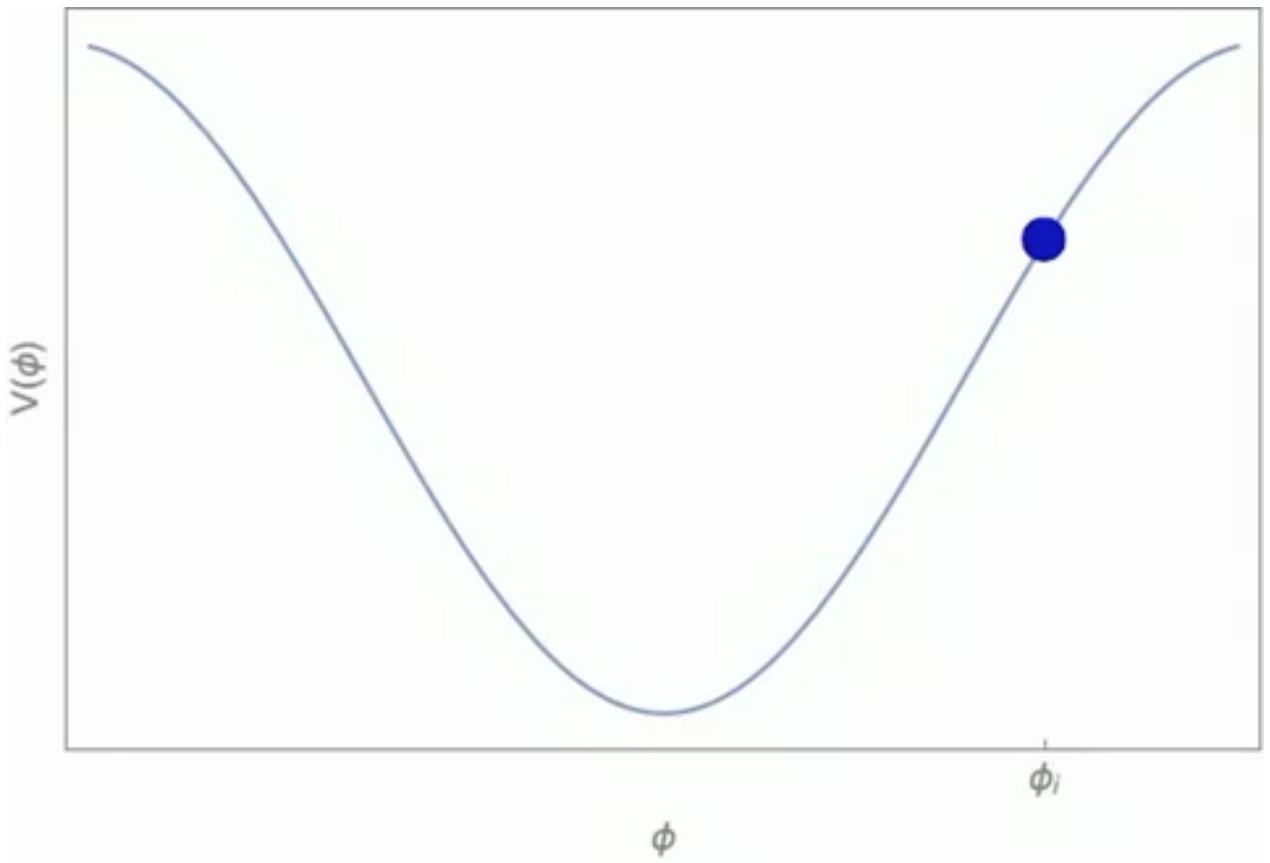

Predict DM density as a function of *m*, *f*:

$$\frac{\rho_{\rm a}}{\rho_{\rm cdm}} \sim \left(\frac{m}{\rm eV}\right)^{1/2} \left(\frac{f}{10^{11}{\rm GeV}}\right)^2 \left(\frac{a_i}{f}\right)^2$$

QCD axion

$$\frac{\rho_{\rm a,QCD}}{\rho_{\rm cdm}} \sim \left(\frac{f}{\text{few} \times 10^{11}{\rm GeV}}\right)^{7/6} \left(\frac{a_i}{f}\right)^2$$

Preskill, Wise, Wilczek (1983)
…

Light bosonic dark matter

- Dark Photons can also be produced by inflationary perturbations in the early universe

$$\left(\partial_t^2 + \frac{3k^2 + a^2m^2}{k^2 + a^2m^2} H\partial_t + \frac{k^2}{a^2} + m^2\right) A_L = 0$$

longitudinal mode with momentum *k*

- Relic abundance set by the mass of the vector and the Hubble scale during inflation

$$\frac{\Omega_{\rm vector}}{\Omega_{\rm cdm}} \sim \left(\frac{m}{\rm eV}\right)^{1/2} \left(\frac{H_I}{5\times 10^{12}{\rm GeV}}\right)^2$$

[P.W. Graham, J. Mardon, S. Rajendran, arXiv:1504.02102]

Gravitational Wave signatures

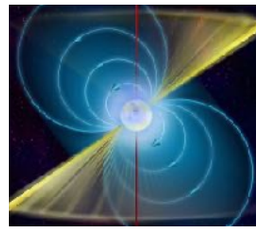

Continuous Wave Searches

Current searches for gravitational waves from asymmetric rotating neutron stars

- Weak signals require long coherent integration time

coherent: T_{coh} sensitivity ~ $T_{coh}^{1/2}$

semicoherent: T_{coh} T_{coh} T_{coh} T_{coh} T_{coh} sensitivity ~ $T_{coh}^{1/2}$ $N_{seg}^{1/4ish}$

All-Sky O1 Upper Limits

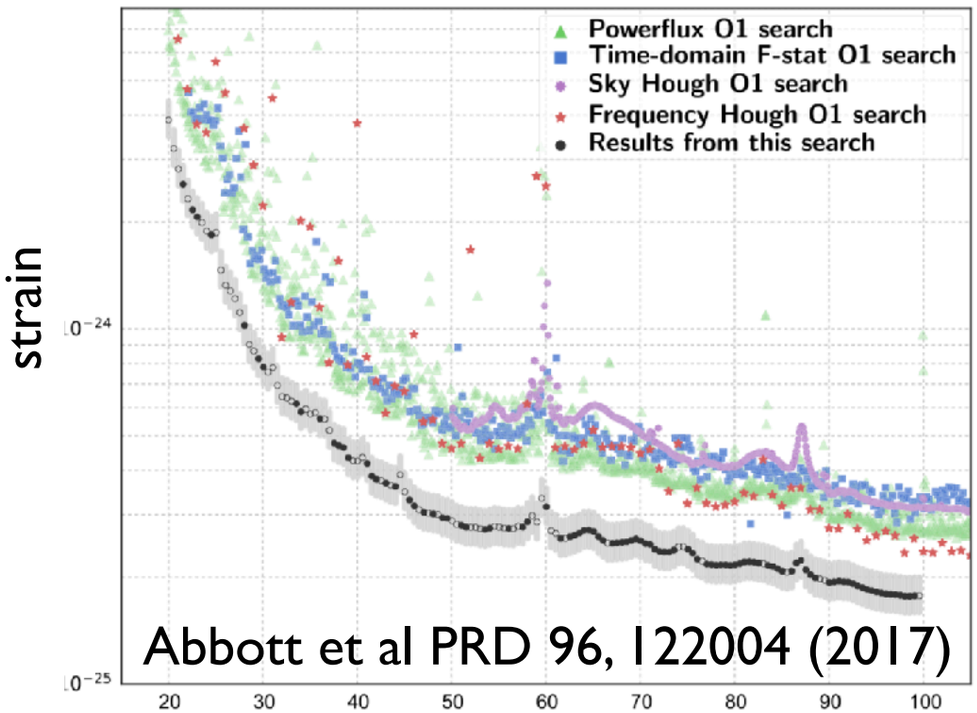

Abbott et al PRD 96, 122004 (2017)

e.g.,

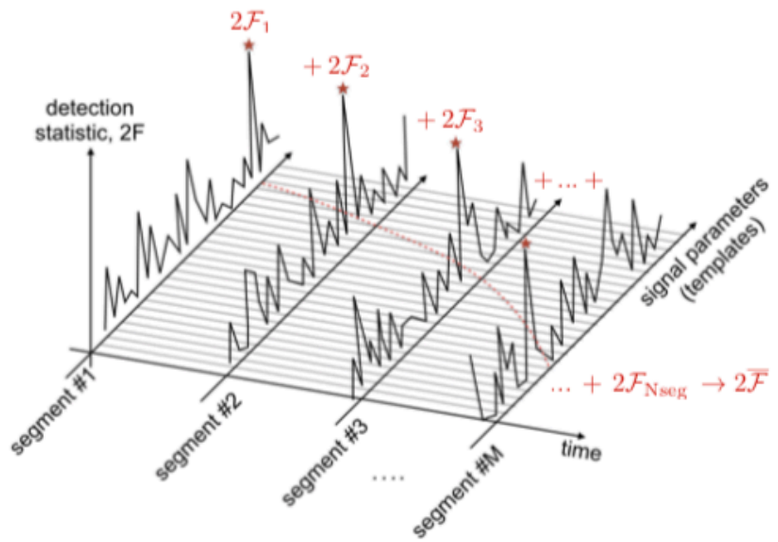

Sylvia Zhu, 2019

all-sky search
minimal assumptions

$N \sim Tcoh^6 \sim 10^{17}$

63

Gravitational Wave Signals

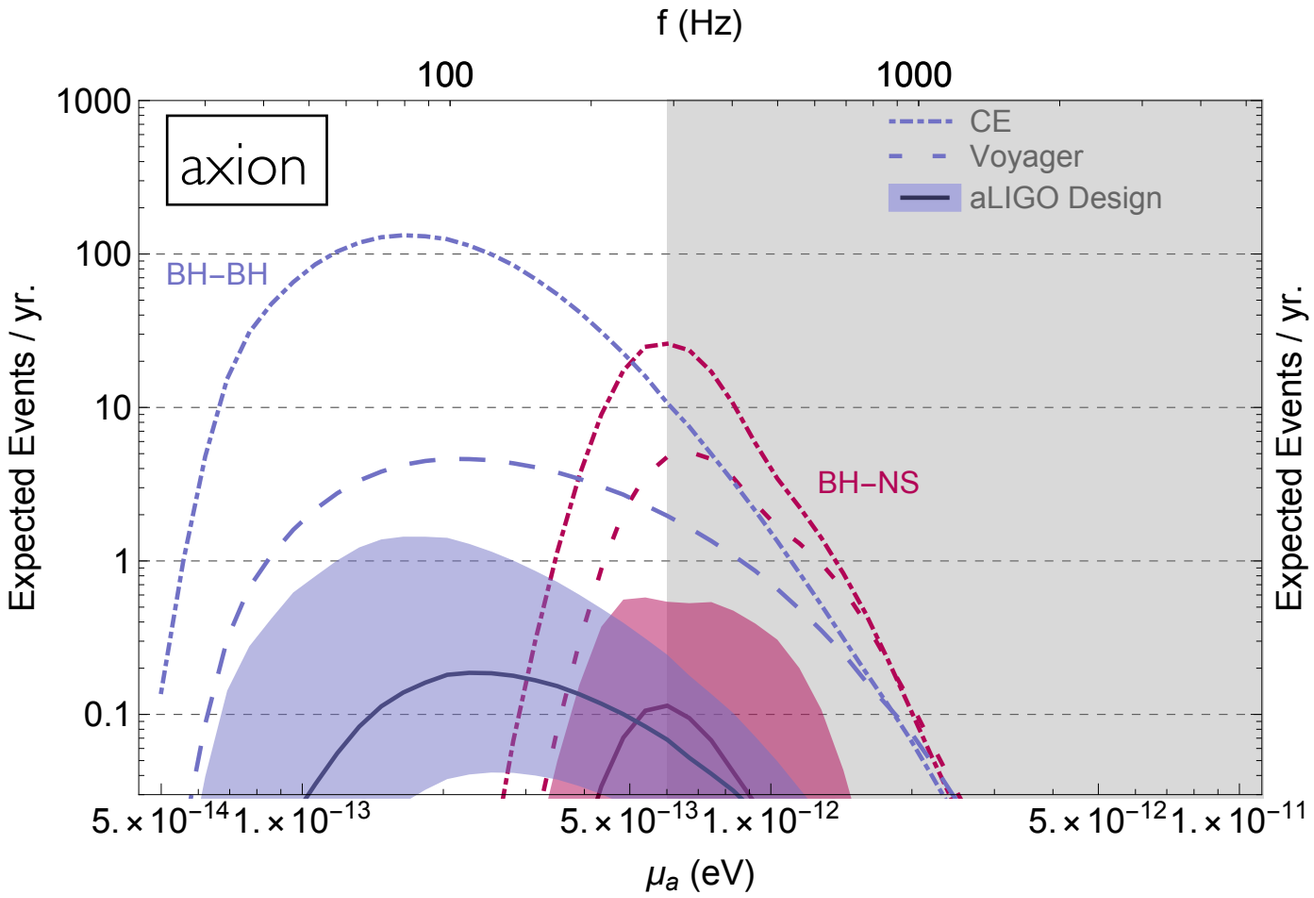

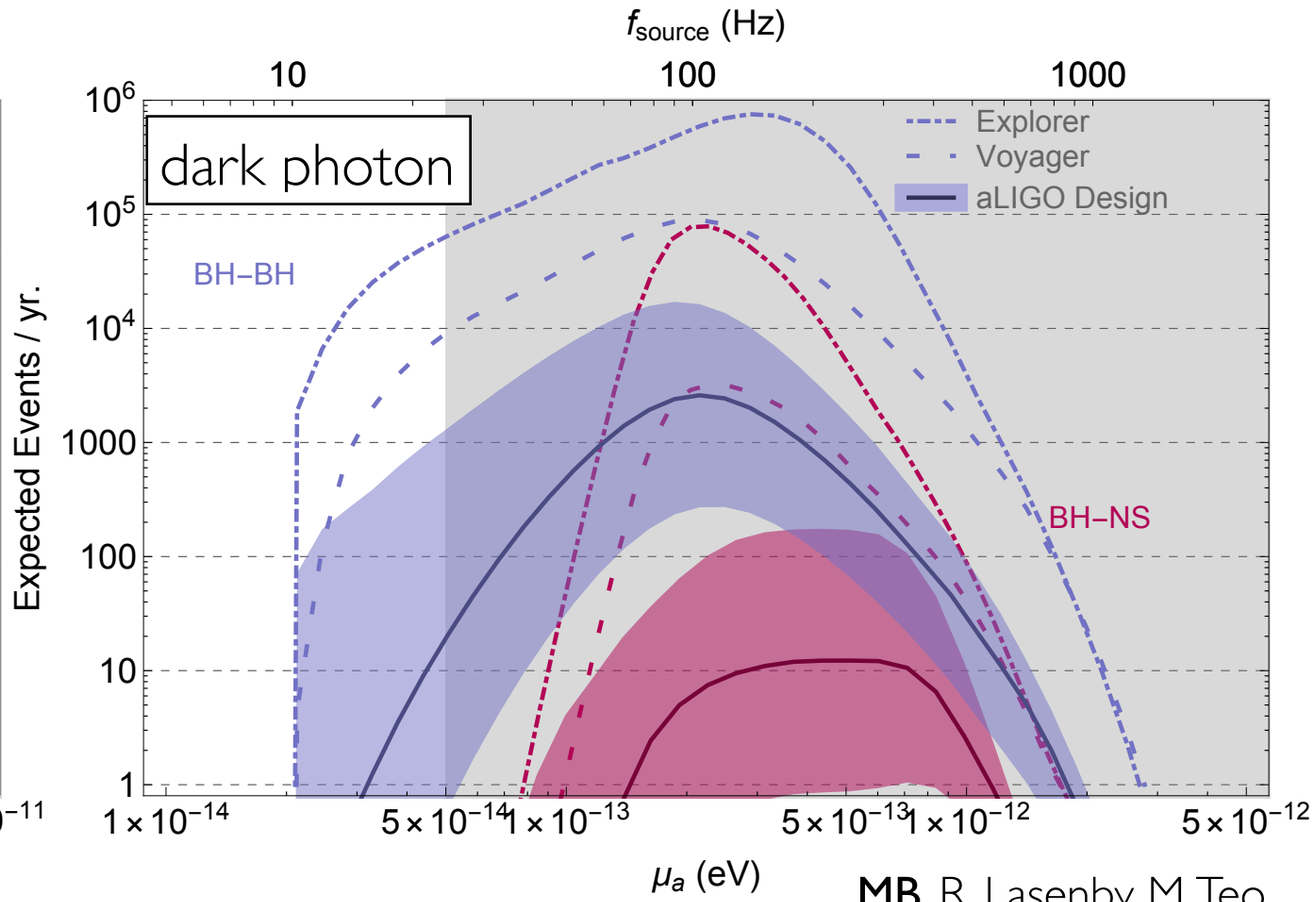

MB, R. Lasenby, M. Teo

A. Arvanitaki, **MB**, S. Dimopoulos, S. Dubovsky, R. Lasenby

- **Short, bright signals** — directed follow-up searches to recently born BHs from 10-1000 Mpc away
- Measure BH mass, spin, and particle mass: fully study gravitational atom
- Especially promising at future GW observatories, methods investigations ongoing
  - M. Isi, L. Sun, R. Brito, A. Melatos

Gravitational Wave Signals

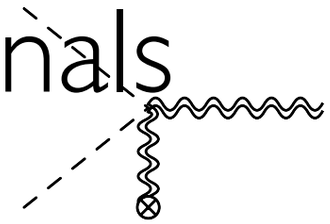

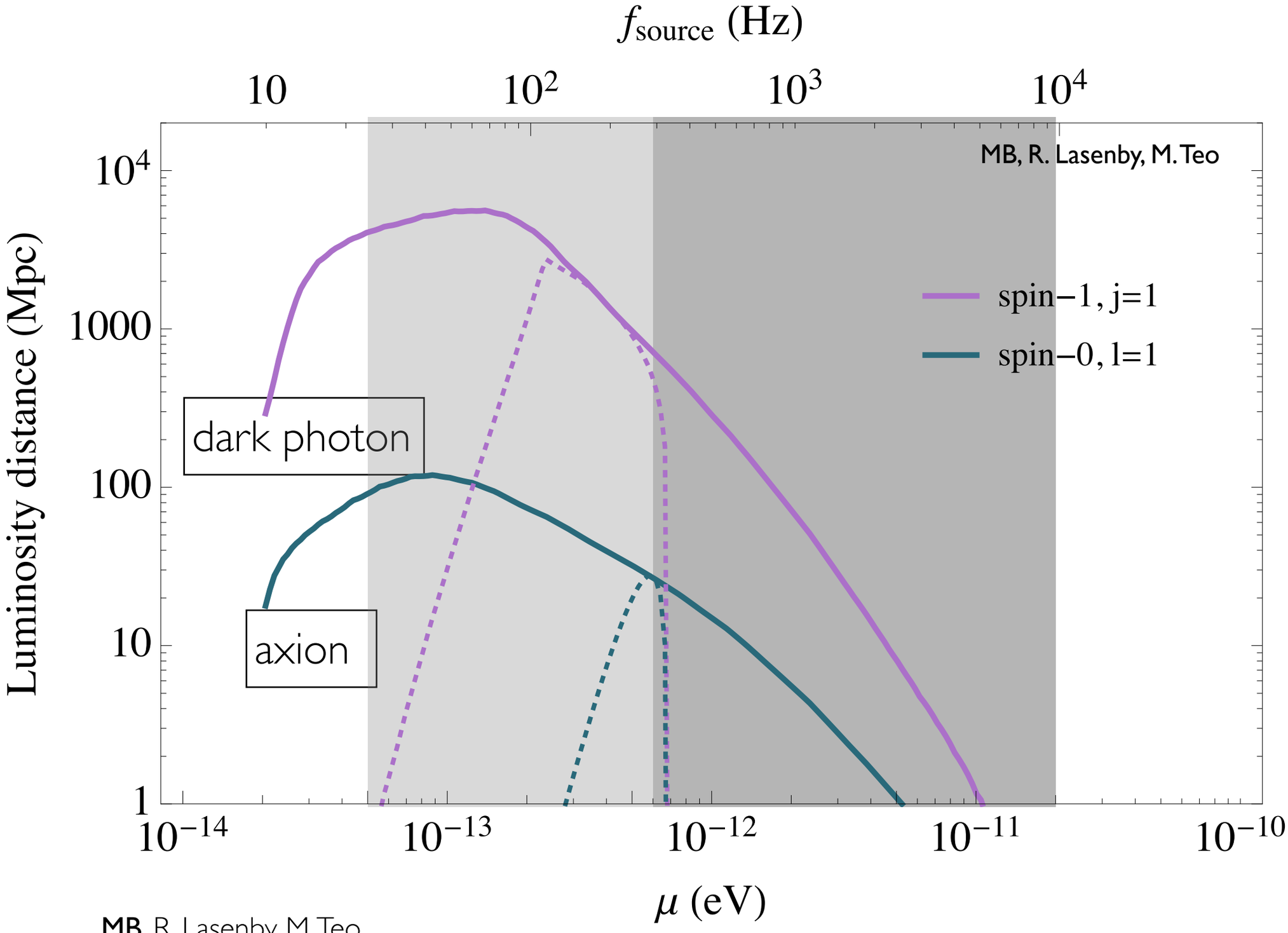

Spin-1 particle annihilations give higher rates, but more constrained

Realistically, limited by number of heavy black holes (>100 Msun)

MB, R. Lasenby, M. Teo

Gravitational Wave Signals

- Up to 10^8 black holes born in the Milky Way over age of universe
- Each can potentially grow a cloud of axions and subsequently source gravitational waves

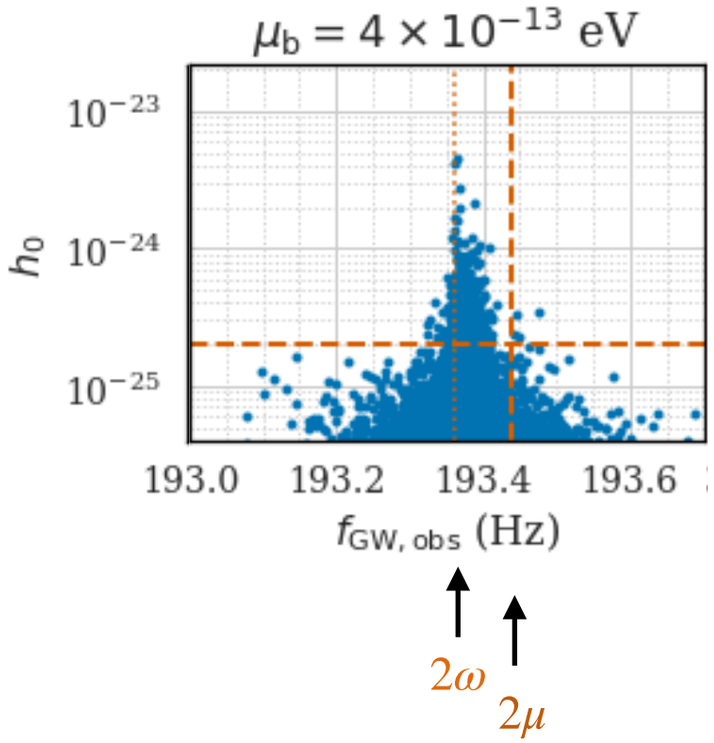

Up to 1000s of signals observable with Advanced LIGO searches

- Signals clustered at frequency ~twice the axion mass
- Binding energy (constant) and doppler shift (time-dependent) change frequency at LIGO
- Heavier black holes produce larger signals, lower frequencies

Zhu, **MB**, Papa, Tsuna, Kawanaka, Eggenstein (2003.03359)

Gravitational Wave Signals

- **Weak, long signals** last for ~ million years, visible from our galaxy, limited by LIGO noise floor
- Event rates up to 10,000 — can be observed and studied in detail
- Searches ongoing with O1/ O2 data

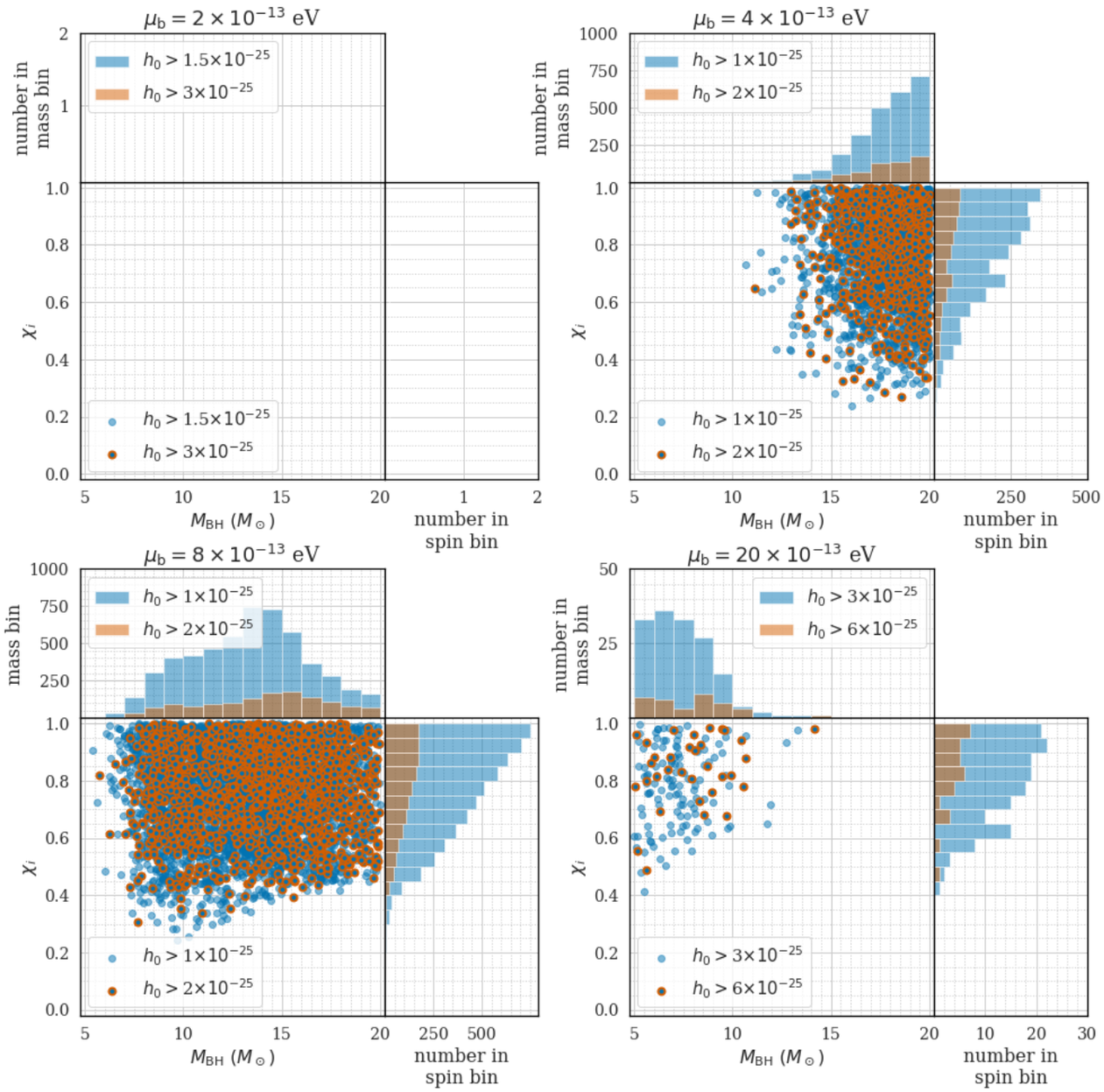

S. J. Zhu, **MB,** M. A. Papa, D. Tsuna, N. Kawanaka, H.B. Eggenstein *(2020)*

Gravitational Wave Signals

- **Weak, long signals** last for ~ million years, visible from our galaxy, limited by LIGO noise floor
- Event rates up to 10,000 — can be observed and studied in detail
- Searches ongoing with O1/ O2 data

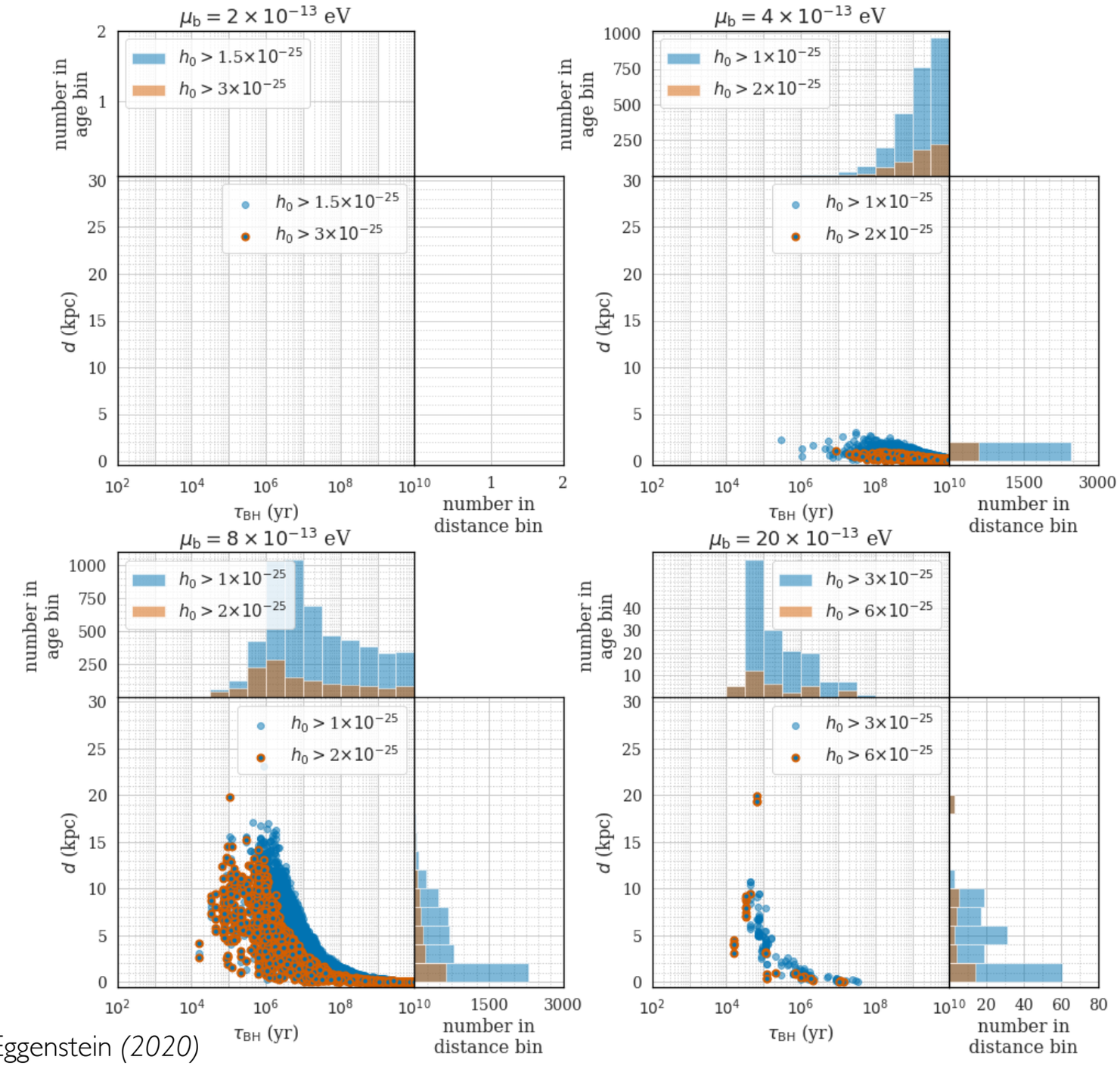

S. J. Zhu, **MB,** M. A. Papa, D. Tsuna, N. Kawanaka, H.B. Eggenstein *(2020)*

Gravitational Wave Signals

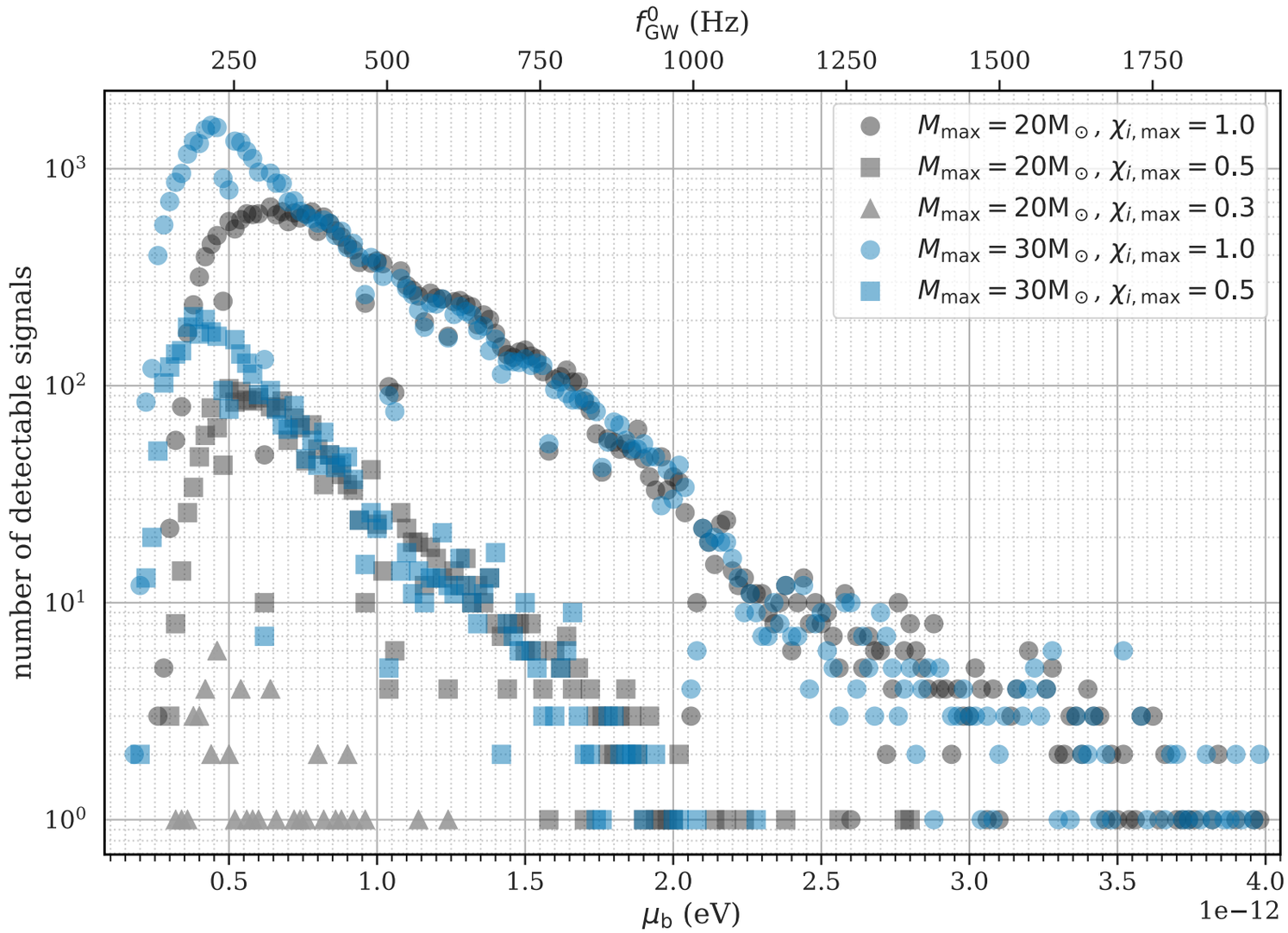

Zhu, **MB**, Papa, Tsuna, Kawanaka, Eggenstein PRD 2020

- **Weak, long signals** last for ~ million years, visible from our galaxy
- Very sensitive to number of rapidly rotating black holes
- Weak dependence on mass distribution except at low axion masses

- Up to 1000 signals above sensitivity threshold of Advanced LIGO searches today
- Can disfavor axions of mass ~10^{-12} eV with assumptions on black hole populations
- Further characterization of continuous wave searches in dense signal regime is ongoing

Black hole spins

Black Hole Spins

Black hole spin and mass measurements can be used to constrain axion parameter space

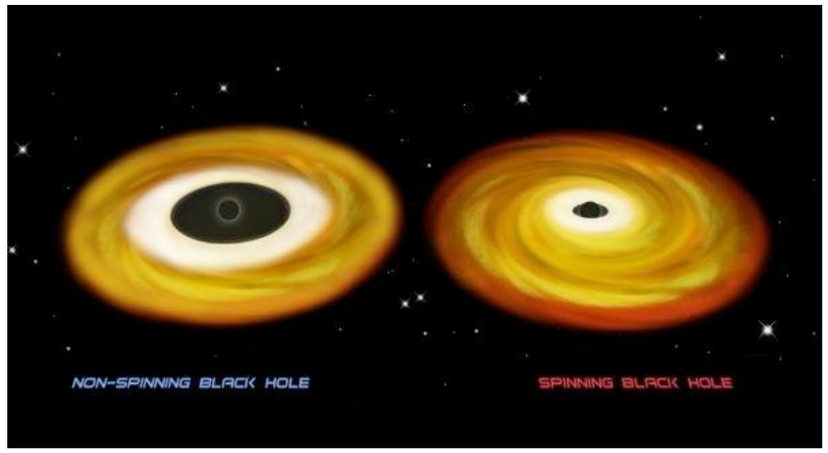

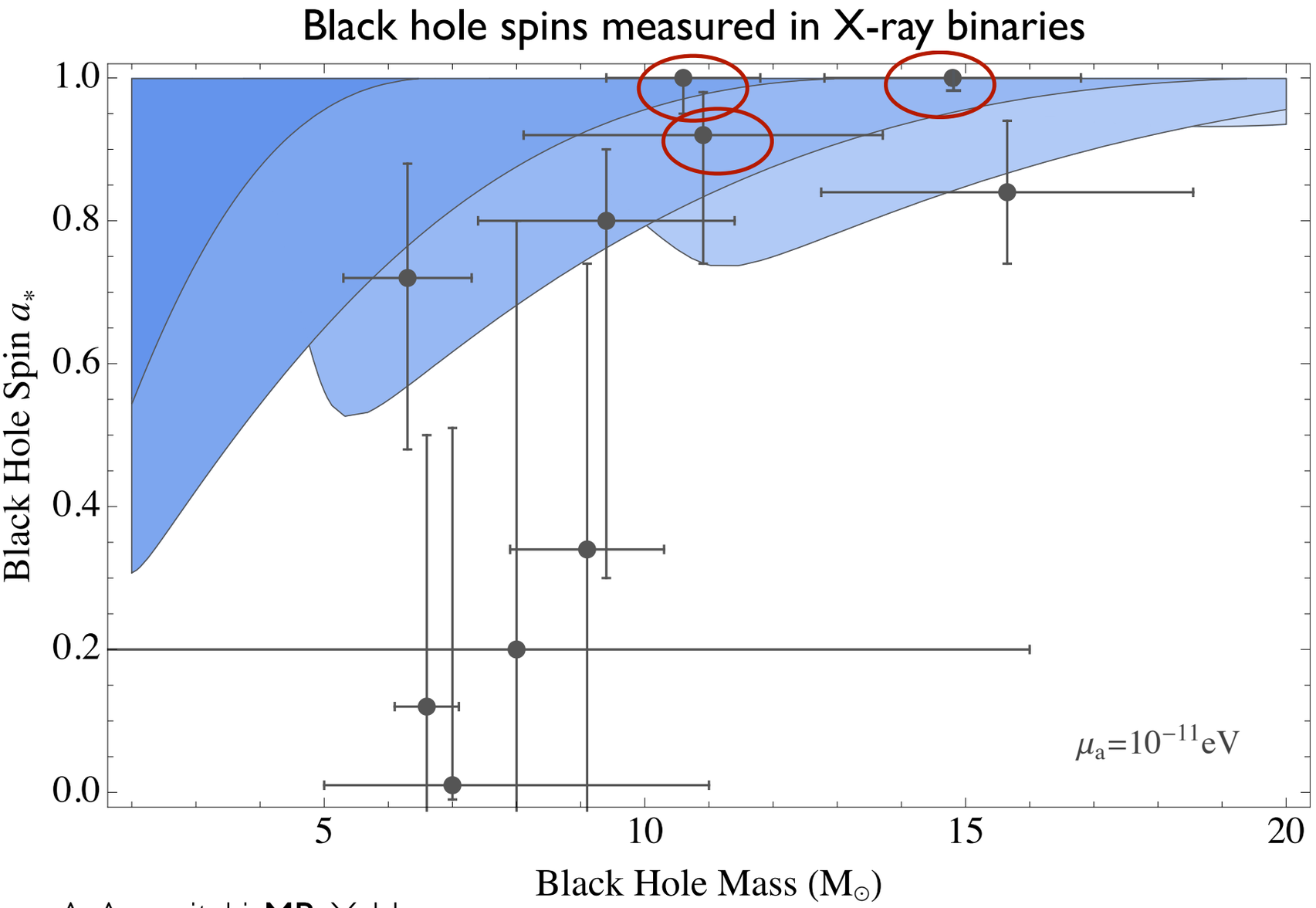

A. Arvanitaki, **MB**, X. Huang

Black Hole Spins

Use measurements of rapidly rotating black holes to constrain parameter space

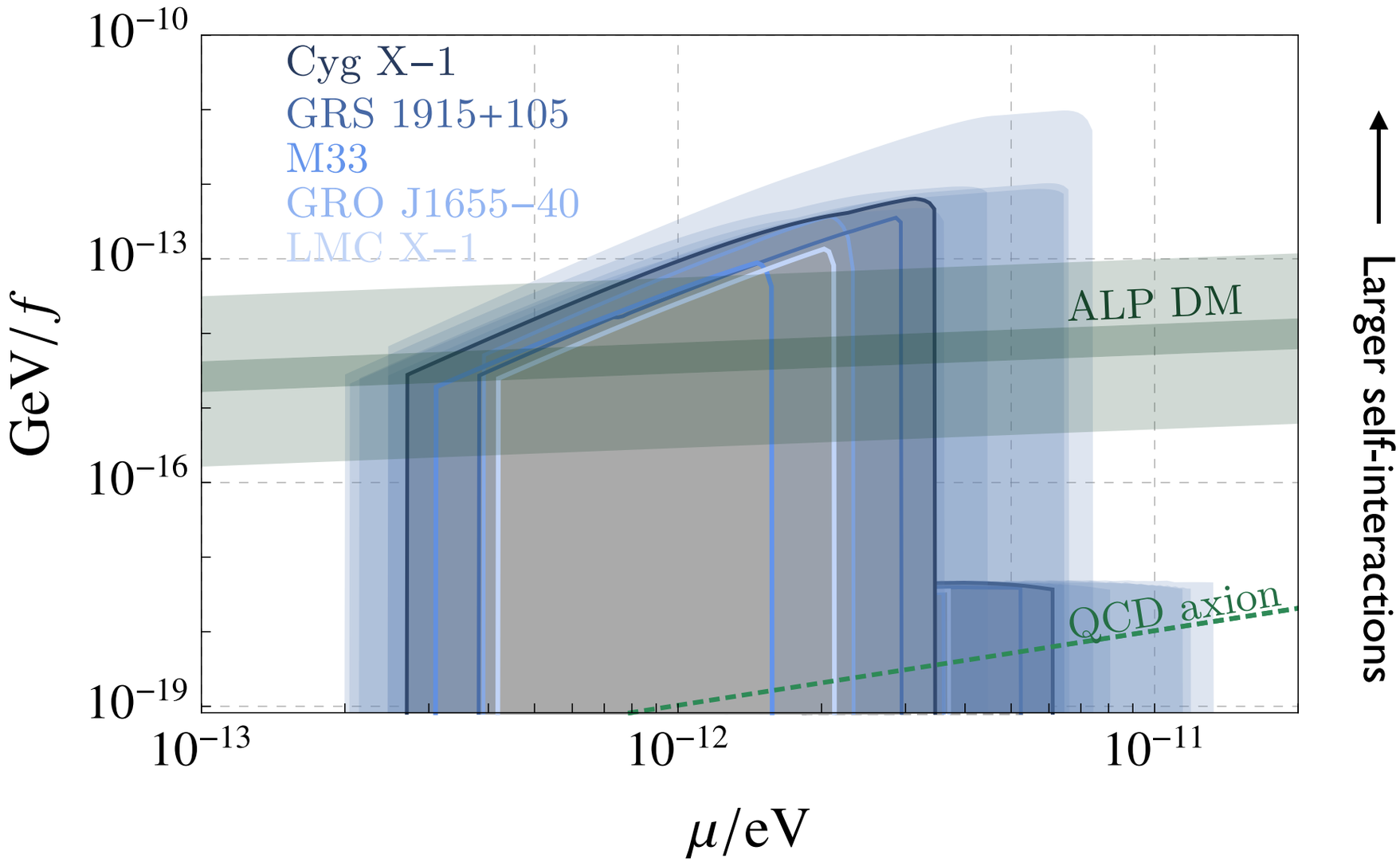

- As self-interactions increase, the number of axions in each level is bounded and spin extraction from the black hole slows

MB, M. Galanis, R. Lasenby, O. Simon PRD 2021

Black Hole Spins at LIGO

If light axion exists, some initial merger BHs would have low spin due to superradiance, limited by age of binary system

A. Arvanitaki, **MB**, S. Dimopoulos, S. Dubovsky, R. Lasenby

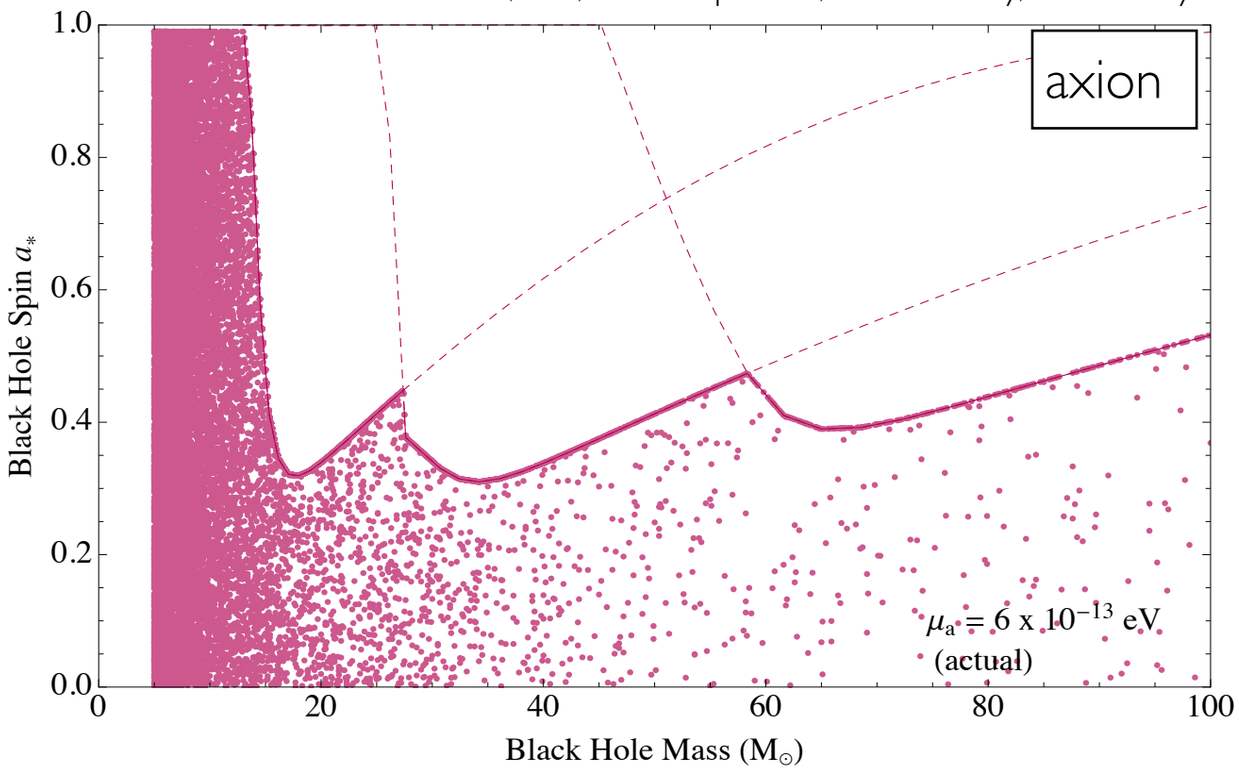

MB, R. Lasenby, M. Teo

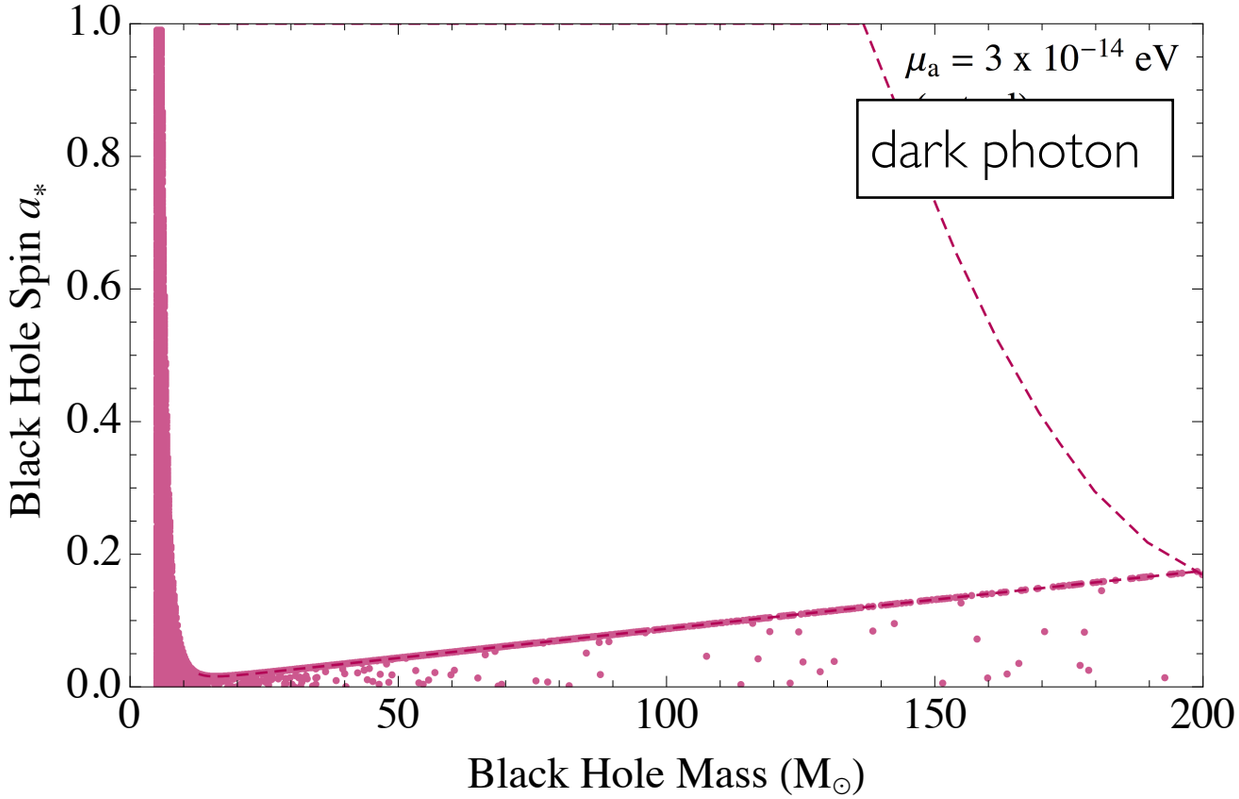

9-240 BBHs/Gpc^3/yr. — 1000s of BHs merging in low-redshift universe

With ~100-300 spin measurements, possible to see statistical evidence for light boson in the mass range 10^{-11} — 10^{-13} eV

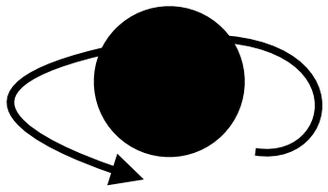

Black Hole Spins

- Two leading methods: continuum fitting and X-ray reflection
- Based on finding the innermost stable orbit of the accretion disk
- Uncertainty dominated by observational errors; smaller at extremal spins

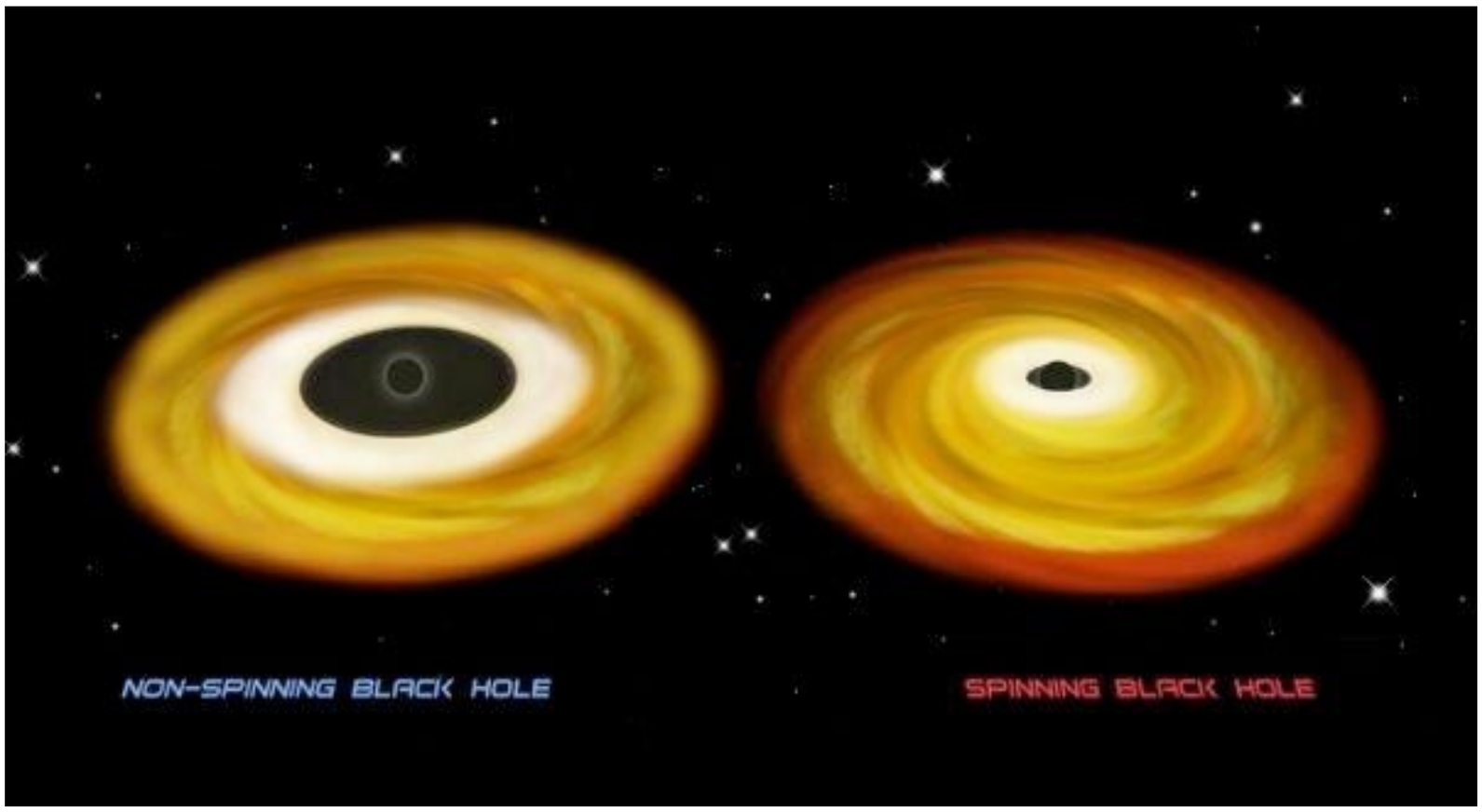

Xray line BH spin measurement

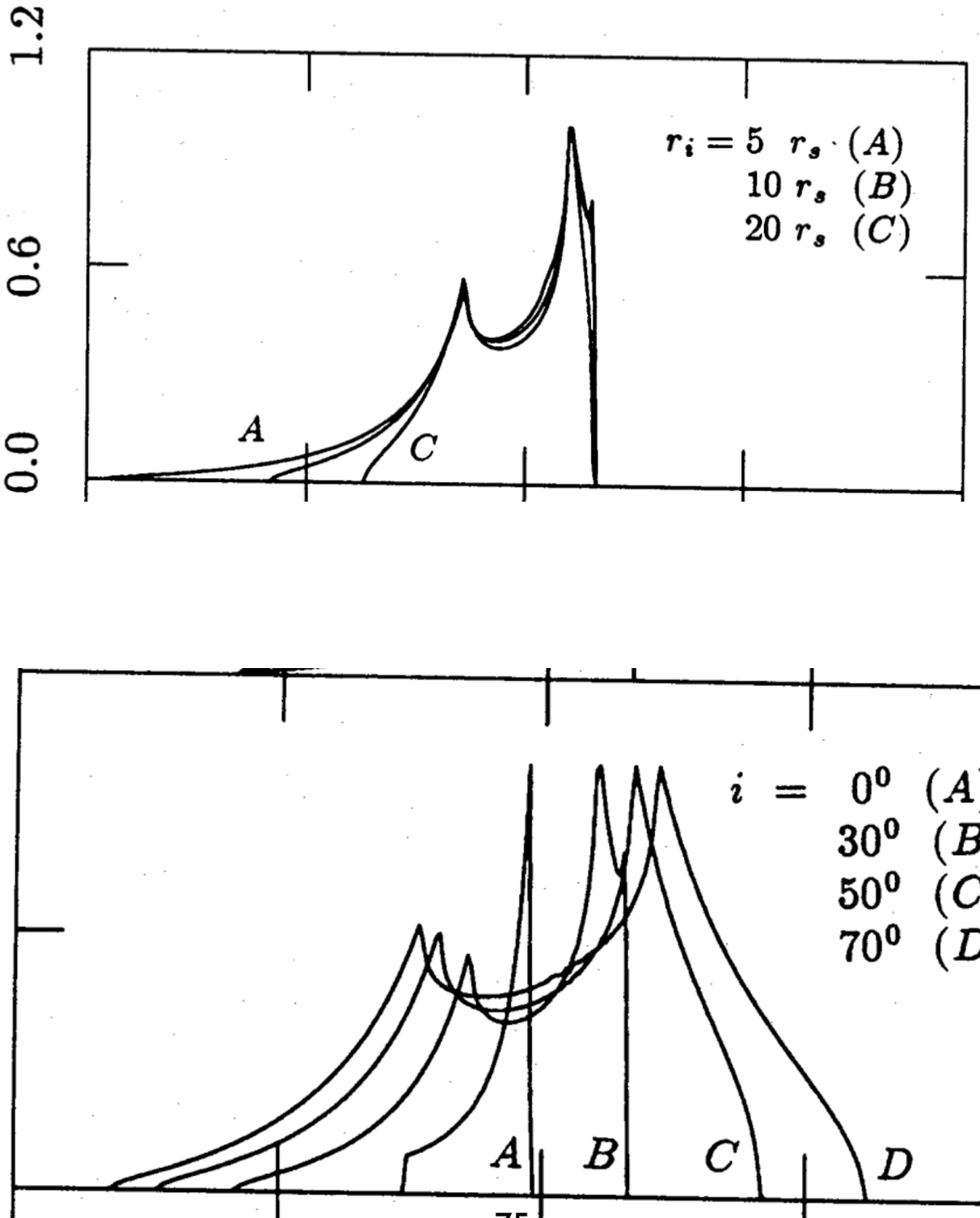

Continuum measurement

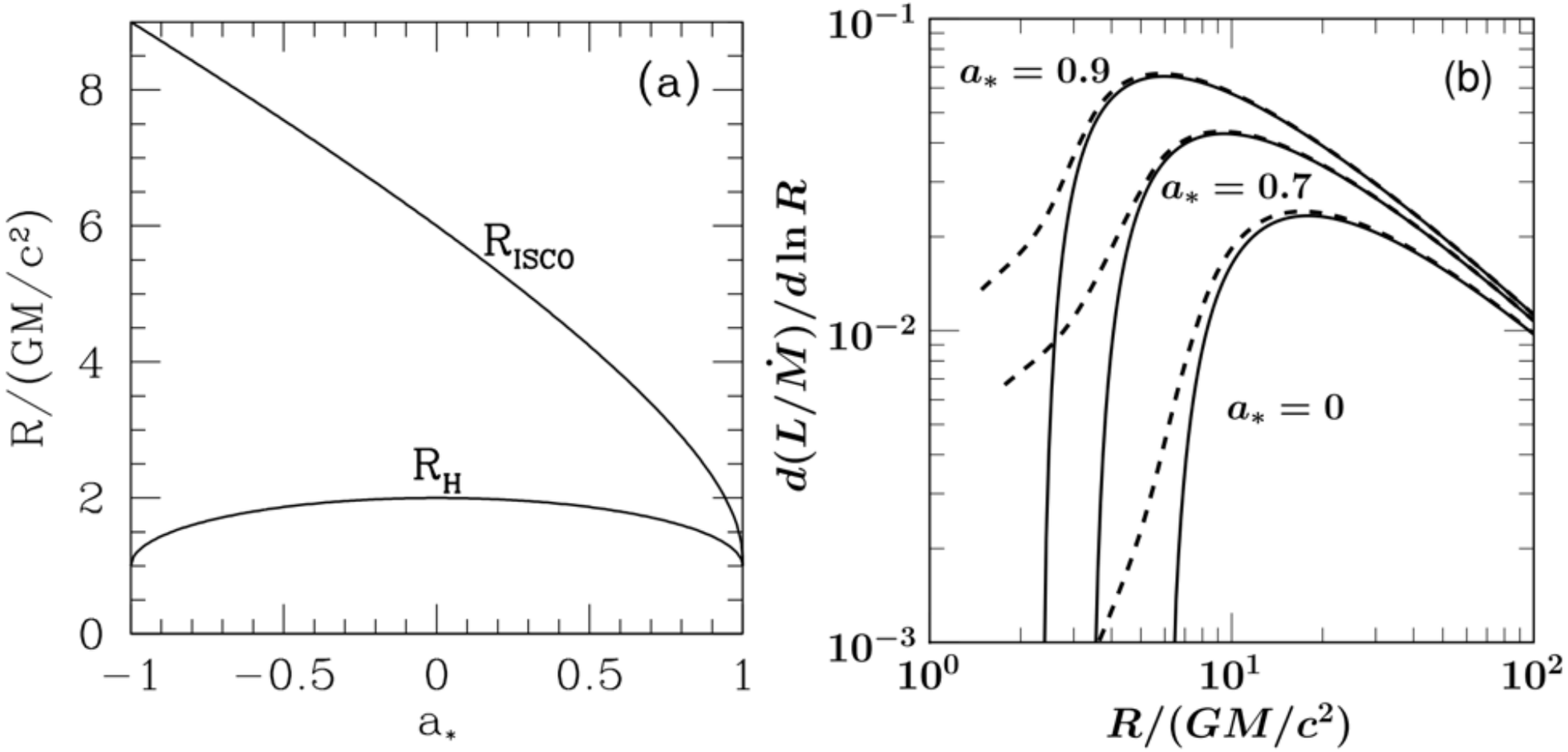

Fig. 3 (a) Radius of the ISCO $R_{\rm ISCO}$ and of the horizon $R_{\rm H}$ in units of GM/c^2 plotted as a function of the black hole spin parameter a_*. Negative values of a_* correspond to retrograde orbits. Note that $R_{\rm ISCO}$ decreases monotonically from $9GM/c^2$ for a retrograde orbit around a maximally spinning black hole, to $6GM/c^2$ for a non-spinning black hole, to GM/c^2 for a prograde orbit around a maximally spinning black hole. (b) Profiles of $d(L/\dot{M})/d\ln R$, the differential disk luminosity per logarithmic radius interval normalized by the mass accretion rate, versus radius $R/(GM/c^2)$ for three values of a_*. Solid lines are the predictions of the NT model. The dashed curves from Zhu et al. (2012), which show minor departures from the NT model, are discussed in Section 5.2.

Black Hole Spins

Five stellar black holes and four SMBHs combine to disfavor the range:

$$2.5 \times 10^{-19} < \mu_V < 2.1 \times 10^{-17}\mathrm{eV}$$

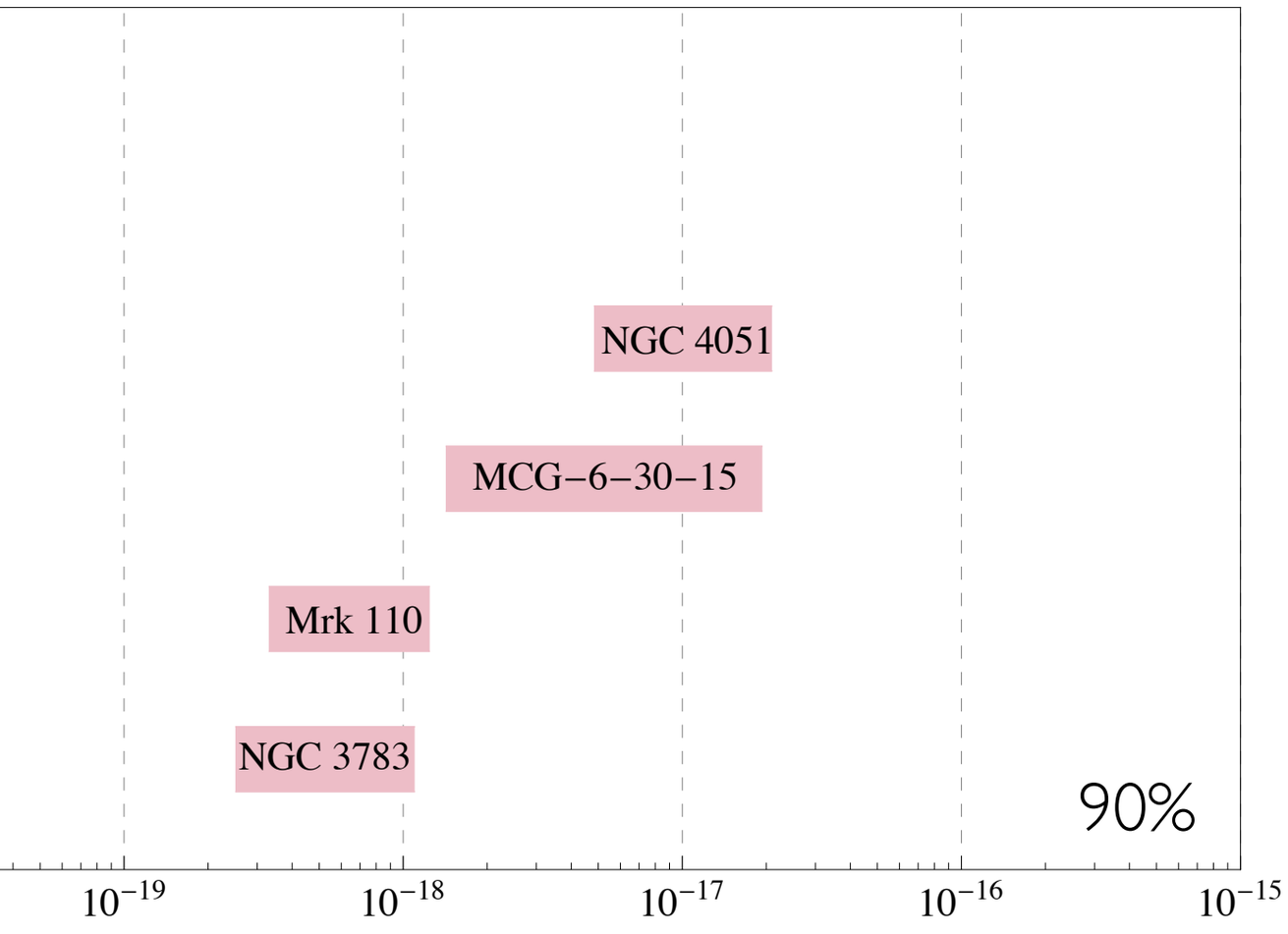

$$2 \times 10^{-11} \gtrsim \mu_V \gtrsim 5 \times 10^{-14}\mathrm{eV}$$

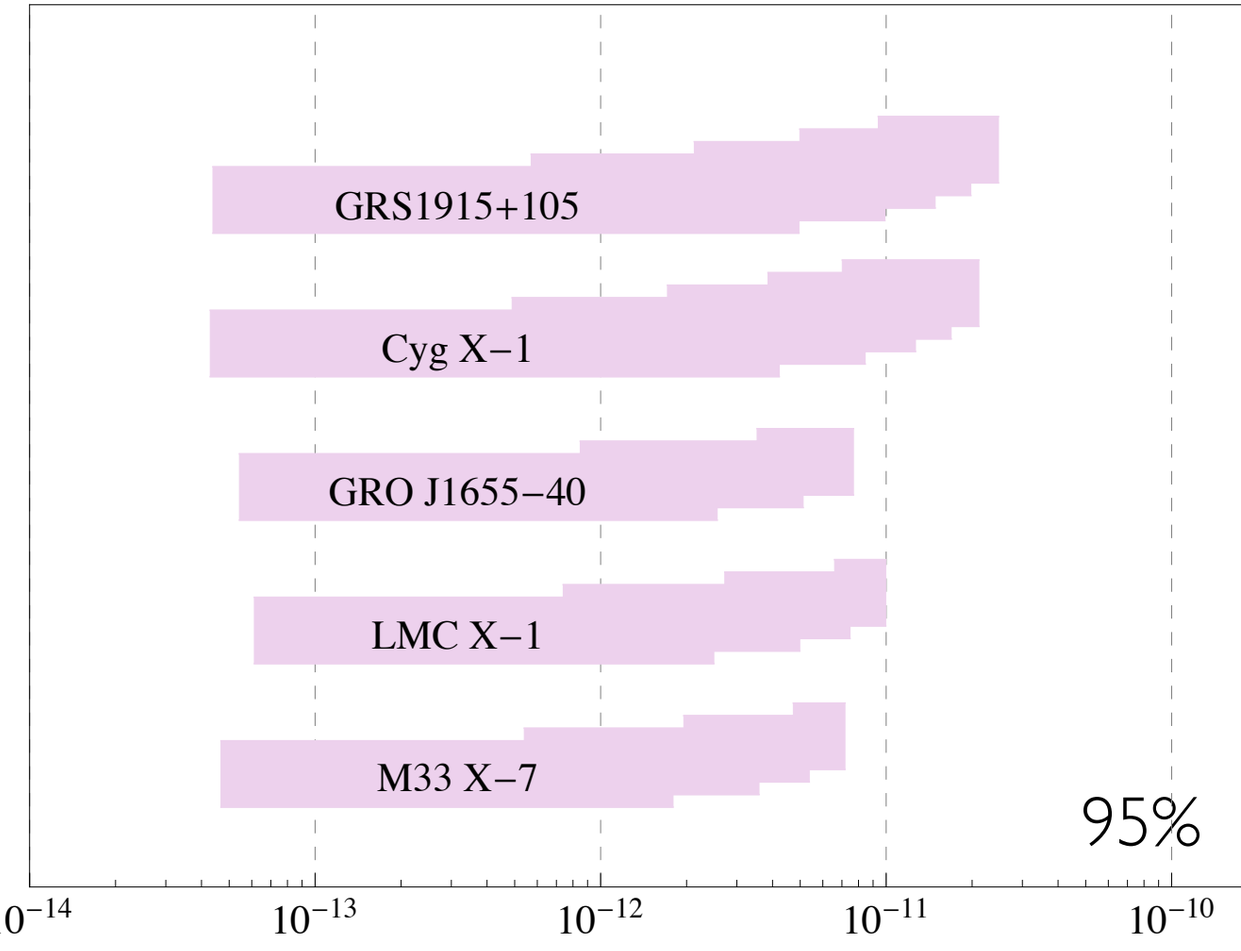

Black Hole Spins

Use measurements of rapidly rotating black holes to constrain parameter space

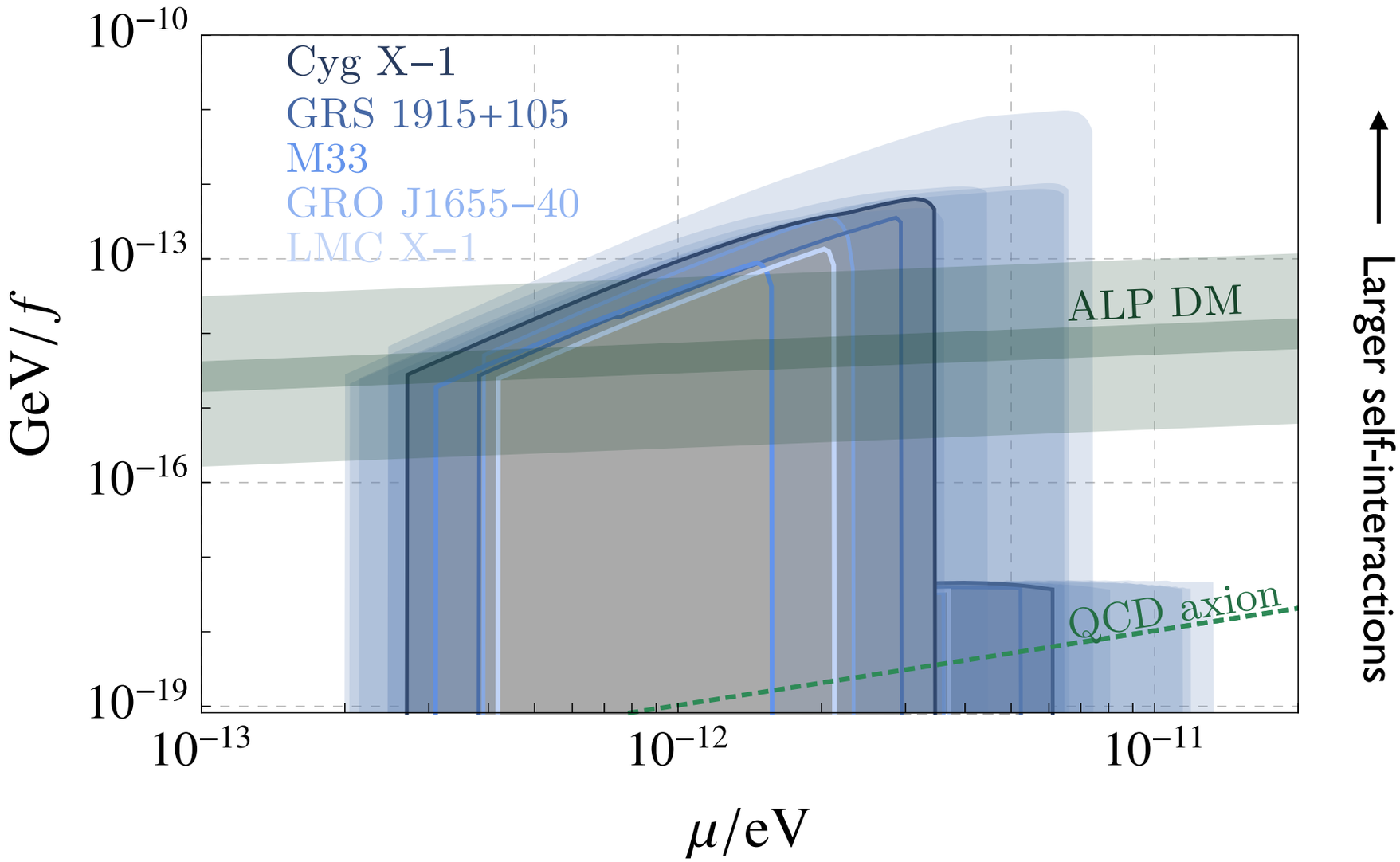

- As self-interactions increase, the number of axions in each level is bounded and spin extraction from the black hole slows

MB, M. Galanis, R. Lasenby, O. Simon PRD 2021

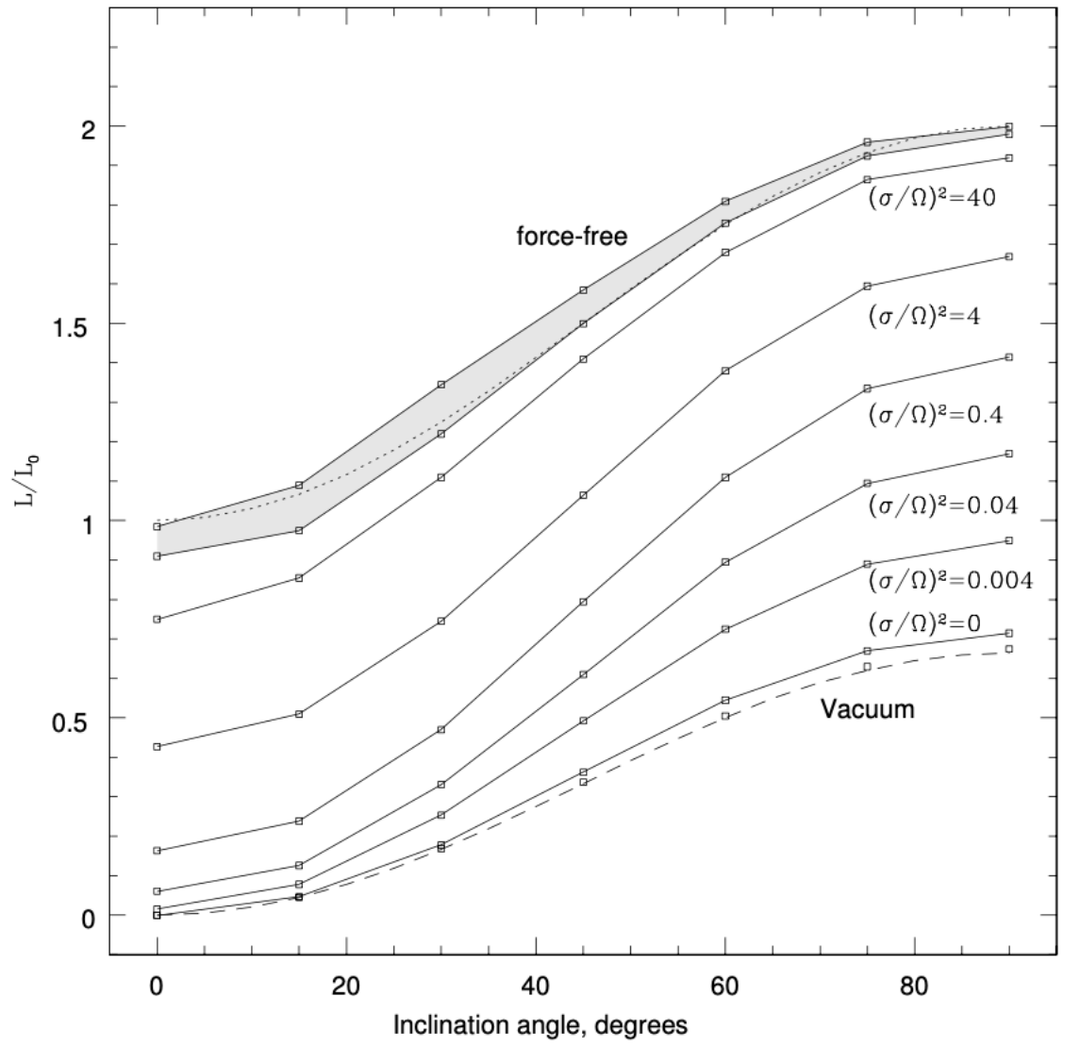

FIG. 2.— Spin-down luminosity dependence on inclination angle for force-free, a sequence of resistive, and vacuum dipoles. Spin-down is normalized by 3/2 times the spin-down power of the orthogonal vacuum rotator. We see a smooth monotonic transition from force-free to vacuum with decreasing conductivity.

$$E^i = -e^{-r/a}\frac{\sqrt{N}\alpha^{3/2}\epsilon\mu\sigma\omega}{\sqrt{\pi}(\sigma^2+\omega^2)}\begin{pmatrix}\omega\cos(\mu t)-\sigma\sin(\mu t)\\ \sigma\cos(\mu t)+\omega\sin(\mu t)\\ 0\end{pmatrix}$$

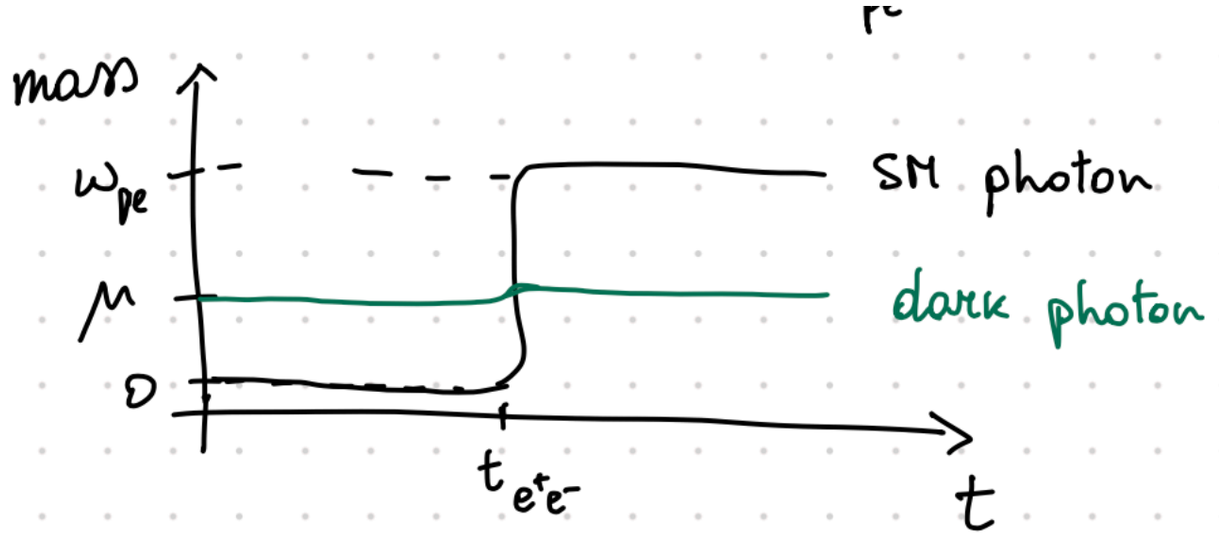

$$J^i = \sigma(E^i+\varepsilon E'^i) = -\frac{e^{-r/a}\sqrt{N}\alpha^{3/2}\varepsilon\mu\sigma\omega^2}{\sqrt{\pi}(\sigma^2+\omega^2)}\begin{pmatrix}\sigma+i\omega\\ -\omega+i\sigma\\ 0\end{pmatrix}e^{-i\omega t},$$

$$P_{\text{Joule}} = \int_V d^3x J_i(E^i+\varepsilon E'^i), \qquad \lim_{r\mu\to\infty} A^i_{SM} = \frac{e^{i\mu r}}{r}\int_V d^3x' J^i(x')e^{-i\omega n'_k x^k} \mapsto P_{EM}.$$

$$P_{\text{Joule}}M/M_{\text{cloud}} = \frac{\tilde{\sigma}\alpha\varepsilon^2}{1+\tilde{\sigma}^2}, \qquad P_{EM}M/M_{\text{cloud}} = \frac{512\pi^2}{3}\frac{\tilde{\sigma}^2\alpha^6\varepsilon^2}{1+\tilde{\sigma}^2},$$

Simulation: B field

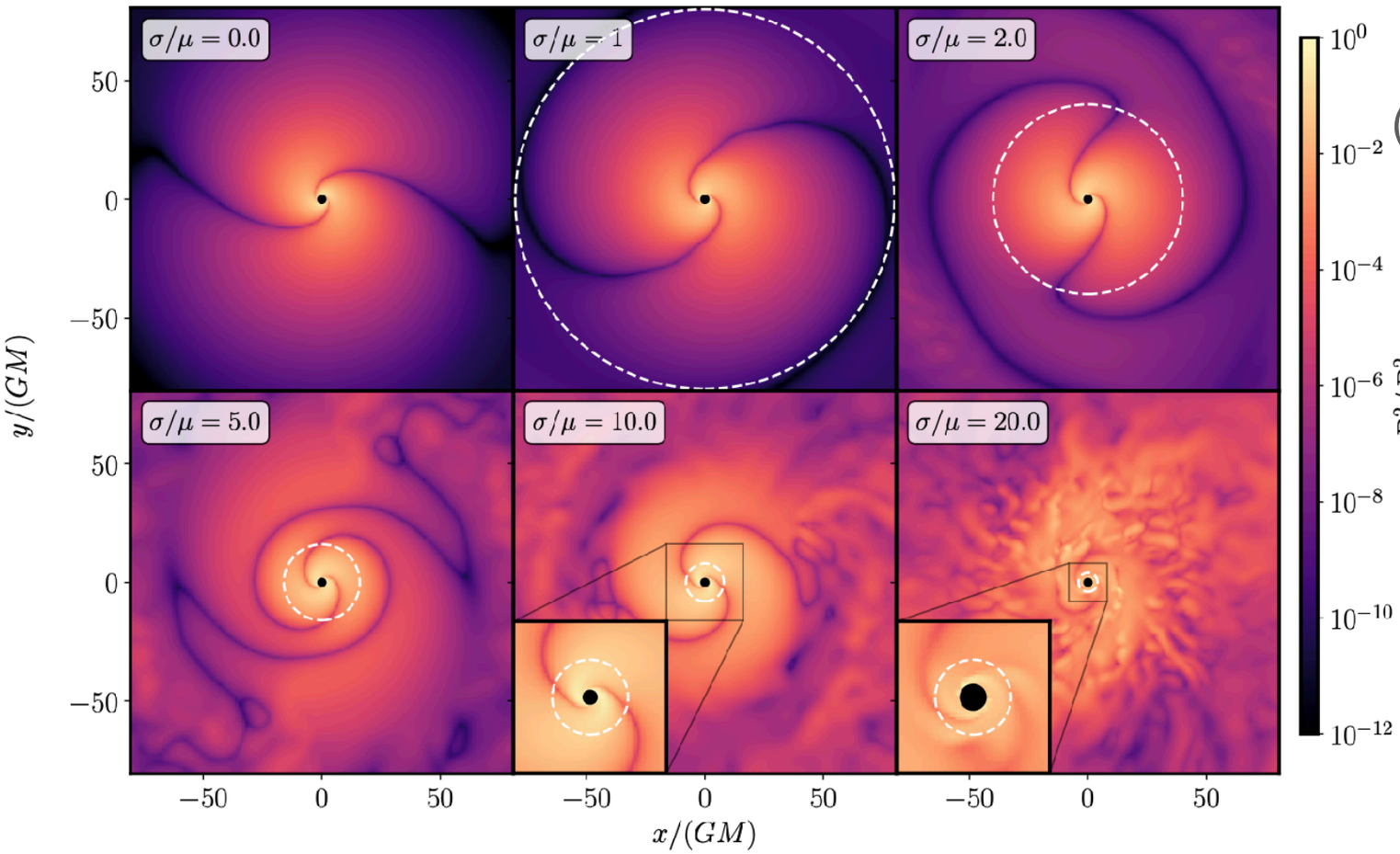

Induction equation:

(Ohm's + Faraday's + Ampere's law)

$$\partial_t \vec{B} = \frac{\epsilon\mu^2}{\sigma}\vec{B}' + \frac{1}{\sigma}\nabla^2\vec{B} + \nabla \times (\vec{v} \times \vec{B})$$

Magnetic Reynolds number $R_m = \sigma v l$

$R_m \gg 1$ Advection (laminar flow)

$R_m \ll 1$ Diffusion

Interplay between the two regimes leads to turbulence.

Simulation: energy dissipation

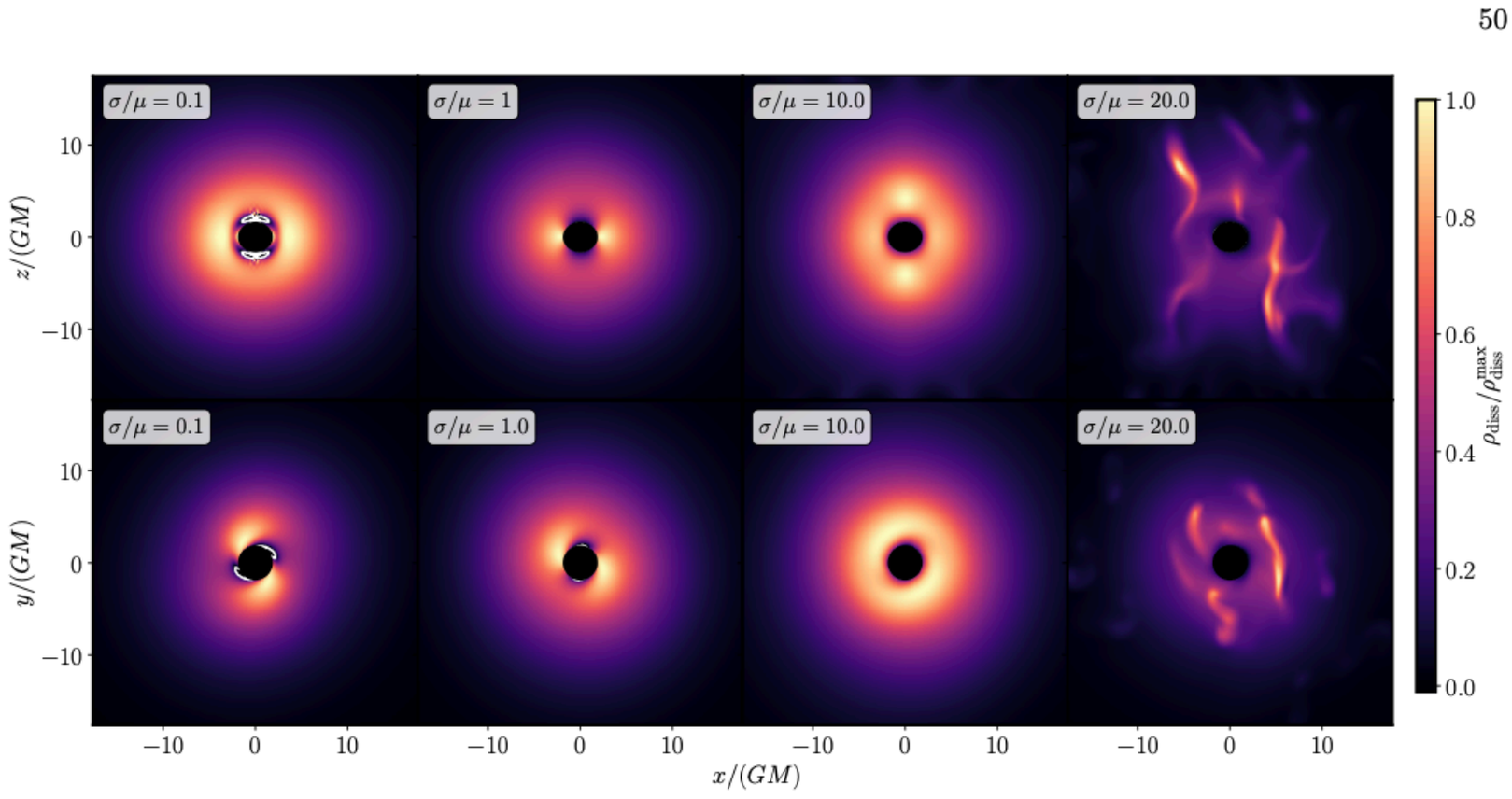

Simulation: energy dissipation